1 2 9 0

UNIVERSIDADE D
COIMBRA

Óscar Emanuel de Melo Rodrigues

The Heart of the Question: Exercise During Gestational Diabetes, Does It Work?

Dissertação no âmbito do Mestrado em Bioquímica orientada pela Doutora Susana P. Pereira e pelo Professor Doutor António J. Moreno e apresentada ao Departamento de Ciências da Vida da Faculdade de Ciências e Tecnologia da Universidade de Coimbra

Janeiro de 2020

UNIVERSIDADE D
COIMBRA

The Heart of the Question:

Exercise During Gestational Diabetes, Does It Work?

Óscar Emanuel de Melo Rodrigues

Master Dissertation in Biochemistry

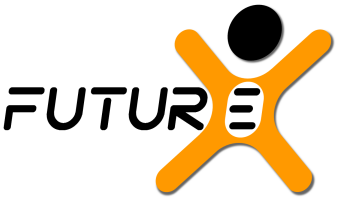

Óscar Rodrigues: The Heart of the Question: Exercise During Gestational Diabetes, Does it Work?

Master dissertation in Biochemistry, January 2020.

This work was performed at the Center for Neuroscience and Cell Biology, UC Biotech Building, Biocant Park, University of Coimbra, Portugal, in MitoXT group under the supervision of Dr. Susana P. Pereira (CNC, University of Coimbra) and Prof. Dr. António J. Moreno (Department of Life Sciences, University of Coimbra).

This work was financed by the COMPETE 2020 - Operational Programme for Competitiveness and Internationalisation and Portuguese national funds via FCT – Fundação para a Ciência e a Tecnologia, under projects: PTDC/DTP-DES/1082/2014, POCI-01-0145-FEDER-016657; UID/NEU/04539/2019; PTDC/ASP-HOR/29152/2017, POCI-01-0145-FEDER-029152; and the fellowship: SFRH/BPD/116061/2016.

ACKNOWLEDGEMENTS

Este trabalho é o culminar de um ano de trabalho, longo e exaustivo, durante o qual contei com o apoio e suporte de muitas pessoas, sem as quais não teria sido possível. No decorrer deste trabalho aprendi imenso a nível científico e profissional, mas mais ainda, descobri sobre mim, aprendi a lidar com as minhas frustrações e acho que saio um ser humano mais forte e mais preparado para a vida real após percorrer este percurso.

Em primeiro lugar, um agradecimento aos meus orientadores, Doutora Susana P. Pereira e Professor Doutor António J. Moreno, por permitirem a realização desta tese. Estendo ainda este agradecimento ao Doutor Paulo J. Oliveira por me ter aceite no seu laboratório e pela dedicação em garantir as condições necessárias para o sucesso deste trabalho.

Gostaria também de agradecer aos nossos colaboradores da Universidade do Porto sem os quais este trabalho não teria sido impossível. Doutor António Ascensão e ao Doutor José Magalhães agradeço por me terem acolhido no seu laboratório e por sempre disponibilizarem todas as ferramentas necessárias à realização deste trabalho. Um obrigado também aos incansáveis Pedro Coxito, Jelena Stevanovic, Jorge Beleza e Manoel Ríos. Estendo ainda este agradecimento ao Doutor David Rizo-Roca e à Doutora Estela Santos-Alves, que foram também parte determinante para o sucesso deste trabalho.

Agradeço às entidades de financiamento que suportaram os recursos que permitiram a realização desta tese: COMPETE 2020 - Operational Programme for Competitiveness and Internationalisation and Portuguese national funds via FCT – Fundação para a Ciência e a Tecnologia, under projects: PTDC/DTP-DES/1082/2014, POCI-01-0145-FEDER-016657; UID/NEU/04539/2019; PTDC/ASP-HOR/29152/2017, POCI-01-0145-FEDER-029152; and the fellowship: SFRH/BPD/116061/2016.

Agradeço à Universidade de Coimbra, em especial ao Departamento de Ciências da Vida, ao CNC – Centro de Neurociências e Biologia Celular, ao UC Biotech e ao CIAFEL – Centro de Investigação em Atividade Física, Saúde e Lazer por me acolherem e proporcionarem todas as instalações e ferramentas físicas para a realização desta tese.

Um agradecimento muito especial à Doutora Susana P. Pereira que ao longo deste ano foi mais que uma orientadora. Agradeço por todo o esforço, dedicação, ajuda, compreensão, por acreditar e confiar em mim, dando-me a confiança que muitas vezes senti que não tinha. Mais do que orientação a nível científico, foi uma orientação de toda uma experiência de vida, um "farol" constante iluminar o caminho correto. Agradeço todos os ensinamentos e conselhos,

e sei que os irei levar comigo para toda a vida. Esta tese simboliza isso mesmo. Um Grande Obrigado!!

Ao Mestre João Martins um enorme obrigado por toda a colaboração e apoio na realização deste trabalho. Quer seja pela sua frontalidade, boa disposição, ou excelente conhecimento científico, foi uma das pessoas mais determinantes para o sucesso deste trabalho. Obrigado por todas as horas dispensadas, pelas conversas estimulantes e por toda a experiência partilhada.

Agradeço a todos os membros do MitoXT pelo bom ambiente vivido nos laboratórios, por todas as conversas altamente estimulantes depois do almoço e pela ajuda sempre facilmente prestada. Sem dúvida que tornaram mais fácil ultrapassar os momentos desafiantes vividos no laboratório. Em especial, um agradecimento ao Doutor José Teixeira, ao Ricardo Amorim, ao Rui Simões e à Adriana Carvalho por estarem sempre disponíveis a ajudar seja no laboratório, seja com input científico para este trabalho.

Ao André Barbosa, agradeço todas as risadas e palhaçadas nas viagens Cantanhede-Coimbra/Coimbra-Cantanhede. Sem dúvida uma das maiores surpresas que este ano me trouxe. Obrigado pela tua amizade e constante palavra de apoio.

Às meninas de mestrado, Rafaela, Margarida, Gabriela, Sara Valente, um grande obrigado por estarem sempre prontas para um lanchinho e organizar uma jantarada! A vossa boa disposição foi uma constante durante este ano e adorei partilhar esta experiência convosco.

Agradeço à Doutora Teresa Oliveira por todos os ensinamentos e por me mostrar as boas práticas laboratoriais para realizar a técnica de PCR.

Um obrigado especial ao meu colega de orientação e grande amigo Luís Grilo. Durante este ano foi uma ajuda constante e pronto-socorro que nunca hesitou quando lhe pedi ajuda. Obrigado por tudo o que me ensinaste, por seres um companheiro de inúmeras batalhas e por me desafiares naqueles dias em que a motivação faltou. Foste determinante para que esta tese atingisse a sua forma final.

À Helena Aires agradeço por ter sempre uma palavra de apoio e de calma nos momentos mais stressantes. Ainda, um obrigado por me ter aceite como seu colega de casa emprestado. Agradeço ainda à Catarina Leoa, pela dose de loucura que consegue sempre animar qualquer um.

Ao Sandro Silva e à Pastora, um obrigado por toda a sabedoria e ensinamentos durante a minha formação académica. Parte do sucesso desta tese também se deve a tudo o que me ensinaram.

Ao André Gaspar, John, Morgan, Guida, João Cardoso, meus grandes companheiros de toda a viagem académica! Obrigado por todas as risadas, noitada, conversas, apoio e amizade ao longo destes anos. Vocês fazem parte da pessoa que me tornei e foram essenciais naqueles dias em que me fizeram esquecer a tese e me transportaram para uma altura em que a universidade significava algo bem diferente de pressões e responsabilidades. Obrigado por tudo seus nabos!

Aos de sempre e para sempre, Linhares, Pedro, Carmen, Maria João, Micas, Ana Filipa, Rafaela, Luís Oliveira e Beatriz, obrigado por toda a amizade e apoio ao longo de todos os anos, pelos cafezinhos e canecas ao fim de semana, e por serem sempre um porto de abrigo! Obrigado por tudo maltinha!!

Ao pessoal da minha banda Gil Pedrosa e Nuno Batista, à grande Serenela Duarte e ao Mafrilaz um grande obrigado por me acompanharem na minha paixão pela música e por todas as grandes noites que passamos e que foram um escape constante do stress da vida real!! Espero que continuem a sentir a música e a vivê-la da melhor maneira.

Agradeço agora ao meu amor, Sara Canário, a pessoa mais importante da minha vida, à minha companheira nesta viagem. Foste a pessoa mais determinante para que conseguisse ultrapassar este momento difícil na minha vida. O teu amor, a tua força e confiança em mim foram sempre uma inspiração, não só para chegar a esta etapa, mas para todos os dias tentar ser a melhor versão de mim possível. Obrigado por todas as lágrimas, sorrisos, dificuldades, e vitórias que partilhamos durante este percurso. És a minha pessoa, o meu abrigo. Amo-te para sempre! Agradeço ainda à minha segunda mãe, a uma grande mulher e melhor sogra do mundo, a dona Manu!! Obrigado por ter sempre uma palavra de apoio e ser um exemplo de força e boa disposição.

Agradeço, por fim às duas pessoas mais importantes para o meu desenvolvimento pessoal e profissional, e que representam tudo aquilo que um dia eu ambiciono ser. Ao meu Pai, Óscar sénior e à minha Mãe, dona Nucha, um obrigado por serem todos os dias uma inspiração e um exemplo de bondade, de profissionalismo, de amor, de cidadania, de carinho, de respeito, de tudo. Não há palavras para descrever o quanto vos admiro e respeito, nem sei como um dia poderia retribuir todo o amor incondicional e confiança que sempre me deram. Peço desculpa pela minha rabugice e estupidez que tantas vezes teve de ser absorvida por vocês. Amo-vos muito, e desejo-vos sempre tudo de bom! UM ENORME OBRIGADO!

Finalmente, agradeço à minha avó, Graciete Guarda pela pureza de espírito, inocência e por ser a pessoa que mais acreditou que eu iria ser capaz. A ela não só agradeço todo o apoio como dedico esta tese.

Obrigado a todos que de uma maneira ou de outra contribuíram para a conclusão desta tese, sem vocês nunca teria terminado esta etapa.

Muito Obrigado!!

ABSTRACT

Pregnancy is a demanding process that requires critical adaptations of the female organism to support the new blooming life growing inside the womb. Several body systems, such as cardiovascular, renal, respiratory, gastrointestinal and endocrine, must undergo crucial physiological modifications, to allocate a healthy fetus development and ensure maternal health and survival. However, due to the extensive set of adaptations that the pregnant women's body undergoes, some pathologies can occur. Gestational Diabetes Mellitus (GDM) is a metabolic disorder with a first onset during pregnancy, which affects 5-10% of the pregnant women, being characterized by an increased insulin resistance and mild hyperglycemia. This could have serious implications to the mother's health, with a 7-fold increased risk of developing type 2 diabetes and cardiovascular diseases (CVD) in the following 5 years. CVD are the major cause of death in the world, accounting for about 50% of all deaths, being also the principle cause of morbidity and fatality in diabetic patients.

The objective of this project was to assess the suitability of physical exercise, as a non-pharmacological therapy for gestational diabetes, to improve maternal cardiac function, by means of increased mitochondria respiratory efficiency and antioxidant defenses, also providing better insulin sensitivity. A secondary objective of this work was to characterize the pregnancy-mediated mitochondrial respiratory adaptations.

We developed a Sprague-Dawley model of GDM, that resulted from the ingestion of a high-fat high-sugar (HFHS) diet, starting at 6 weeks of rodents age and 7 weeks before pregnancy. The controls were fed with normal chow pellets (C). The females were impregnated with 13 weeks of age. The animals were fed with the respective diet during the 3 weeks of pregnancy, the 2.5 weeks of weaning, as well as 5.5 weeks after the weaning. The period of pregnancy coincided with the exercise protocols on an adapted treadmill. The experimental groups are distributed as follows: non-pregnant C_S (n=7); HFHS_S (n=11); HFHS_E (n=6); Pregnant: C_S (n=7); HFHS_S (n=6); HFHS_E (n=6). Mothers (24-weeks-old) were euthanized 5.5 weeks after weaning with a total of 18 weeks in nutrition intervention. Animals were sacrificed according to the guidelines for care and use of laboratory animals in research, advised by the Federation of European Laboratory Animal Science Association. Body weights were measured, and blood glucose levels were evaluated through oral glucose tolerance test. Cardiac mitochondria were isolated and oxygen consumption rate and membrane potential were measured with Clark-type and TPP^+ electrodes, respectively. Expression of fatty acid and mitochondrial biogenesis related genes was measured by qPCR technique. Protein levels of

mitochondrial complexes and ATP synthase, and proteins related to mitochondrial biogenesis, glucose metabolism, mitophagy and inflammation were measured using Western-blot. Data were compared between the experimental groups using the most pertinent statistical test, and $p<0.05$ was considered as statistically significant, and $p<0.1$ as statistical tendency.

The ingestion of an HFHS diet isolated or in combination with exercise induce alteration in cardiac mitochondrial respiratory states, leading to decreased respiratory control ratio, ADP/O ratio, and maximum oxygen consumption rate, with effect specially in complex I and in non-pregnant groups. Also, it led to increased state 2 and state 4 which together with the previous results suggest that the experimental treatments led to mitochondrial uncoupling. Moreover, it decreased the expression of complex III subunit UQCRC2, which may lead to deficient assembly of the respirasome (CI/CIII/CIV), thus explaining the predominance of alterations related to complex I. Regarding pregnancy, it was observed an apparent protective effect against the effects of the HFHS diet combined with exercise, suggesting that pregnancy induces cardiac mitochondrial adaptations in order the better cope with the challenges of pregnancy.

In conclusion, exercise was not able to improve cardiac mitochondria respiratory efficiency of the animals that exhibited GDM hallmarks, even exacerbating the effects of the HFHS diet. It is possible the intensity or the time-window of the exercise may be an explanation for the absence of the known positive effects of exercise. Moreover, pregnancy by itself can act as a modulatory agent of the cardiac mitochondrial function. Further studies exploiting different approaches on exercise and better characterization of the pregnancy mediated cardiac mitochondrial alteration may provide a better medical care and improve pregnancy outcome.

Keywords: Gestational diabetes mellitus, cardiovascular diseases, high-fat-high-sugar diet, physical exercise, mitochondrial dysfunction.

RESUMO

A gravidez é um processo altamente exigente para o organismo feminino, que necessita fazer adaptações críticas para suportar a formação e o desenvolvimento de uma nova vida no seu ventre. Vários sistemas, cardiovascular, renal, respiratório, gastrointestinal e endócrino, têm que realizar alterações fisiológicas cruciais para um desenvolvimento fetal saudável, e para que a mãe sobreviva ao processo gestacional. No entanto, por vezes, as adaptações podem ser demasiado exigentes, podendo levar ao aparecimento de certas patologias. A Diabetes Mellitus Gestacional (DMG) é um distúrbio metabólico, sendo diagnosticado apenas durante a gestação, e que afeta 5-10% das gravidezes, sendo caracterizado por um aumento da resistência à insulina e por uma hiperglicemia moderada. Esta emergente doença pode implicar graves consequências para a saúde materna, sendo que aumenta em 7 vezes a probabilidade de nos 5 anos após a gravidez, uma mãe que teve DMG desenvolva diabetes do tipo 2 e/ou doença cardiovascular. As doenças cardiovasculares são a principal causa de morte a nível mundial, sendo responsáveis por 50% do total de mortes. São também a principal causa de morte em pacientes com diabetes.

O objetivo deste projeto foi avaliar a adequabilidade do exercício físico, como terapia não-farmacológica, para tratar a DMG, melhorando a função cardíaca materna através do aumento da eficiência respiratória mitocondrial, do aumento da defesa antioxidante, e ainda proporcionando uma melhor sensibilidade à insulina. Um objetivo secundário deste projeto foi caracterizar as alterações da função mitocondrial promovidas pela gravidez.

Foi desenvolvido um modelo de DGM em Sprague-Dawley, que resultou da ingestão de uma dieta rica em açucares e gorduras (HFHS), a partir de 7 semanas antes da gravidez. Os animais controlo com uma dieta standard. As fêmeas foram impregnadas às 13 semanas de vida. Os animais foram alimentados com as respetivas dietas durante as 3 semanas de gravidez, as 2.5 semanas de amamentação, assim como durante as 5.5 semanas após esse período. O período de gravidez coincidiu com o protocolo de exercício, realizado numa passadeira adaptada. Os grupos experimentais ficaram então distribuídos assim: Não-grávidas: C_S (n=7); HFHS_S (n=11); HFHS_E (n=6); Grávidas: C_S (n=7); HFHS_S (n=6); HFHS_E (n=6). As mães (24 semanas de idade) foram sacrificadas 5.5 semanas após o fim da amamentação tendo ficado com um total de 18 semanas de tratamento com a dieta. O sacrifício ocorreu de acordo com as normas estipuladas pela Federation of European Laboratory Animal Science Association. O peso corporal foi medido, assim como os níveis sanguíneos de glucose através do teste oral de tolerância à glucose. As mitocôndrias cardíacas foram isoladas e a taxa de consumo de oxigénio e o potencial membranar foram medidos com elétrodos tipo-Clark e TPP^+. A expressão de genes

relacionados com o metabolismo de lípidos e com a biogénese mitocondrial foram medidos através da técnica de qPCR. O nível de proteínas dos complexos mitocondriais, da ATP sintase, de biogénese mitocondrial, do metabolismo de glucose, mitofagia, e inflamação, foram avaliados através da técnica de Western-Blot. Os dados foram comparados entre os diferentes grupos e foram tratados usando o teste estatístico mais pertinente. $p<0.05$ foi considerado como diferença estatística, e $p<0.1$ como tendência.

O consumo de uma dieta HFHS, quando isolada, ou combinada com exercício induziu alterações nos estados respiratórios das mitocôndrias cardíacas, levando a uma diminuição no RCR, no ADP/O, e no consumo máximo de oxigénio, com efeito especialmente quando foram usados substratos para o complexo I e nos grupos não-grávidos. Mais ainda, causou o aumento do estado 2 e 4 que em conjunto com os resultados anteriores sugerem que os tratamentos experimentais levaram a um desacoplamento mitocondrial. Continuando, a dieta HFHS combinada com exercício causou a diminuição da expressão da subunidade UQCRC2 do complexo III, que pode levar a uma montagem deficiente do respirassoma (CI/CIII/CIV). Em relação à gravidez, foi observado um aparente efeito protetor, sugerindo que pode induzir adaptações a nível das mitocôndrias cardíacas para que estas estejam melhor preparadas para lidar com os desafios da gravidez.

Em conclusão, o exercício não foi capaz de melhorar a eficiência respiratória mitocondrial cardíaca dos animais que mostraram sinais de DMG, pelo contrário, atuou aumento os efeitos já observados pela dieta HFHS. É possível que a intensidade ou a janela de tempo do exercício possa ser uma explicação para a ausência dos efeitos benéficos que já se sabe que o exercício pode ter. Mais, a gravidez por si só pode atuar como um agente modelador da função cardíaca mitocondrial. Estudos futuros explorando diferentes abordagens de exercício e uma melhor caracterização dos efeitos mediados pela gravidez poderão levar a um melhor cuidado/acompanhamento médico, assim como aumentar o sucesso da gravidez.

Palavras-Chave: Diabetes Mellitus gestacional, doenças cardiovasculares, dieta rica em açucares e gorduras, exercício físico, disfunção mitocondrial.

TABLE OF CONTENTS

LIST OF FIGURES

LIST OF TABLES

LIST OF ABBREVIATURES AND ACRONYMS

ACAA2	Acetyl-CoA Acyltransferase 2
ACC	Acetyl-CoA Carboxylase
ACOX1	Acyl-CoA Oxidase 1
ADP	Adenosine Diphosphate
AGE	Advanced Glycation End-product
AMP	Adenosine Monophosphate
ATP	Adenosine Triphosphate
ATP5A	ATP Synthase F1 subunit Alpha
BMI	Body Mass Index
BSA	Bovine Serum Albumin
C	Control diet
CAT	Carnitine Acyltransferase
CPT-2	Carnitine Palmitoyltransferase 2
CPT1	Carnitine Palmitoyltransferase 1
CVD	Cardiovascular Diseases
Cyt-c	Cytochrome C
DMSO	Dimethyl sulfoxide
DOX	Doxorubicin
Drp1	Dynamin related Protein 1
ETC	Electron Transport Chain
F-1,6-B	Fructose-1,6-Biphosphate
F-6-P	Fructose-6-Phosphate
FA	Fatty Acids
FABP	Fatty Acid Binding Protein
$FADH_2$	Reduced Flavin Adenine Dinucleotide
FAT	Fatty Acid Transporter
FCCP	Carbonyl Cyanide-4-(trifluoromethoxy)phenylhydrazone
FELASA	Federation for European Laboratory Animals Science Associations
FFAs	Free Fatty Acids
Fis1	Mitochondrial Fission Protein 1
FMN	Flavin Mononucleotide
G-3-P	Glyceraldehyde-3-Phosphate

G-6-P	Glucose-6-Phosphate
G/M	Glutamate/Malate
GAPDH	Glyceraldehyde-3-Phosphate Dehydrogenase
GDM	Gestational Diabetes Mellitus
GDP	Guanosine Diphosphate
GLUT	Glucose Transporter
GSH	Reduced Glutathione
GTP	Guanosine Triphosphate
HFHS	High-Fat High-Sugar diet
HIB	Heart Isolation Buffer
HIB+	Heart Isolation Buffer supplemented with BSA
HIF1	Hypoxia Inducible Factor
HRB	Heart Reaction Buffer
HRP	Horseradish Peroxidase
HWB	Heart Washing Buffer
IL-6	Interleukin 6
IRS-1	Insulin Receptor Substrate 1
KGDH	Alpha-Ketoglutarate Dehydrogenase
LDHB	Lactate Dehydrogenase B
LDHD	Lactate Dehydrogenase D
LVH	Left Ventricle Hypertrophy
MAP	Mean Arterial Blood Pressure
MCD	Malonyl-CoA Decarboxylase
MCT-1	Monocarboxylic Acid Transporter 1
MDA	Malondialdehyde
Mfn1	Mitofusin 1
Mfn2	Mitofusin 2
MTCO2	Mitochondrially Encoded Cytochrome C Oxidase 2
mtDNA	Mitochondrial DNA
NADH	Reduced Nicotinamide Adenine Dinucleotide
nDNA	Nuclear DNA
NDUFB8	NADH:Ubiquinone Oxidoreductase subunit B8
NP	Non-pregnant
NRT	No Reverse Transcriptase Control

NTC	Non-Template Control
OCR	Oxygen Consumption Rate
OGTT	Oral Glucose Tolerance Test
Opa1	Optic Atrophy 1
OXPHOS	Oxidative Phosphorylation
P	Pregnant
PBS	Phosphate Buffered Saline
PDH	Pyruvate Dehydrogenase
PDK4	Pyruvate Dehydrogenase Kinase 4
PE	Physical Exercise
PGC1-α	Peroxisome Proliferator-activated Receptor 1α
pGDM	Previous Gestational Diabetes Mellitus pregnancy
P_i	Inorganic Phosphate
PKC	Protein Kinase C
POLmt	Mitochondrial RNA Polymerase
PPARα	Peroxisome Proliferator-Activated Receptor alpha
PVDF	Polyvinylidene Fluoride
qPCR	Real-time Polymerase Chain Reaction or Quantitative PCR
RCR	Respiratory Control Ratio
ROS	Reactive Oxygen Species
RT	Room Temperature
RT-PCR	Reverse-Transcription PCR
S	Sedentary
SCE	Saturated Calomel Electrode
SDHB	Succinate Dehydrogenase B
SDS	Sodium Dodecyl Sulfate
SOD	Superoxide Dismutase
T2D	Type 2 Diabetes
TBP	TATA-box Binding Protein
TBS	Tris-buffered Saline with Tween20
TCA cycle	Tricarboxylic Acid Cycle
mTFA	Mitochondrial Transcription Factor A
TNF-α	Tumor Necrosis Factor Alpha

TnnT2	Cardiac Type Troponin T2
Tom20	Translocase of Outer Mitochondrial Membrane 20
TPP^+	Tetraphenylphosphonium$^+$
UCPs	Mitochondrial Uncoupling Proteins
UCP2	Mitochondrial Uncoupling Protein 2
UQCRC2	Ubiquinol-Cytochrome C Reductase Core Protein 2
VDAC2	Voltage-dependent Anion Channel 2
VPA	Voluntary Physical Activity
WB	Western Blot
WHO	World Health Organization

CHAPTER 1 - INTRODUCTION

1.1. Maternal Physiological Adaptations to Pregnancy

During pregnancy, the women undergoes major adaptations in order to cope with the physical and metabolic demands of growing a new life inside the womb. This occurs so that the maternal organism is able to endure the necessary requirements to survive from conception until delivery, and also support a healthy and safe development for the fetus. Cardiovascular, respiratory, endocrine, renal and gastrointestinal systems, all sustain vital physiological adaptations[1]. Also, morphologically, the women body suffers a transformation, so it can carry the extra weight gained, not only from the baby, but also from tissue growth and fat accumulation[2].

1.1.1. Cardiovascular and Hemodynamic Adaptations

The cardiovascular system is responsible for pumping a continuous blood flow through the vessels, allowing whole-body communication, nutrient supply, gas exchanges, toxins removal, immune system defense, and others[3,4]. During gestation, this system will be overloaded to support the mother and the fetus development. The cardiac output rise from 4.6 L/min to 8.7 L/min during pregnancy [5]. This represents an increase of almost 50% in behalf of 15-20 higher heart rate, and 20-30% augmented stroke volume[5]. The mean arterial blood pressure (MAP), essential to a proper perfusion of the organs, is related with the cardiac output and the systemic vascular resistance. As the cardiac output increases during pregnancy, it would be expected that arterial pressure would spike. However, it minimally drops. This happens because during pregnancy estrogen stimulates the production of nitric oxide, responsible for reducing vascular resistance, allowing a minor decline in MAP[6,7]. Increased cardiac output is essential since the placenta and uterus require 25% more blood flow which is vital for fetus development[1]. Also, kidneys, breasts, and skin demand a greater blood influx. This series of alterations allow the

maternal organism to endure with the increasing basal oxygen consumption[8]. In order to sustain the increased blood flow the maternal heart undergoes structural alterations during gestation, such as increased ventricle muscle mass and contractility, becoming thicker, and also with larger valvular annular diameters[9].This allows the ejection of a larger volume of blood to achieve the needed requirements [9].

It is important to understand these physiological alterations during childbearing in order to accurately diagnose a certain cardiovascular pathology. Otherwise, physiological modifications could be misunderstood and lead to unnecessary treatment, or even camouflage an underlying disease[10]. Even with this knowledge, physicians often have trouble identifying an impending shock due to illness. For example, as women have a 30% increase in blood volume, they can lose up to 1500 mL before showing any clinical signs[10]. For instance, a common method is to monitor fetal distress and heart rate because it is remarkably sensitive to any alterations in maternal state and may hint about maternal cardiovascular health[10].

In this context, the cardiovascular system is susceptible to an intensive amount of stress during gestation, sustaining profound alterations in order to successfully cope with pregnancy demands, without developing a cardiovascular inefficiency.

1.2. Gestational Diabetes Mellitus

Gestational Diabetes Mellitus (GDM) is the most common disease during pregnancy, affecting 5-10% of pregnant women. Diagnosed in the 2nd or 3rd trimester of gestation, this condition has its first onset during pregnancy, and it is characterized by a state of glucose intolerance[11]. The diagnostics may be performed in two distinct phases: in the first pre-natal medical appointment, the plasma glucose levels are measured. If higher or equal than 92 mg/dL and lower than 126 mg/dL, the pregnant woman is diagnosed with GDM. A higher value of 126 mg/dL, or an occasional glycemic plasma level over 200 mg/dL, could lean towards the presence of diabetes

before the pregnancy, which excludes GDM. In case of a value lower than 92 mg/dl value, a second trial is required. This consists in an Oral Glucose Tolerance Test (OGTT), performed between the 24th and 28th weeks of pregnancy, comprising the intake of an overload dose of glucose, after 8 to 14 h of fasting, through the ingestion of 75 g of glucose diluted in 300 mL of water. After this, the levels of glucose are measured at 3 different time points: 0, 1, and 2 hours post ingestion. A positive GDM diagnose is achieved when one or more values are higher than the following reference values: 0 h ≥ 92 mg/dL; 1 h ≥180 mg/dL; 2 h≥153 mg/dL[12].

Gestational diabetes mellitus rose from 2.9% to 8.8%, in the last 20 years, which may be related with an increase in overweight and obese people who also get pregnant[13], since those conditions have already been appointed as major risk factor for the development of GDM[14]. In fact, the incidence of obesity has nearly tripled since 1975[15]. Overweight and obesity were defined by the World Health Organization (WHO) as an abnormal or excessive fat accumulation that may impair health[15]. The classification and stratification to classify the overweight sever according to a person's weight is attributed by using the Body Mass Index (BMI), which correlates the person's height and weight of a person, being defined by person's weight in kilograms divided by the square of its height in meters. The result is a score that allows to group the populations in categories. The overweight state is defined by a BMI score greater than or equal to 25, while obesity is defined by a BMI score greater than or equal to 30. These values are used for adults, however, different thresholds are considered, for different aged groups[15]. Concerning data report that in the US 60% of the women in the beginning of pregnancy are overweight, and from those 30% are already obese[13]. Other risk factors have also been considered such as family history of diabetes, lifestyle during and before pregnancy, previous GDM in another pregnancy, or the family origins[14].

In our perspective, it is important to highlight lifestyle and diet induced obesity, because they have been suggested as the root of the recent increase in the incidence of the disease and also because these risk factors can be manipulated during an experimental setup to test their effect.

1.2.1. Gestational Diabetes Mellitus Pathophysiology

As mentioned before, the metabolic alterations in the female body to accommodate the pregnancy can result in the development of pathology, which is the case of GDM. The mechanism accepted for the development of GDM is centered in abnormal insulin sensitivity and impaired glucose homeostasis[13]. During pregnancy, it is expected that a mild loss in insulin sensitivity occurs, decreasing cellular glucose intake, elevating its blood level, in such a way that availability to deliver nutrients to the fetus while resourcing the mothers' organism is optimal[16]. One possible explanation relies on increasing progesterone levels that accompanies pregnancy[16]. This hormone can suppress the expression of Insulin Receptor Substrate-I (IRS-I), which is essential for signal transduction when insulin binds to its receptor. Decreased IRS-I expression disrupts insulin signaling, causing insulin insensitivity, thus resistance[16]. Further, estrogen elevated levels during pregnancy can also diminish the sensitivity to insulin[16]. However, if the pregnant woman presents one or more risk factors, the insulin resistance that normally would have a physiological role, can surpass that level and become detrimental for the organism[13]. In this scenario, the insulin biological action is ineffective, the blood sugar level spikes, and this abnormal blood sugar accumulation will cause beta-pancreatic cells disfunction in terms of insulin production, leading to the development of GDM [1].

1.2.2. Short- and Long-Term Implications of Gestational Diabetes Mellitus

The GDM pathology could have serious implications both in the mother and the fetus. As described before, an insulin resistance state occurs during GDM. This leads to a reduced uptake

of glucose in tissues, and consequently to its accumulation in the blood. The high glucose levels in the blood will stimulate the pancreatic beta-cells to secrete more insulin, however in an inefficient amount, being incapable of overcoming the insulin resistance developed[17]. The placenta is one of the most important tissues formed during gestation, being the main interface between mother and fetus. Research studies have demonstrated that factors secreted by the placenta, such as adipokines, could be an underlying mechanism for the development of GDM, instigating augmented insulin resistance[18]. Despite this putative signaling function, one of the major placental roles is to provide a barrier between maternal and fetal circulation, allowing a selective permeability. Regarding the permeability to glucose and insulin, the placenta allows supply of glucose to the fetal blood, however it blocks the passage of insulin[19]. This results in increased supply of glucose, due to maternal blood hyperglycemia, to which the fetal organism is not prepared to cope, causing a series of short and long-term complications[13,17,19]. In the short-term, the fetus may develop increased body weight, waist circumference and fat accumulation, resulting in macrosomia, respiratory distress, birth trauma and cardiac malformations, among others[19–21]. Additionally, the exposure to an adverse environment in the womb, can implicate a series of long-term consequences, highly associated with metabolic disorders, such as obesity, type 2 diabetes (T2D), insulin resistance, fatty liver disease, and cardiovascular diseases (CVD)[21].

Concerning the mother, GDM has known short-term implications, increasing the risks of complications during pregnancy, such as premature birth, caesarean section, polyhydramnios, hypertensive disorders, such as preeclampsia, delivery complications due to macrosomic babies and in rare cases, baby loss[13,17,18,22]. Regarding long-term implications, women with previous GDM (pGDM) becomes more predisposed to develop a series of complications that highly increase the risk of developing CVD[23], such as atherogenic lipid profile, tendency to obesity, increased blood pressure and increased inflammatory markers, and decreased endothelial

function[24]. Several studies show that 5-20 years after delivery, the risk of developing T2D increases 7 times in pGDM women comparing with non-diabetic pregnancies[25]. Additionally, in the following 4 years postpartum, the spectrum of glucose intolerance is predominant in pGDM women, with increased insulin resistance and abnormal insulin secretion[24]. Moreover, in pGDM women, the risk of developing metabolic syndrome, a condition defined by high blood sugar and lipids level, a large waist circumference and insulin resistance, increases by 3-fold in the 9 years after birth[26]. This long-term postpartum predisposition to a series of GDM-related pathologies, causes a major distress to the cardiovascular system, in such a way that eventually the heart and vessels will be pushed far from their adaptation capacity, becoming dysfunctional and susceptible to CVD, which may result in death.

1.3. Cardiovascular Diseases

Cardiovascular diseases are the most prevalent cause of death worldwide, with more than 17 million deaths registered every year, according with World Health Organization[27]. With over 4 million deaths, CVD is accountable for 50% of all deaths in worldwide[28], with an epidemic rate that keeps accelerating[29], urging the need to better understand the mechanisms underlying this disease[30].

Cardiovascular diseases are a class of diseases that affects the heart and blood vessels[29], namely coronary heart disease, stroke, heart failure, hypertensive heart disease, cardiomyopathy, arrhythmia, and congenital heart disease. This kind of conditions are most of the times associated with risk factors such as gender, ethnicity, socioeconomic status, genetic predisposition, age, tobacco and alcohol consumption, diet, stress, hypertension, sedentarism, being overweight or obese, among others[31–33]. Although there are a panoply of factors, most of them are associated with lifestyles, and this has been appointed as a crucial element to prevent the development of CVD[34]. Evidences, of this lifestyle-mediated influence, are persistence of

behaviors such as tobacco and alcohol consumption, the increase in high-caloric diets with predominance of saturated fats, salt and refined carbohydrates and, the continuous increase in sedentarism with concomitant decline in physical activity. All these factors had been associated with a high morbidity of cardiovascular diseases, and contributing to the constant increasing proportion of death registered every year[35]. Although every factor has an impact in increasing CVD risk, some authors propose that diet intervention could be the upmost key factor to reduce the occurrence of cardiovascular events[36].

1.4. Heart Disease – The Diabetes Burden

Cardiovascular diseases are the dominant cause for morbidity and fatality for patients with Type 2 Diabetes[37,38]. T2D is a disease that affects about 415 million people in the world, although its estimated that millions are still not diagnosed[38]. This metabolic disorder results of inefficient insulin secretion in pancreatic β-cell and insulin resistance, being characterized by high circulating levels of blood sugar[38]. In spite of genetic predisposition to obesity and/or insulin resistance, it is generally accepted that the primary contributors for this global rise, is an excess of saturated fat and high-sugar diets, with high calorie intake, and a sedentary lifestyle[39]. Those factors have been boosting the incidence of T2D to alarming epidemic levels, which increases the need and impact of new studies and findings to improve the prevention and management of the disease. Although the principal characteristic of T2D is high levels of blood sugar, or hyperglycemia, this is a weak predictor when associated to the promotion of CVD[40]. However, moderate to severe insulin resistance is a better predictor of an increased risk of CVD, being also associated with obesity, dyslipidemia, hypertension, endothelial dysfunction and procoagulant state[40]. This implies that even if a patient has a healthy heart and vessels, T2D will rise the chances of cardiovascular deterioration, which will lead on to the development of cardiomyopathy (group of diseases that strike the heart muscle)[41].

1.4.1. Diabetic Cardiomyopathy

The mechanisms involved in the pathophysiology of diabetic cardiomyopathy are somewhat understood, however this is a multifactorial condition[42] (

Figure 1). The most accepted hypotheses are the ones that are focused in mechanisms that reduce ventricular contractibility in response to T2D, such as impaired calcium homeostasis and increment of oxidative stress[42]. It is widely accepted that Fatty Acids (FA) are the prime substrate used by the adult heart, however the cardiac metabolic network is extraordinarily adjustable, being able to switch the substrates preferences in function of substrate availability, or due to a conditioning caused by a pathology[43]. In the case of metabolic cardiomyopathy associated with diabetes or obesity, despite a state of hyperglycemia, glucose transporters expression and glucose uptake in the heart tissue are reduced, due to impaired insulin signaling[41–43]. Contrasting, increased influx of FAs to the mitochondria and subsequent overreliance on β-oxidation implies a higher oxygen requirement that can become damaging to cardiomyocytes, since it leads to incomplete oxidation of FAs and consequent production of its by-products, uncoupling of the mitochondrial respiratory chain, alterations in the internal mitochondria membrane lipid composition, and excessive ROS production[39,42,43]. Those factors could lead to a status of mitochondrial dysfunction, with decreased bioenergetics efficiency, increased reactive oxygen species (ROS) production, altered gene regulation and unbalanced calcium homeostasis, resulting in mitochondrial damage with progressive bioenergetic decline that finally could impair cardiac function, promoting the development of CVD[43,44].

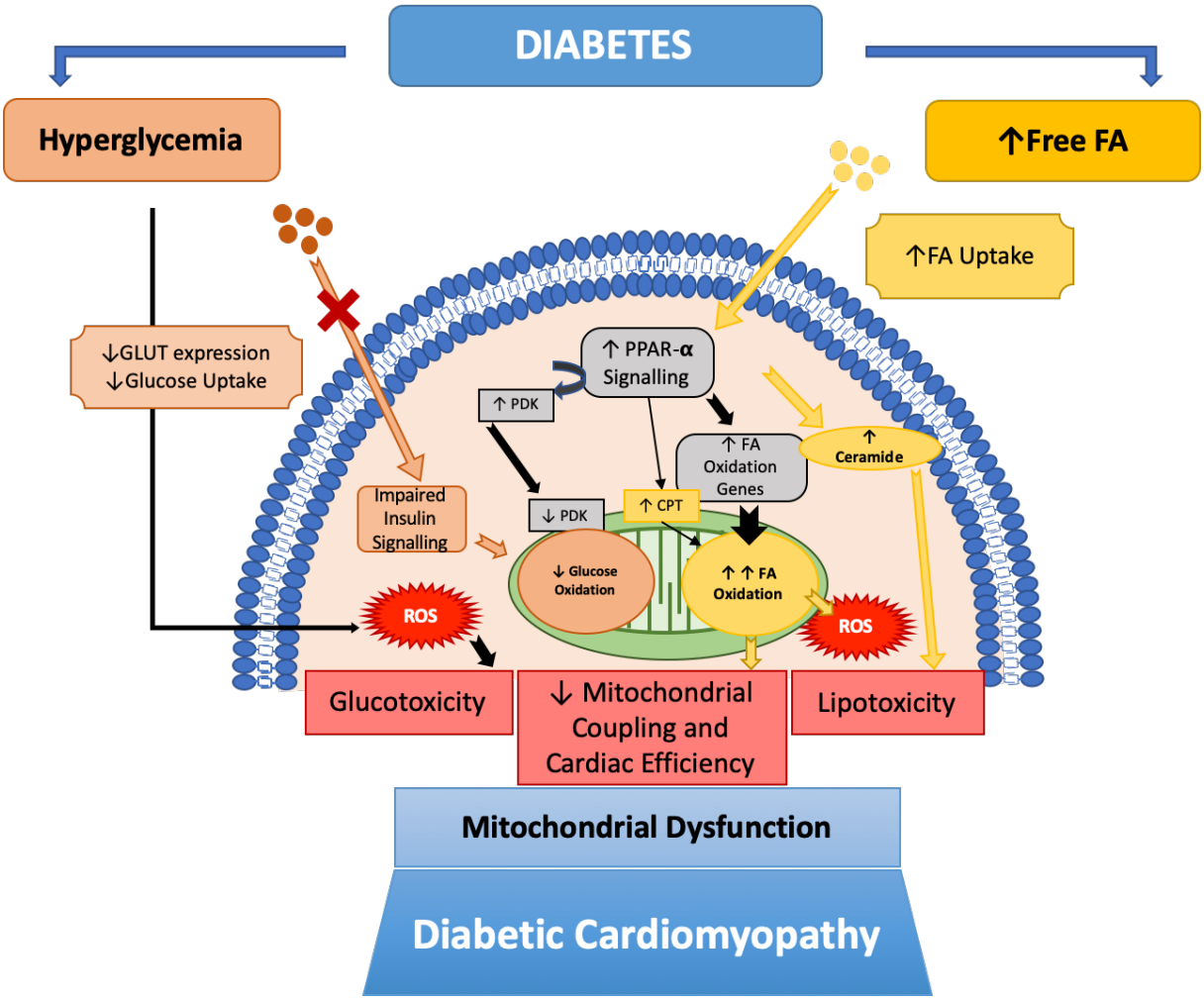

Figure 1. ***Schematic representation of the proposed mechanisms that lead to cardiac dysfunction, in a diabetic cardiomyopathic state.*** *Figure adapted from Boudina, S. & Abel, E. D Diabetic cardiomyopathy revisited (2007)* [42].

1.4.2. Diabetes Management and CVD Risk Decline

It is important to manage diabetes in order to eliminate symptoms that would decrease life quality and to prevent the development of future complications. The first line of approach includes lifestyle interventions such as healthy eating or increase physical activity. However, in many cases this line of action does not achieve the intended results due to the lack of compliance with the clinical guidelines, a challenging topic, and a pharmacological treatment arise as an alternative approach.

The most common pharmacological approach to treat diabetes includes agents that can help regulate glucose homeostasis, or the injection of insulin, in order to overcome the deficient pancreatic cells production. One of the most widely used antihyperglycemic pharmacological agent to treat T2D is Metformin. Although its mechanisms are not fully understood, it has been reported that this pharmaceutical agent increases AMP/ATP and ADP/ATP ratios, in such way that interacts with several pathways leading to an improvement of glycemic control[45]. However, this is not the only known agent, belonging to a larger group of oral antihyperglycemic and hypoglycemic agents, which are used to control glucose homeostasis. Besides Metformin, there are other classes of agents, such as Sulfonylureas, that enhance insulin secretion, Glyburide, a second generation sulfonylurea-class compound, Glimepiride, that increases insulin secretion, whole-body glucose uptake, and insulin sensitivity, Thiazolidinediones, a pharmacological alternative to insulin therapy, and finally Alpha-glucosidase inhibitor, that slows the carbohydrates absorption in the bowel[46]. Other alternative therapies include insulin therapy and analogues, in which occurs direct administration of insulin or an analogue, aiming to mimic a normal physiological secretion of nondiabetic pregnancies[46]. In cases of GDM, insulin is considered the prime pharmacological therapy for glycemic control, being supported by the Federal Drug Association, the American Diabetes Association, and the American College of Obstetricians and Gynaecologists[46]. Glyburide and Metformin have also been used with efficiency to manage hyperglycemia in GDM[46], however both of these drugs can cross the placenta and interact with the fetus, although no short-term impairments have been reported[47]. It is well known that most drugs taken by the mother will cause fetal exposure, besides placental ability to limit this interaction[47]. Regarding GDM, it is not known whether the administration of insulin, glyburide or metformin could somehow alter fetal development and, if so, cause long-term impairments caused by intrauterine exposure to antihyperglycemic drugs[47]. Nevertheless, recent studies performed with metformin have showed that there is little evidence

suggesting any short-term harmful effect for the fetus, however with a putative harmful effect at long-term, due to intrauterine fetal exposure. These evidences combined with its cheapness and effectiveness in blood glucose levels management has led to a recent increase in the usage of this drug, replacing the preference for insulin treatment[48–50].

Albeit successful pharmacological management of glycemic level during GDM, this is not considered as a first-line therapy, being non-pharmacological therapies the first measures to counteract GDM[46].

Ideally, non-pharmacological interventions would always be the first strategy to reduce the impact of GDM. In few cases, non-pharmacological interventions reverse some of GDM outputs, greatly diminishing the risk of developing CVD[46,47,51]. Alterations and adaptations in lifestyles can mitigate diabetic symptoms and consequences[52], being the less invasive therapy for the organism. Diabetes self-management programs provide the base to assist patients to perform better choices of lifestyle, by a process of learning new skills and habits, allowing a person with diabetes to make daily self-management decisions[53]. This is a claim of the American Diabetes Association, that defends that every patient diagnosed should receive the tools to perform self-management, without using drugs, improving the patient care, health, knowledge, and reducing expenses[53]. Dietary adaptations are already a well-established lifestyle alteration that highly contributes to the management of GDM, being the first measure to counter the disease[53]. One emerging strategy to overcome the effects of diabetes and to prevent further complications, such as CVD, is physical exercise (PE), which is a non-pharmacological method, that has already been described as cardio protective, and as a vital part of healthy lifestyle in non-pregnant subjects[54]. However, the relevant mechanisms, the impact and potential of exercise to reduce insulin resistance on GDM pregnancies and prevent harmful outcomes remains poorly understood.

1.5. Cardiac Dysfunction and Metabolism

There is a large variety of mechanisms suggested as the underlying origin for cardiac dysfunction, such as oxidative stress, inflammation, atherosclerosis or endothelial dysfunction[24]. It is important to keep in mind that the heart is an extremally oxidizing organ, that incessantly pumps blood through the body, which implies a huge energy requirement. If this metabolic supply gets diminished, the heart will lose its efficiency, leading to the development of disease[44]. However, this may not have been caused by a reduction in substrates availability, but instead to a variation in their abundance, such as in a state of exercise, in which the heart intake and oxidation of lactate becomes predominant, although the availability of FAs is not reduced [43]. Also during fasting or ketogenic diets, the abundance of ketone bodies in the blood flow increases, and so the heart starts to oxidize them for energy production[43]. Regarding pathological hypertrophy of the left ventricle (LVH**),** cardiomyocytes rely on glucose metabolism and decrease FA oxidation, the regular main source of ATP, in order to cope with the diminished amount of oxygen that is able to reach the cardiac hypertrophic muscle[55]. The switch from FAs to glucose metabolism will improve the efficiency of ATP production, since carbohydrates have approximately a 30% higher efficiency of ATP produced per mole of O_2, comparing with FA oxidation[56]. This means that the oxidation of glucose molecules requires less oxygen, which is itself an advantage, since the cardiac muscle cannot oxygenate properly. However if glucose metabolism becomes predominant, the overall ATP synthesis by oxidation will decrease, and lead to a state of "Glucotoxicity"[57]. Contrarily, in the cardiac dysfunction in obesity and diabetes, as aforementioned, FA uptake and its oxidation are increased, and glucose oxidation is reduced. However this metabolic profile has been associated with increased cardiac oxygen consumption, reduced efficiency and increased oxidative stress, suggesting that an increase in the rate of FA oxidation could be harmful and impair cardiac function, since it leads

to a state of fragility of the cardiomyocytes, and a high risk of developing cardiovascular disease[43].

1.5.1. Mitochondria - the Heart of Energy

In cardiac muscle cells, mitochondria represent one third of the cell volume, suggesting the importance of their processes for proper cardiac myocyte function[43]. Mitochondria are responsible for the generation of at least 95% of the ATP consumed by the heart, but also, those organelles regulate intracellular calcium homeostasis, ROS production, signaling pathways, and cell apoptosis[43]. Thus, in several cases of heart pathologies, it is accurate to refer that perturbations in mitochondrial balance, energy production and propagation could be the underlying cause for disease[44]. Mitochondrial dysfunction can result from distinct factors, including ageing, genetics, inflammation, sugar and processed foods consumption, sedentary lifestyle, environmental toxins or radiation, sleep deprivation, stress, among others[58]. Interestingly, some of these factors are also correlated with increased risk of CVD, which reinforce the tight relation between mitochondrial function and cardiac pathologies[34,58]. The mechanisms that lead to damaged mitochondria include mutations in the expression of mitochondrial proteins, either from mitochondrial DNA (mtDNA) or nuclear DNA (nDNA), and acquired defects in mitochondrial quality control, which cause defective mitochondrial dynamics, mitophagy and protein turnover, inducing a vicious cycle of more acquired mitochondrial defects including altered metabolic signaling, defective bioenergetics, defective calcium homeostasis, cell death pathways, and augmented ROS production, that ultimately could promote cardiomyocyte death and cardiac dysfunction[44].

1.5.2. Cardiac Mitochondrial Metabolism

Although cardiac cells are tremendously oxidative, with high energetic demands, the cellular content in ATP is very low[59]. This is explained by a high rate of ATP formation and a high rate of ATP consumption, that results in myocardial ATP pool turnover of just 10 seconds. To maintain this accelerated pace, the heart relies on several sources of carbon, namely FAs or glucose, to generate ATP, being the firsts responsible for 50-70% of the energy produced[59].

FAs circulate in plasma associated with albumin, contained in chylomicron-triacylglycerol, or contained in very-low-density lipoproteins-triacylglycerol. While some FAs can cross myocardial membrane freely, the great majority requires membrane transporters, as tissue specific FA carriers, CD36/FA Transporter (FAT) and FA Binding Protein (FABP)[59,60]. Once inside myocardial cells, FA undergo a catabolic pathway known as β-Oxidation. This process consists in breaking down FAs' chains, generating metabolites that can follow oxidative phosphorylation in the mitochondria, such as acetyl-CoA, NADH and $FADH_2$. Once FA are inside the cell, the enzyme Fatty Acyl CoA Synthetase adds one CoA molecule to the FA chain, becoming Fatty Acyl CoA, which is a mitochondrial-permeable form. Carnitine palmitoyltransferase 1 (CPT-1) is the key enzyme for mitochondrial internalization of FA, because it is responsible for their transfer. This enzyme catalyzes the formation of acyl-carnitine, which is transported to the mitochondrial matrix through Carnitine Acyltransferase (CAT). There, Carnitine palmitoyltransferase 2 (CPT-2) converts acyl-carnitine back to fatty acyl-CoA, that can undergo β-Oxidation[60]. The regulation of this process is performed by malonyl-CoA, since it inhibits CPT-1, the first enzyme in this transport, therefore, a regulator of FA oxidation, in the mitochondria[59,60]. It has been reported that in cases of diabetic cardiomyopathy, the inhibition of Malonyl-CoA Dehydrogenase, responsible for converting malonyl-CoA to acetyl-CoA, can improve cardiac function, since accumulation of malonyl-

CoA inhibits FA metabolism, stimulates glucose metabolism, and reverts the diabetic cardiomyopathic state[61,62]. Once inside mitochondria, β-Oxidation cycles breakdown Fatty Acyl-CoA chain through a series of oxidations, that ultimately will produce one molecule of acetyl-CoA, one of NADH, and one reduced $FADH_2$ co-factor for each cycle. Full oxidation of FA not only produces NADH and $FADH_2$ that can directly provide electrons to the electron transport chain (ETC), but also, the acetyl-CoA generated can enter the TCA cycle, generating more NADH and succinate[60]. For example, palmitic acid, a 16-carbon saturated fatty acid, when fully oxidized, results in the production of 8 Acetyl-CoA, 7 NADH and 7 reduced $FADH_2$ factors, that are equivalent to a net of 106 ATP molecules (considering that NADH = 2.5 ATP and $FADH_2$ = 1.5 ATP)[63].

In a cardiac healthy state, FA are the preferred source of energy since they can generate a larger amount of ATP just from a single molecule, which constitutes a tremendous advantage for an organ that requires constant ATP supply[43,59].

Carbohydrates, such as glucose or lactate, also play a very important role in cardiac metabolism, being the second most used substrate[64]. Lactate metabolism is dependent of its uptake, that is facilitated by a monocarboxylic acid transporter-1 (MCT-1)[65]. When inside the myocytes, lactate is conversed to pyruvate by lactate dehydrogenase, and then pyruvate can enter the Krebs cycle (or tricarboxylic acid cycle, TCA) as acetyl-CoA, in a reaction catalyzed by pyruvate dehydrogenase[65,66].

Glucose metabolism depends on the blood glucose levels and on the presence of specific transporters in the plasma membrane, namely glucose transporters type 1 and 4 (GLUT1 and GLUT4), that translocate glucose from the blood to the cytosol by facilitated diffusion[64]. The fusion of GLUT4 containing vesicles with the plasmatic membrane is dependent of insulin signaling, however GLUT1 action is independent of insulin signalling[67]. The capacity of the

cardiomyocytes to uptake glucose is directly dependent of the quantity of glucose transporters in the plasma membrane[64]. After glucose uptake, the glycolysis reactions occur in the cytoplasm, and can be divided in two different stages: the first 5 reactions comprise the investment stage, and the second set of reactions comprise the pay-off stage. The investment stage starts with glucose phosphorylation to glucose-6-phosphate (G-6-P), catalyzed by hexokinase[68]. This is a key regulatory step in glycolysis, since it is an irreversible reaction that requires the consumption of ATP. Also, this reaction keeps the intracellular glucose concentration at a low level, maintaining the gradient so that the glucose uptake from the plasma continues, and it blocks the glucose from diffusing back to the plasma[68]. The next step consists in an isomerization, from G-6-P to frutctose-6-phosphate (F-6-P) catalyzed by G-6-P isomerase[69]. F-6-P is then phosphorylated by phosphofructokinse-1 resulting in fructose-1,6-biphosphate (F-1,6-B) which is the second regulatory step, since it is irreversible reaction requiring the hydrolysis of another ATP[70]. The fourth reaction consists in the separation of F-1,6-B, in two trioses that are energy charged molecules. The reversible reaction is catalyzed by aldolase that cleaves F-1,6-B in a molecule of glyceraldehyde-3-phosphate (G-3-P) and another of dihydroxyacetone-phosphate[71]. The last reaction of the first stage consist in the reversible conversion of dihydroxyacetone-phosphate to G-3-P, which is catalyzed by triosephosphate isomerase[72]. The final result of the investment phase is the consumption of 2 ATP molecules and the generation of two energized trioses of glyceraldehyde-3-phosphate. From this point starts the pay-off phase in which each are occurring in duplicate. It starts with oxidation of the molecule of G-3-P catalyzed by G-3-P dehydrogenase. In this reaction, NAD^+ receives the H^+ released, leading to the formation of NADH. Also, there is the addition of one P_i to the molecule, generating 1,3-biphosphoglicerate[73]. In the following step, a reaction catalyzed by phosphoglycerate kinase converts 1,3-biphosphoglycerate to 3-phosphoglicerate, with release of P_i that is used to phosphorylate one molecule of ADP, resulting in the formation of ATP[74].

Next there is the isomerization of 3-phosphoglycerate to 2-phosphoglycerate catalyzed by phosphoglycerate mutase, followed by the conversion into phosphoenolpyruvate promoted by enolase, with release of a molecule of H_2O[75,76]. The final step is catalyzed by pyruvate kinase and it consists in another substrate level phosphorylation in which phosphoenolpyruvate is converted to pyruvate, with the release of P_i that is used to phosphorylate one molecule of ADP, resulting in the formation of ATP[77]. Although this is the last reaction, it is one of most important regulated steps, that also determinates the rate at which glycolysis occurs[77].

The final glycolysis yield is the generation of 2 NADH, 2 ATP and 2 pyruvate molecules that can generate Acetyl-CoA, in a reaction catalyzed by pyruvate dehydrogenase, which is fuel for the TCA cycle[78].

ATP is produced mainly in the mitochondria, through oxidative phosphorylation (OXPHOS) associated with TCA cycle. This cycle consists in a metabolic cyclic pathway that oxides acetyl-CoA, provided by β-oxidation or glycolysis, to carbon dioxide, producing 3 molecules of NADH, 1 molecule of succinate and 1 GTP molecule. GTP can be converted to ATP by the action of the mitochondrial nucleoside diphosphate kinase[79]. NADH and succinate will feed the electron transport chain (ETC), which in tight relation with the ATP synthase, comprise OXPHOS machinery[80].

The first step of TCA is the condensation of acetyl-CoA, a two-carbon compound with an acetyl moiety linked to a coenzyme A, with oxaloacetate resulting in the formation of citrate, which becomes a 6-carbon molecule, that also plays a role in de novo lipogenesis. Citrate synthase is the enzyme responsible for catalyzing this reaction, being followed by the dehydration to cis-aconitate, and hydrated again to form isocitrate, being both reactions catalyzed by aconitase. This enzyme has been appointed as a regulator of TCA cycle, and as being an indicator of oxidative stress[81].

The next step results in the production of the first NADH molecule, as a result of isocitrate dehydrogenase activity. Isocitrate dehydrogenase converts isocitrate to oxalosuccinate, an instable molecule that is quickly decarboxylated to α-ketoglutarate, becoming a 5-carbon molecule. The next step consists in another oxidative decarboxylation, in which α-ketoglutarate is converted to succinyl-CoA by the multi-enzyme complex α-ketoglutarate dehydrogenase (KGDH)[80]. It has been reported that cardiac mitochondria, when challenged with hydrogen peroxide (H_2O_2), greatly limit NADH-linked ADP-dependent respiratory activity[82]. This was explained by the reversible inhibition of KGDH upon oxidation by H_2O_2, decreasing NADH formation and consequent OXPHOS decrease[82].

Returning to Krebs's cycle, the next step requires a phosphorylation at substrate level, in which succinyl-CoA is converted in succinate by succinyl-CoA thiokinase. In this step there is the formation of GTP that can later be transformed in ATP by nucleoside-diphosphate kinase (GTP + ADP = ATP + GDP)[80,83]. After formation of succinate, flavin-dependent dehydrogenation occurs, catalyzed by succinate dehydrogenase, resulting in the formation of fumarate and reduction of FAD prosthetic group in the enzyme. Besides a role in Krebs cycle, succinate dehydrogenase is also known as succinate-coenzyme Q reductase or complex II, a component of the ETC, being responsible for reducing ubiquinone to ubiquinol[84].

The following step is catalyzed by fumarate hydratase or fumarase, that hydrate the carbon double bond present in fumarate, converting it into malate[80]. The final step of TCA consists in the regeneration of oxaloacetate with the formation of NADH. This is catalyzed by malate dehydrogenase that converts malate to oxaloacetate, that can react again with acetyl-CoA, completing a full cycle and allowing the restart of a new one[80].

1.5.2.1 The Electron Transport Chain – "Electro-Train"

The ETC consists of four multi-subunit complexes, NADH dehydrogenase-ubiquinone oxidoreductase (Complex I), succinate dehydrogenase-ubiquinone oxidoreductase (Complex II), ubiquinone-cytochrome-c oxidoreductase (Complex III), and cytochrome-c oxidase (Complex IV). ATP Synthase sometimes appears in literature appears as Complex V, although it is not part of the ETC[85–87]. The ETC also comprises two electron carriers, namely cytochrome-c (cyt-c) and ubiquinone (co-enzyme Q10)[85] and the primary functions are the transport of electrons across complexes until the final acceptor, which is O_2, leading to the production of H_2O, and simultaneously there is the ejection of protons in complexes I, III, and IV from the mitochondrial matrix to the intermembranar space[86,87]. The electrons can enter the ETC in complex I or complex II. The movement of protons promoted by electron transport will generate a protonmotive force that is used to drive protons across ATP synthase which generates ATP[86,87].

Complex I is responsible for the transfer of 2 electrons from NADH to ubiquinone. First, NADH will donate the electrons to a flavin mononucleotide (FMN) prosthetic group, being then transferred to a second prosthetic group, iron-sulfur clusters, that finally donate the electrons to the ubiquinone[86,88]. This movement of electrons allows the translocation of for H^+ from the mitochondrial matrix to the intermembranar space[88]. The reaction occurs as follows:

$$NADH + H^+ + CoQ + 4H^+ \rightarrow NAD^+ + CoQH_2 + 4H^+$$

Regarding complex II, it is the complex more distinct among the others, since its subunits are only encoded by nDNA, whereas some subunits from the remaining complexes have some mtDNA encoded subunits[88]. Also, as aforementioned, complex II acts as a direct enzymatic

segment of the TCA cycle, catalyzing the reaction of succinate to fumarate[84]. It can be a second point of entrance for electrons, however the reaction is thermodynamically insufficient to allow the translocation of protons, being the only complex that does not ejects protons out of mitochondrial matrix[86]. Although its role on TCA cycle, this complex is able to feed the electron flow through its prosthetic groups. It has one flavin adenine dinucleotide (FAD), covalently bound to the active site, and three iron-sulfur clusters[88]. Mechanistically, after the conversion of succinate to malate, this results in the reduction of the prosthetic group FAD to $FADH_2$, that will then transfer the electrons through the FeS clusters, and finally reducing ubiquinone to ubiquinol[88]. The reaction occurs as follows:

$$\text{Succinate} + \text{CoQ} + 2\text{H}+ \rightarrow \text{Fumarate} + \text{CoQH}_2$$

Independently of the electron entrance complex, the transport follows to complex III. The ubiquinol resultant from the reactions catalyzed either by complex I or II, is able to diffuse along the lipidic bilayer until it reaches the active site (Q_0) of complex III where it is oxidized back to ubiquinone, and there is reduction of cytochrome c [88]. Simultaneously, there is translocation of two protons from the mitochondrial matrix to the intermembrane space. However, the reaction is not completed and what follows is truly remarkable. Inside complex III there is an additional site where ubiquinone is reduced back to ubiquinol, using electrons from ubiquinol turnover at Q_0 and protons from the mitochondrial matrix[88]. This results in a catalytic cycle with a final output of two electrons to reduce cytochrome c, two electrons that reduce ubiquinone back to ubiquinol and a total of 4 protons translocated to the intermembrane space, being the full reaction as follows:

$$2\text{CoQH}_2 + 2\ \text{cyt-c}^{3+} + \text{CoQ} + 2\text{H}^{+} \rightarrow 2\text{CoQ} + 2\ \text{cyt-c}^{2+} + \text{CoQH}_2 + 4\text{H}^{+}$$

The final step is catalyzed by complex IV, where cytochrome-c is oxidized giving its electrons to molecular oxygen, reducing it to water. For the complete reaction, four electrons and four protons are required in order to form two water molecules by reduction of O_2. As mentioned, the electrons come from cyt-c, and the protons are translocated from the mitochondrial matrix[88]. Moreover, the reaction increases its energy efficiency since it was later discovered that there are four extra protons that are translocated from the mitochondrial matrix for each full catalytic cycle. This final reaction occurs as follow:

$$4\ \text{cyt-c}^{2+} + O_2 + 8H^+ \rightarrow 4\ \text{cyt-c}^{3+} + 2H_2O + 4H^+$$

Finally, the ATP synthase is one of the most ubiquitous proteins in living organisms, that catalyzes the most prevalent chemical reaction in the biological world – ATP synthesis[89]. Moreover, the mechanism through which ATP is synthesized is almost unique, being only matched by bacterial and archaeal flagella[89]. It functions by rotating over itself in a process that is extremely rare in biological systems, since we do not see animals with wheels or fishes with propellers. Although it is fundamental for energy production in mitochondria, the ATP synthase is not considered as an integral component of the ETC since it does not participate directly in the electron transfer. It has a knob-like structure, with a domain that extends to the mitochondrial matrix, which is named F_1-ATPase, constituted by three α and three ß subunits around a smaller γ subunit, being responsible for ATP synthesis[90]. And a second domain, F_o, responsible by proton translocation, which is constituted also by the γ subunit and a ring of smaller subunits that are hydrophobic allowing this domain to be embedded in the inner membrane of mitochondria, attaching the whole multimeric F_1F_o-ATPase system[89]. This complex system uses the protonmotive force generated by the ETC to transport protons back to the mitochondrial matrix, to produce ATP from ADP and inorganic phosphate[90]. This reaction occurs in the catalytic domain of F_1, which contains three catalytic sites. The most accepted

theory for ATP synthesis is defined by a binding-change mechanism, in which each active site can assume any of the three different conformational states[90]. The three different conformations can be defined as: conformation O (stands for "Open") in which the ATP affinity is lower; conformation L that binds ADP and P_i loosely; and conformation T that tightly bind ADP and P_i[90]. Moreover, at any one point, the three active sites will have one of the possible conformations, respectively. The movement of protons across F_o generates torque power that allow the conformational changes in the catalytic sites of F_1, promoting the phosphorylation of ADP to ATP[90]. Interestingly, in some situations, the ATP synthase can hydrolase ATP, pumping protons out of the mitochondrial matrix to restore membrane potential. If the ATP synthase rotates in a clockwise direction, it will synthetize ATP and the conformational changes go from T ➔ L ➔ O, however the opposite stream is observed in a hydrolytic function. The reaction occurs as follows:

$$10H^+ + 3ADP + 3Pi \rightarrow 10H^+ + 3ATP$$

Producing the much-needed ATP, able to store and transport chemical energy within cells, the "molecular currency" in intracellular energy transfer that the cardiac cells can use.

1.5.3. A Dangerous Triad – Mitochondria, Oxidative Stress, and Cardiomyocytes

Oxidative stress can be defined as an imbalance between the formation of oxidant agents and the antioxidant defenses[91]. This means that either there is excessive formation of ROS that cannot be compensated by the antioxidant enzymes and antioxidants, or there is a reduction in the levels of antioxidant defenses, or both in a bad-case scenario. Furthermore, if the levels of antioxidant defenses are too high, this represents an imbalance since the defenses surpass the oxidative agents. In physiological levels, ROS can act as signaling molecules important for

several cellular processes[92]. For example, after exercise practice, the increased level of ROS triggers mitochondrial biogenesis, and also improves the recruitment of antioxidant defenses[92]. Interestingly, some post-workout milk shakes and meals are rich in antioxidants, which means that their ingestion after the practice of exercise increases the levels of antioxidant defenses in the organism and can mitigate the exercise beneficial impact mediated by ROS, thus reducing the recovery capacity of an athlete[93]. In general, a diet rich in antioxidative agents is advised, nevertheless this example shows how important it is to understand the relation between oxidative and protective agents and the balance between them[94].

The reactive oxygen species, namely superoxide anion ($O_2^{\bullet -}$), hydrogen peroxide (H_2O_2), and hydroxyl anion ($OH^{\bullet -}$) are mainly produced in the mitochondria along the electron transport chain, in particular on complexes I and III, through the interaction of leaked electrons and oxygen, leading to the formation of superoxide. These species are not very reactive, however they can react with nitric oxide, leading to the formation of a powerful oxidant and nitrating agent called peroxynitrite ($ONOO^{\bullet -}$)[95]. Superoxide anion can suffer spontaneous dismutation within the mitochondria, nevertheless there are enzymatic defenses, namely superoxide dismutase (SOD) that can convert superoxide to hydrogen peroxide, a free radical that is stable and membrane permeable, allowing it to easily diffuse within the cell. It can cause some oxidative damage, however, is uncapable of interacting directly with lipids or DNA[95]. Hydrogen peroxide can be decomposed by enzymatic defense mechanisms present in cytosol or within the mitochondria such as glutathione peroxidase, catalase, or thioredoxin reductase[91,95]. If not removed, hydrogen peroxide can interact with ferrous ions, and through the Fenton's reaction lead to the formation of free hydroxyl radicals which are highly reactive with a strong oxidizing power, with the potential to damage every type of biomolecule, which makes this compound extremely dangerous for the organism[95]. Moreover, there is not an

enzymatic defense to remove this toxic compound, being necessary the intervention of nonenzymatic agents that can scavenge radicals, such as glutathione or vitamin E[95].

The formation of ROS can become toxic to the cell in cases where the antioxidant defenses fail or when there is a degree of mitochondrial dysfunction that lead to an increased production of ROS. At noxious levels ROS can interact with DNA, protein or lipids, causing lipid peroxidation, mtDNA damage, or protein carbonylation, which can lead to cellular damage. If the degree of that damage becomes irreversible, then there is more dysfunction, leading to an even higher production of ROS, creating a vicious cycle, that ultimately can implicate the whole organism[95]. This highlights again how important it is to maintain the balance between ROS production and antioxidant defenses.

As aforementioned, cardiomyocytes greatly rely on mitochondria, being a fundamental organelle for energy production through oxidative phosphorylation. However, this also implicates that mitochondria are the main source of ROS production in cardiomyocytes, as a byproduct of physiological aerobic metabolism. It has been already been described that oxidative stress and damage could play an important role in several cardiac pathologies, being implicated in the pathophysiology of cardiac failure, in myocardial hypertrophy, and in diabetic cardiomyopathy[42,96–98]. Thus, it is possible to expect that ROS also plays a role in the putative deleterious effects that GDM could have on the cardiomyocytes.

1.5.3.1 ROS Imbalance in GDM

It is known that oxidative stress has a detrimental impact in type 1 and type 2 diabetes, however it is not fully understood if a similar relation is present in GDM[99]. Nevertheless, increasing evidences show that GDM follows a similar trend in its relationship with oxidative stress, being reinforced by the impact of this stress in the pathophysiology of the disease[100]. Moreover, it has been reported that a decrease in antioxidant defenses and an increase in oxidative stress may

contribute to the development of further complications in GDM[101]. In addition, Zhang et al observed that patients with GDM had increased plasmatic levels of malondialdehyde (MDA) which is a known marker of lipid peroxidation resultant of oxidative stress[102], as well as reduced levels of SOD and GSH, both important antioxidative agents that help regulate oxidative status[99]. All together, these studies suggest that GDM alters the production of oxidative agents and antioxidative defenses causing oxidative stress and damage, which could contribute to development of short- and long-term repercussions observed in GDM[99–101].

1.6. Physical Activity as a Non-pharmacological Therapy for Diabetes and CVD

Various advantages of physical activity practice have been described and highlight the improvements in cardiac function and a protective effect, largely reducing the mortality and morbidity risk, due to CVD[54]. In relation with other diseases, multiple epidemiological studies relate the practice of physical activity with a reduced risk of developing osteoporosis, some kinds of cancer and type 2 diabetes[103]. By studying this component Sarvas et al. assessed the impact that voluntary physical activity (VPA) had on the prevention of T2D, acknowledging that voluntary physical activity could effectively prevent insulin resistance even in young healthy mice, meaning that could prevent one of the first steps of developing T2D[104]. Also, on this disease, physical activity stimulates a better regulation in glucose homeostasis, accounting that skeletal muscle is responsible for 80% of insulin induced glucose uptake[103]. Moreover, concerning the cardioprotective effect, there are several studies that point out physical activity as a powerful, non-invasive and non-pharmaceutical, method, that is capable of improve heart function[105,106]. These studies have been mostly performed in relation with cancer, however its beneficial cardiac effects seem independent of the disease. Doxorubicin (DOX) is a chemotherapeutic agent used to treat various types of cancer, due to its antineoplastic biological

activity. Although being extremely effective, this drug presents cardiovascular toxicity, resulting in cardiomyopathy, which can be fatal[106]. Marques-Aleixo et al. have found that VPA during DOX treatment could mitigate the cardiac toxicity, through the improvement of mitochondrial function[106]. Recent data, provided by Antunes et al. showed that exercise, a subcategory of physical activity that is planned, structured, repetitive and intentional, is an effective non-pharmacological therapy to mitigate the effects of cachexia, a common syndrome developed in CVD patients, especially in chronic heart failure. Exercise was able to remodel various signaling pathways altered during cachexia syndrome, thus improving heart function[105].

It is clear that exercise largely contributes to improve cardiac function, preventing future pathologies, and to promote a better management of metabolic disorders, such as diabetes in non-pregnant subjects. Regarding GDM, it has already been demonstrated that one of the first therapeutic interventions should be diet and lifestyle adaptations, being also recommended the initiation of PA. Furthermore, in a recent study performed to assess the impact of physical exercise in GDM pregnancies, it was observed that aerobic and resistance exercises alone or combined does not represent any adverse effects for the mother or the fetus[107]. Interestingly, the practice of exercise led to an improved regulation of glucose homeostasis, through the decline of the blood sugar levels[107].

Although there is already some data regarding the impact of exercise during pregnancy, the lack of more studies that validate this perspective results in different opinions among the medical community. On one side, several physicians started to consider exercise, or an active lifestyle, as a fundamental component of a healthy pregnancy, and in opposition, the majority of the obstetricians, which consider that pregnancy should be a phase of low intensity effort for the women, advising plenty of resting periods throughout the whole gestation[108–110].

Without a clear and solid research on those both point of views, it is important that new studies emerge in order to settle which is the most beneficial behavior for both mother and fetus, and if existing, the possible harmful effects, regarding inactivity or activity during pregnancy.

1.6.1. Exercise and Cardiac Improvement Through Mitochondrial Function

Nowadays, it is inconceivable not to recognize the plethora of health promoting effects that come with the practice of physical activity. In fact, physical activity is associated with reduction of adipose tissue, better regulation of glucose homeostasis, more muscular strength and better whole-body tissue oxygenation due to improved cardiorespiratory fitness, which are extremely important outcomes of exercise intervention in obesity, metabolic syndrome, T2D, and heart disease patients[103]. Some of these favorable effects rely on the premise that mitochondrial disfunction is one of the underlying mechanism of the disease, and that exercise will improve mitochondrial function[44,103]. Actually, there are a large variety of mitochondrial evidences that support the positive effects of exercise[103,111]. Mitochondria are organelles with specific dynamics, called fission and fusion processes that allow a constant remodeling of the mitochondrial network[92]. Also, mitochondrial content within the cell is variable through processes of mitochondrial biogenesis, which increase synthesis, and mitophagy, that is responsible for degradation of mitochondria[111]. Exercise has been reported as a powerful stimulator of mitochondrial biogenesis, thus increasing its content inside the cell, in response to the accruing effects of each session of exercise. This is mainly due to the activation of exercise-induced biogenesis pathways, following physical activity, that result in the induction of the expression of the gene peroxisome proliferator-activated receptor 1α (PGC-1α) [112,113]. It is also observed the increased expression of Mitochondrial Transcription Factor A (mTFA)[103,114]. These molecules will lead to increased mitochondrial biogenesis and volume,

and also to a better coupling of the mitochondrial electron transport chain, thus making the production of ATP a more efficient process[103].

Exercise is also responsible for inducing production of stress signals, such as ROS, that could be responsible for mitochondrial biogenesis[103]. As mentioned before, in excessive amount, those oxidant species would interact with protein, lipids and DNA, and cause oxidative damage, sometimes in an irreversible way[44]. At certain intensities, exercise can be too stressful, leading to the production of an injurious amount of ROS. However, exercise generally produces ROS at a signaling level, that not only activate the expression of PGC-1α but also, trigger the recruitment of antioxidant defenses to prevent any type of cellular damage, in a way that in future stressful events of oxidative stress the cell will be more prepared to cope with it[92].

In a basal state or under stress, the autophagy process coordinates with mitophagy in order to assure mitochondrial shape, network and function[92]. Autophagy is an intracellular degradation system that disassembles unnecessary or dysfunctional components, balancing sources of energy at critical times. Mitophagy is the selective catabolism of superfluous or damaged mitochondria by autophagy[92]. This balance is tightly controlled by fusion and fission dynamics, which includes mitofusins 1 and 2 (Mfn1 and Mfn2), optic atrophy 1 (Opa1), dynamin related protein 1 (Drp1) and mitochondrial fission protein 1 (Fis1). Disruption in the fission dynamics could lead to an excessive gathering of damaged mitochondria, resulting in cell-dysfunction[92]. Also, mitochondrial fusion dynamics, mediated by Mfn1 and Mfn2, will increase mitochondrial renewal, improving their health and function. In cancer cachexia, aforementioned, it has been reported that Mfn2 has a crucial role for preventing muscle wasting through its overexpression, thus improving mitochondrial function[115]. Moreover, it has been described that fusion proteins are highly regulated by PGC-1α, so considering the exercise-induce response, stimulating PGC-1α expression, it is accurate to state that exercise will not only improve mitochondrial

function through biogenesis, but further by promotion of fusion dynamics, providing renewal of the mitochondrial network[116].

The association between mitochondrial morphology and function has been reported, suggesting that mitochondrial quality control occurs in parallel with morphology regulation through mitochondrial dynamics[117]. Fusion and fission processes have been thought to be a promotor of either a more interlinked, elongated and/or connected mitochondria, which could lead to mitochondrial function improvement. Those processes could also lead to a more discontinued and fragmented mitochondrial network, which can suggest mitochondrial dysfunction[118]. It is then implied that mitochondrial morphology can be altered to perform the multivariant functions inherent to it, mentioned previously, such as energy production, cellular calcium homeostasis, or cell apoptosis[44].

All the mechanisms described above have been reported as being responsible for the exercise-induced improvement of the mitochondria, with a better mitochondrial respiratory efficiency and a more robust antioxidant defence[103].

1.8 Pertinency, Hypothesis, and Objective

It has become evident in recent decades that the prevalence of metabolic-rooted pathologies is increasing, with incidence levels of obesity, diabetes, non-alcoholic fatty liver disease, metabolic syndrome and CVD raising every year. One metabolic disease that has followed this trend is GDM, that emerges as the most common disease that occurs during pregnancy. Moreover, being GDM such a prominent disease, is fundamental to better understand its mechanisms in order to improve prevention, diagnosis, treatment, and management of long-term effects.

In this work, we hypothesized that physical activity during pregnancy can be a powerful modulator of maternal cardiac mitochondrial state, acting as a non-pharmacological therapy to counteract the negative outcomes associated with GDM, namely in the maternal cardiac health. Considering this, it is important to better understand the impact that PA has in the maternal heart.

Our main objective is to characterize the impact of physical activity, during a situation of GDM, on cardiac mitochondrial function. Further, we also have a secondary goal that consists in the characterization of the pregnancy-modulated mitochondrial function, since knowledge about this subject is somewhat missing in the literature.

CHAPTER 2 - MATERIALS AND METHODS

2.1. Reagents

The reagents used were of the highest grade of purity commercially available (Table 2.1). All aqueous solutions were prepared in ultrapure water (type I). For nonaqueous solutions, ethanol (99.5%, Sigma-Aldrich, Barcelona, Spain) or dimethyl sulfoxide (DMSO, Sigma-Aldrich) were used as solvents.

Table 1. List of reagents used in the present work and the respective common name, Chemical Abstracts Service (CAS) registry number, supplier reference, and company.

Reagent	Supplier	CAS-Number	Reference	Brand HQ
40% Acrylamide/Bis Solution	Bio-Rad	—	161-0148	Hercules, California, USA
Absolute Ethanol (200 proof) Molecular Biology Grade	Fisher Scientific	64-17-5	BP2818100	Waltham, Massachusetts, USA
Blotting-Grade Blocker	Bio-Rad	9000-71-9	170-6404	Hercules, California, USA
Bovine Serum Albumin	Sigma	9048-46-8	A4503	St. Louis, MO, USA
Carbonyl cyanide 3-chlorophenylhydrazone	Sigma	555-60-2	C2759	St. Louis, MO, USA
Chloroform	Sigma	67-66-3	650498	St. Louis, MO, USA
Clarity Western ECL Substrate	Bio-Rad	—	170-5061	Hercules, California, USA
Distilled Water DNase/ RNase Free	Gibco	—	10977-035	Waltham, Massachusetts, USA
Dithiothreitol (DTT)	Sigma	3483-12-3	D9163	St. Louis, MO, USA

Glacial Acetic Acid	PanReac AppliChem	64-19-7	131008.1611	Barcelona, Spain
Glycerol	Sigma	56-81-5	G6279	St. Louis, MO, USA
Glycine	Fisher Scientific	56-40-6	BP381-1	Waltham, Massachusetts, USA
Guanidine Hydrochloride	Fisher Scientific	50-01-1	BP178	Waltham, Massachusetts, USA
HEPES	Sigma	7365-45-9	H4034	St. Louis, MO, USA
Isopropanol	Sigma	67-63-0	190764	St. Louis, MO, USA
L-Glutamic Acid	Sigma	56-86-0	G8415	St. Louis, MO, USA
L-Malic Acid	Sigma	97-67-6	M7397	St. Louis, MO, USA
2x Laemmli Sample Buffer	Bio-Rad	—	161-0737	Hercules, California, USA
Methanol	Sigma	67-56-1	M/4000/17	St. Louis, MO, USA
Oligomycin Streptomyces diastatochronogenes	Sigma	1404-19-9	O4876	St. Louis, MO, USA
Ponceau S	Sigma	6226-79-5	P3504	St. Louis, MO, USA
Precision Plus Protein™ WesternC™ Standards	Bio-Rad	—	161-0376	Hercules, California, USA
Rotenone	Sigma	83-79-4	R8875	St. Louis, MO, USA
Sodium Chloride (NaCl)	Sigma	7647-14-5	71376	St. Louis, MO, USA
Sodium Deoxycholate	Sigma	302-95-4	D6750	St. Louis, MO, USA

Sodium Dodecyl Sulphate (SDS)	Bio-Rad	151-21-3	161-0301	Hercules, California, USA
Sodium Phosphate Dibasic (Na_2HPO_4)	Labkem	10028-24-7	SOPH-02A-500	Dublin, Ireland
Sodium Phosphate Monobasic (NaH_2PO_4)	Labkem	10049-21-5	SODH-01A-500	Dublin, Ireland
SsoFast™ EvaGreen® Supermix	Bio-Rad	—	172-5204	Hercules, California, USA
Subtilisin Fraction type VIII	Sigma	9014-01-1	P5380	St. Louis, MO, USA
Succinic Acid	Sigma	110-15-6	S3674	St. Louis, MO, USA
Tetramethyl ethylenediamine (TEMED)	NZYtech	110-18-9	MB03501	Lisbon, Portugal
Tetraphenylphosphonium Chloride	Sigma	2001-45-8	218790	St. Louis, MO, USA
Trans-Blot® Turbo™ 5x Transfer Buffer	Bio-Rad	—	10026938	Hercules, California, USA
TripleXtractor RNA™	GRiSP Research Solutions	—	GB23.0050	Porto, Portugal
Tris – HCl, 0,5M pH=6.8	Bio-Rad	—	161-0799	Hercules, California, USA
Tris – HCl, 1.5M pH=8.8	Bio-Rad	—	161-0798	Hercules, California, USA
Tris Base	Fisher Scientific	77-86-1	BP152-1	Waltham, Massachusetts, USA
Tween® 20	Sigma	9005-64-5	P9416	St. Louis, MO, USA

2.2. Experimental Design and Animal Care

2.2.1. Animals and Ethics

All animal procedures were approved by the Ethics Committee of the Faulty of Sport of the University of Porto, and the National Government Authority (Nº 0421/000/000/2018), and were performed according to the guidelines for care and use of laboratory animals in research, recommended by the Federation for European Laboratory Animal Science Associations (FELASA) conducted in animal care-approved facilities.

Outbred Sprague Dawley rats, 44 females (CD-SIFE05SS - R/SPF CD) and 20 males (CD-SIMA05SS - R/SPF CD), were purchased from Charles River Laboratories (L'Arbresle, France) with 5 weeks of age.

Upon arrival, the rats were submitted to one-week acclimatization to the new environment, which also served as quarantine period. After this period, animals were paired in type III cages with appropriated bedding and environmental enrichment. The animals were artificially kept on 12 h of light during night and 12 h of dark during the day. The room temperature was maintained at 21-22ºC, moisture at 50-60%, noise level below 55dB, and ad libitum access to food (D12450K, Ssniff, Germany) and water.

In order to test our hypothesis, in the current study we implement a novel diet induced GDM model, that mimics several features of the disease such as gestational glucose intolerance, hyperglycemia, and supra-physiological levels of insulin resistance based on the model previously described by Troy J. Pereira and colleagues[11].

All the animals were weighed weekly, behavioral assessment, exercise protocols, and all manipulations were performed during the active period of the animals (dark phase). Figure 2 summarizes the study design and the interventions.

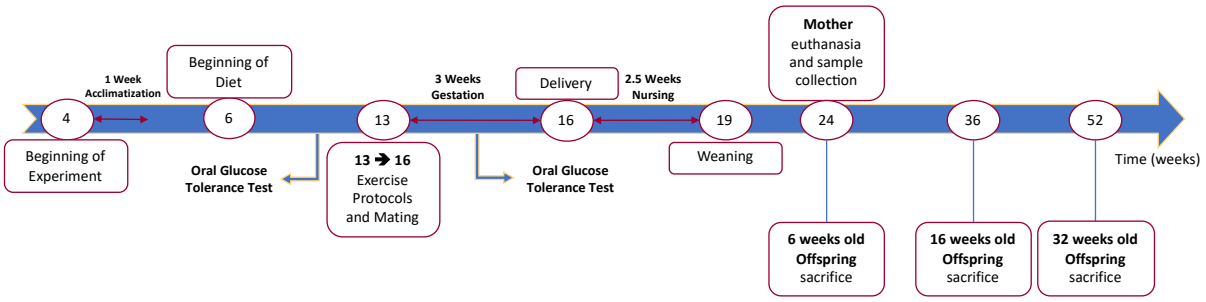

Figure 2. ***Study timeline with maternal age and determinant animal interventions.***

2.2.2. Diet Treatment Protocol

Animals were fed a standard rodent control diet (ssniff® DIO – 10 kJ% fat, no sucrose addition D12450K, Ssniff, Germany) (Figure 3) composed mainly by carbohydrates (70%), being sugar free and with reduced fat content (10%). At 6 weeks of age, 14 animals have been randomly selected to continue to eat the control diet and the remaining 30 females started a high-fat-high-sugar (HFHS) diet to induce the GDM phenotype (ssniff® EF R/M acc. D12451 II) (Figure 3). This diet was rich in fats (42%), mainly saturated and monounsaturated, and in carbohydrates (31%), mainly sugar and dextrin. Both diets were supplemented with essential minerals, vitamins and trace elements. The animals were fed *ad libitum* and the diets were maintained from this time point until sacrifice, resulting in two experimental groups based on diet: rats fed with control diet (C), and rats fed a high-fat-high-sugar diet (HFHS).

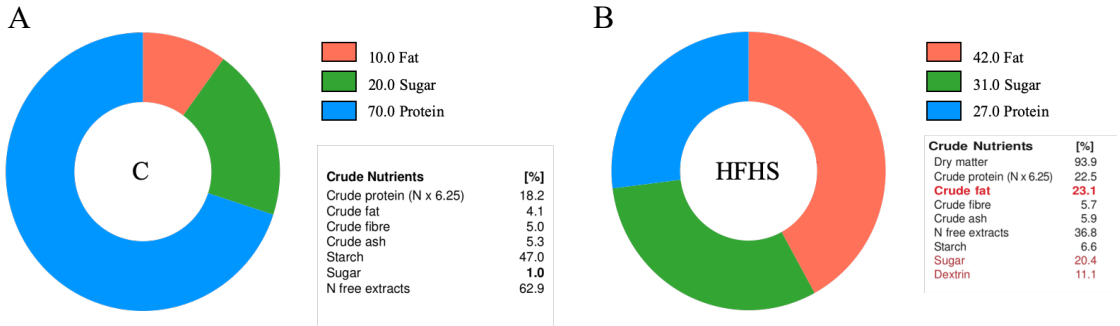

Figure 3. ***Animal diet description and nutrients distribution.*** *Diets were provided* ad libitum as *(A) control diet (ssniff® DIO – 10 kJ% fat, no sucrose addition D12450K) and (B) high-fat-high-sugar diet (ssniff® EF R/M acc. D12451 II). Figure adapted from ssniff®.*

2.2.3. Mating

A fertile male was introduced into each breeding cage to induce pregnancy in 13-week-old females. Pregnancy was assessed by observing vaginal mating plug formation. Mating plug consists in a gelatinous secretion, deposited in female genital tract, by the male, that hardens and seals the vaginal channel. This process occurs in some species to prevent that other males' mate with the same female. Once the mating plug existence was confirmed, the females were considered pregnant (P, n=19), and the remaining without the mating plug were considered non-pregnant (NP).

2.2.4. Exercise intervention with voluntary physical activity (VPA) and endurance training

To test the impact of exercise during pregnancy animals were submitted to an exercise protocol during the three weeks of pregnancy, exercised group (E), and the remaining were considered sedentary (S). The animals of exercising groups performed a physical exercise program (Table 2 and Figure 4) consisting of running on treadmill during three weeks of pregnancy, and additionally had a free access to the running wheel, which mimicked voluntary physical activity (VPA).

A

B

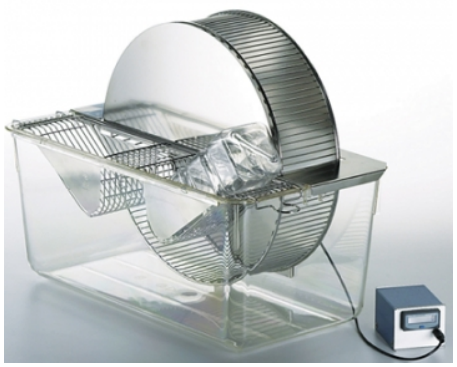

Figure 4. ***Representations of the two systems used to induce PE and VPA:*** *(A) Adapted treadmill developed for rodent PE. (B) Example of a type IV cage with running wheel for VPA, connected to a counter.*

The animals from the exercise intervention were paired allocated in cages type IV with a running wheel (circumference = 103.73 cm, Type 304 Stainless steel, Tecniplast, Casale Litta, Italy) connected to a counter (ECO 701 Hengstler, Lancashire, UK) so the wheel revolutions were recorded, and the traveled distance measured. The female rats had free access to the wheel during the full period of exercise protocols. Since the cage was inhabited by two females, the final distance traveled was divided by two. On top of the VPA animals from the exercise group were adapted to endurance exercise (Figure 4) using a motor-driven treadmill (LE8700, Panlab, Harvard, USA). This protocol consisted in a 2-day period of acclimatization to the treadmill,

that occurred before mating, followed by 7-day gradual increasing intensity of training until achieve the final intensity of physical exercise that was maintained until the end of gestation (see Table 2).

Table 2. Exercise protocol for rodents in adapted treadmill. The treadmill speed is represented in centimeters per seconds.

			Acclimatization Description
Acclimatization (2 days)	Day 1	Duration: 15 min	Acclimatization to the treadmill environment. The rats were on the treadmill, which was static and with electric shock set at 2mA
	Day 2	Duration: 15 min	Acclimatization to the treadmill environment. The rats were on the treadmill, which was static and with electric shock set at 2mA

			Warm-up	**Workout**			**Cool-down**
Gradual increase in PE intensity (7 days)	Day 1	Duration: 22 min	2 min: speed increase until 10 cm/s	3 min at 15 cm/s	15 min at 20 cm/s		2 min: speed decrease until 5 cm/s and stop
	Day 2	Duration: 22 min	2 min: speed increase until 15 cm/s	3 min at 20 cm/s	15 min at 25 cm/s		2 min: speed decrease until 5 cm/s and stop
	Day 3	Duration: 22 min	2 min: speed increase until 15 cm/s	3 min at 20 cm/s	15 min at 25 cm/s		2 min: speed decrease until 5 cm/s and stop
	Day 4	Duration: 32 min	2 min: speed increase until 15 cm/s	3 min at 20 cm/s	15 min at 25 cm/s		2 min: speed decrease until 5 cm/s and stop
	Day 5	Duration: 42 min	2 min: speed increase until 15 cm/s	3 min at 20 cm/s	25 min at 25 cm/s	10 min at 30 cm/s	2 min: speed decrease until 5 cm/s and stop
	Day 6	Duration: 52 min	2 min: speed increase until 15 cm/s	3 min at 20 cm/s	35 min at 25 cm/s	10 min at 30 cm/s	2 min: speed decrease until 5 cm/s and stop
	Day 7	Duration: 62 min	2 min: speed increase until 15 cm/s	3 min at 20 cm/s	45 min at 25 cm/s	10 min at 30 cm/s	2 min: speed decrease until 5 cm/s and stop

		Warm-up	Workout				Cool-down
Final PE intensity (9 Days)	Duration: 62 min	2 min: speed increase until 15 cm/s	3 min at 20 cm/s	35 min at 25 cm/s	10 min at 30 cm/s	10 min at 35 cm/s	2 min: speed decrease until 5 cm/s and stop

2.2.5. Experimental Groups

Animals of similar morphometrics were randomly assigned to eat control diet or to receive HFHS diet. At 12 weeks of age, animals from each group were randomly assigned to the exercise intervention or to remain sedentary. One-week later female rats from all the groups were paired with a fertile male to induce pregnancy. The three independent variables studied were pregnancy, nutrition and, exercise. Resulting in the following six experimental groups (Figure 5):

1) non-pregnant, control diet, sedentary (NP_C_S) with 7 biological replicates;
2) non-pregnant, high-fat-high-sugar diet, sedentary (NP_HFHS_S) with 11 biological replicates;
3) non-pregnant, high-fat-high-sugar diet, exercised (NP_HFHS_E) with 7 biological replicates;
4) pregnant, control diet, sedentary (P_C_S) with 7 biological replicates;
5) pregnant, high-fat-high-sugar diet, sedentary (P_HFHS_S) with 6 biological replicates;
6) pregnant, high-fat-high-sugar diet exercised (P_HFHS_E) with 6 biological replicates.

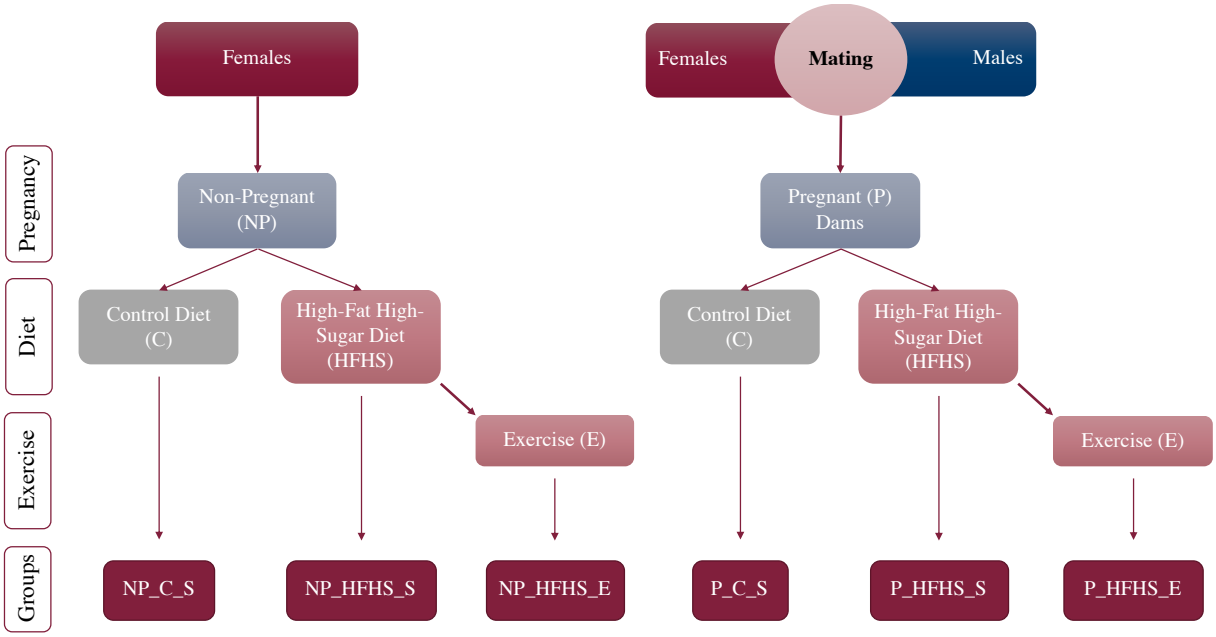

Figure 5. ***Schematic representation of the experimental groups and respective interventions.***

2.3. Animal Procedures

2.3.1. Oral Glucose Tolerance Test

An oral glucose tolerance test (OGTT) was carried out to measure blood glucose levels and assess glycemic control in female rats before mating and on day 16 of pregnancy in the different experimental groups (± 12 and 15 weeks old). The test consists in giving a determined amount of glucose to an individual and collect blood samples at specific time points to see the progression of glucose levels in the blood comparing to the glucose levels before the glucose load. In humans, positive diagnose of GDM is achieved when one or more values are higher than the following reference values: 0 h ≥ 92 mg/dl; 1 h ≥180 mg/dl; 2 h≥153 mg/dl[12]. However, those levels have never been defined yet for Sprague Dawley rats, thus, to confirm a glucose intolerance we compared to the respective control group, because it represents the normal physiological response and glucose tolerance state.

The common routes of glucose administration in rats consist of: 1) intragastric gavage, consisting in a probe that releases glucose directly into the animal stomach or, 2) inject it with a syringe in the intraperitoneal area[119]. However, these methods require highly specialized technicians to cause minimum injuries to the animals, and also involve intensive handling and restraining, causing increased levels of stress, which can modulate the parameters in study, especially blood glucose levels[119]. With this in account and since we were working with pregnant animals, we wanted to find a less stressful way of performing this assessment in the animals, without sacrificing the precision in administering the determined amount of glucose of the common methods used. Zhang et al. developed a method of administrating drugs to mice through an artificially sweetened and flavored jelly, provided that the mice's are acclimatized to eat the jelly[119]. We adapted this method to administrate a precise amount of glucose incorporated in jelly to induce the glucose load and perform the OGTT in Sprague Dawley rats.

To prepare the glucose solution (75%), 0.9 g of glucose was dissolved in approximately 0.8 mL of warm water using a stirring heating plate at 55ºC, after complete dissolution the volume was adjusted to 1.2 mL. Gelatin solution (14%) was prepared by dissolving 0.7 g of gelatin in 5 mL of warm water using a stirring plate at 55ºC, until the solution become clear.

To prepare the oral glucose jelly, the 1.2 ml of glucose solution was transferred to a well of 24-well tissue culture plate, and 0.6 mL of gelatin solution was added. The plate was placed at 4ºC to solidify. Before the OGTT with the oral glucose jelly the animals were acclimatized to jelly and trained to eat the whole amount of jelly.

To perform OGTT the animals were fasted for 6-18 h, and the oral glucose jelly was prepared as aforementioned. To determine the amount of oral glucose jelly to provide for each animal the following formula was applied:

$$a) \quad \frac{2\ g\ Glucose}{1000\ g\ Body\ Weight} = \frac{x\ g\ Glucose}{y\ g\ Body\ Weight}$$

$$b) \quad \frac{0.9\ g\ Glucose}{z\ g\ Jelly} = \frac{x\ g\ Glucose}{Z\ g\ Jelly}$$

The blood glucose level was assessed before the beginning of the test, by measurement of blood taken from the tail vein. During the test, the blood was removed from the same location, at 15, 30, 60, 90 and 120 minutes after administration of the oral glucose jelly. The OGTT was realized before mating (12th week) and at the middle of gestation (15th week), to confirm that pregnancy was the catalyzing challenge to develop glucose intolerance during gestation, as it occurs in GDM, and reinsure that the animals were not diabetic before pregnancy.

2.3.2. Animal Euthanize and Tissue Collection and Processing

The female rats were euthanized at 24 weeks old, 8 weeks after delivery (Figure 2). Rats have a 2.5 weeks offspring nursing period and the protocol was extended more 5.5 weeks after nursing to assess long-term lasting implications in maternal health and to minimize the interference of imminent weaning experience.

The estrus cycle was determined by vaginal smear[120] and animals in the metestrus phase of the cycle were selected for euthanasia. The chosen animals were fasted for 12 h. Just before the euthanasia the glycemic level and bodyweight were determined. Animal euthanasia was performed between 8:00 and 10:00 AM under anesthetic conditions. Firstly, animals were placed in an induction camera at 1.5 L/m O_2 5% isoflurane, and then kept at deep anesthetic state with 0.8 L/m O_2 4% de isoflurane. The abdominal cavity was opened to elicit blood from the inferior vena cava, followed by the opening of the thoracic cavity to remove the tissues of interest, namely the heart. The heart was removed, weighed, rinsed with ice-cold PBS (NaCl, KCl, Na_2HPO_4, and KH_2PO_4) and segmented for different experimental protocols.

2.3.2.1. Cardiac Tissue for Mitochondrial Isolation

A segment of the heart was immersed in ice-cold Heart Isolation Buffer (HIB), prepared with 250 mM sucrose, 0.5 mM EGTA, 10 mM HEPES, pH=7.4 with KOH, supplemented with 0.1% fatty acid free Bovine Serum Albumin (A4503, Sigma; Saint Louis, USA) (HIB+) and finely minced to facilitate the blood removal and posterior mitochondrial isolation.

2.3.2.2. Cardiac Tissue for Biochemical Analysis

A segment of the heart was snap-frozen in liquid nitrogen and stored at -80ºC until used for posteriorly analysis.

2.4. Determining Cardiac Mitochondria Bioenergetics

2.4.1 Cardiac Mitochondria Isolation

Heart mitochondria were isolated following a protocol previously described by Pereira et al. and adapted from Silva and Oliveira [121,122]. Minced heart was washed with HIB+ to completely remove any traces of contaminating blood. Minced blood-free tissue was then resuspended in 20 ml of HIB+ and homogenized with a Potter-Elvehjem tightly fitted homogenizer at 4ºC. After 3-4 homogenizations, the HIB+ was supplied with 0.2 ml protease (subtilisin fraction type VIII, Sigma; Saint Louis, USA) per gram of wet tissue and incubated during 1 min (4ºC) and then re-homogenized. The protease was removed from the homogenate by centrifugation at 13 000 G for 10 min at 4ºC (2-16KC centrifuge with rotor 12139-H, Sigma Laborzentrifugen, Osterode am Harz, Germany). The supernatant was discharged, and the pellet was gently resuspended in HIB+ and transferred to another Potter-Elvehjem, for a manual homogenization. The suspension was centrifuged at 800 G for 10 min at 4ºC (Sigma Laborzentrifugen, Osterode am Harz, Germany). After this centrifugation the mitochondria remained in the supernatant, supernatant was collected to new centrifuge tubes, and centrifuged at 10 000 G during 10 min at 4ºC (Sigma Laborzentrifugen, Osterode am Harz, Germany). This last supernatant was discharged, and the mitochondrial pellet was resuspended with a smooth brush and washed in Heart Washing Buffer (HWB – 250 mM sucrose, 10 mM HEPES, KOH pH=7.4). The suspension was centrifuged again at 10 000 G for 10 min at 4ºC (Sigma Laborzentrifugen, Osterode am Harz, Germany) and the supernatant was discharged and the pellet (isolated mitochondria) was resuspended in 100-300 µL of HWB.

The isolated mitochondria were kept on ice and used on bioenergetic assays within 3 h of isolation. The mitochondrial protein content was quantified by the biuret method.

2.4.2. Protein Quantification by Biuret Assay

For mitochondrial protein quantification, the colorimetric biuret method was used[123]. Through spectroscopy, it is possible to determine the color developed in the reaction of the copper sulfate with biuret in the presence of compounds with peptide bonds in alkaline conditions, detecting polypeptide chains[123].

The assays were performed in 96 multi-well plates, and after a period of 15 min of incubation at 22ºC, the color formation was read at 595 nm in Multiskan GO 1500-10 with SkanIt™ Software 3.2 (Thermo Fisher Scientific, Massachusetts, USA).

The standard curve was performed using BSA as standard (0; 0.05; 0.1; 0.15 and 0.2 mg/mL).

2.4.3. Mitochondrial Oxygen Consumption and Membrane Potential

For characterization of mitochondrial performance modulation, under the experimental conditions tested it is crucial to measure the mitochondrial bioenergetic state. The bioenergetic state involves compelling mitochondrial coupling of substrate oxidation by the ETC with ATP synthase and its efficiency, which operates in tight relation with mitochondrial membrane potential[122]. The ETC coordinates extrusion of protons across the membrane with the movement of electrons through its complexes', resulting in the reduction of O_2 to H_2O and the generation of a protonmotive force. This protonmotive force can be used to pump protons back to the mitochondrial matrix, through the ATP synthase, generating energy to phosphorylate ADP in ATP[122].

2.4.3.1. Oxygen Consumption Rate – Clark-Type Electrode

The final electron acceptor in ETC is oxygen. This reaction occurs in complex IV, cytochrome c oxidase, culminating in the formation of H_2O. This means that mitochondrial electron transport efficiency across the different complexes can be assessed by measuring the rate of

consumption of the final electron acceptor, oxygen. In our work, we used OxyGraph (Hansatech Instruments, Norfolk, England) which is a Clark-Type Oxygen Electrode to measure the disappearance of oxygen in the medium due to its consumption by mitochondria.

The electrode consists in a platinum electrode negatively polarized at 0.7 V in opposition to a silver reference electrode. This structure is protected from the reaction medium by a membrane permeable to oxygen, since direct contact with biological preparations could contaminate the platinum electrode, decreasing the electrochemical sensitivity. The electrolytical oxygen reduction that occurs in the platinum electrode is proportional to the oxygen concentration in the medium, and this generates a potential between the 2 electrodes. The potential is transferred to a computer that registers the oxygen concentration in the medium. Since this represents an accelerated consumption of oxygen, the medium needs to be under stirring so it can re-oxygenate.

The mitochondrial OCR assays were performed in 1 mL of Heart Reaction Buffer (HRB – 130 mM Sucrose, 10 mM HEPES, 65 mM KCl, 2.5 mM KH_2PO_4, 20 μM EGTA, at pH=7.4), in which 0.5 mg/mL mitochondria were suspended. To assess complex I NADH dehydrogenase-ubiquinone oxidoreductase supported O_2 consumption, 10 μL glutamate 0.5 mM/malate 1 mM were used. For complex II succinate dehydrogenase-ubiquinone oxidoreductase assays, 10 μL succinate 1 mM and 1 μL of rotenone 1.5μM (inhibitor of Complex I) were used. To induce a mitochondrial phosphorylative state, also named state 3, 8 μL of ADP 30 mM were added to the chamber, and for stimulation of mitochondrial maximum oxygen consumption 2.5 μL of Carbonyl cyanide-*4*-(trifluoromethoxy)phenylhydrazone (FCCP) 0.1 mM was used.

An example of a record obtained with the method described above can be observed in Figure 6. With this assay, we are able to determine four mitochondrial states: state 2, state 3, state 4 and FCCP (uncoupled) state, that allow to infer about mitochondrial phosphorylative performance. State 2 represents a basal mitochondrial oxygen consumption rate derived from

endogenous substrates and from proton leakage. State 3 represents a state where the ATP production is stimulated by the injection of ADP to the medium. That results in an increase in the ETC activity which ultimately results in increased consumption of oxygen, the final acceptor in the for electrons in the ETC. State 4 occurs after the full consumption of ADP being characterized by a complete or almost complete return to a basal oxygen consumption. Finally, the FCCP state, or uncoupled state, represents the maximum oxygen consumption rate in mitochondria due to the action of FCCP that allows the passage of protons through the inner membrane, instead of ATP synthase, which results in disruption of the mitochondrial membrane potential. To mitigate this effect, the ETC increases the transport of electrons to a maximum resulting in maximum oxygen consumption rate.

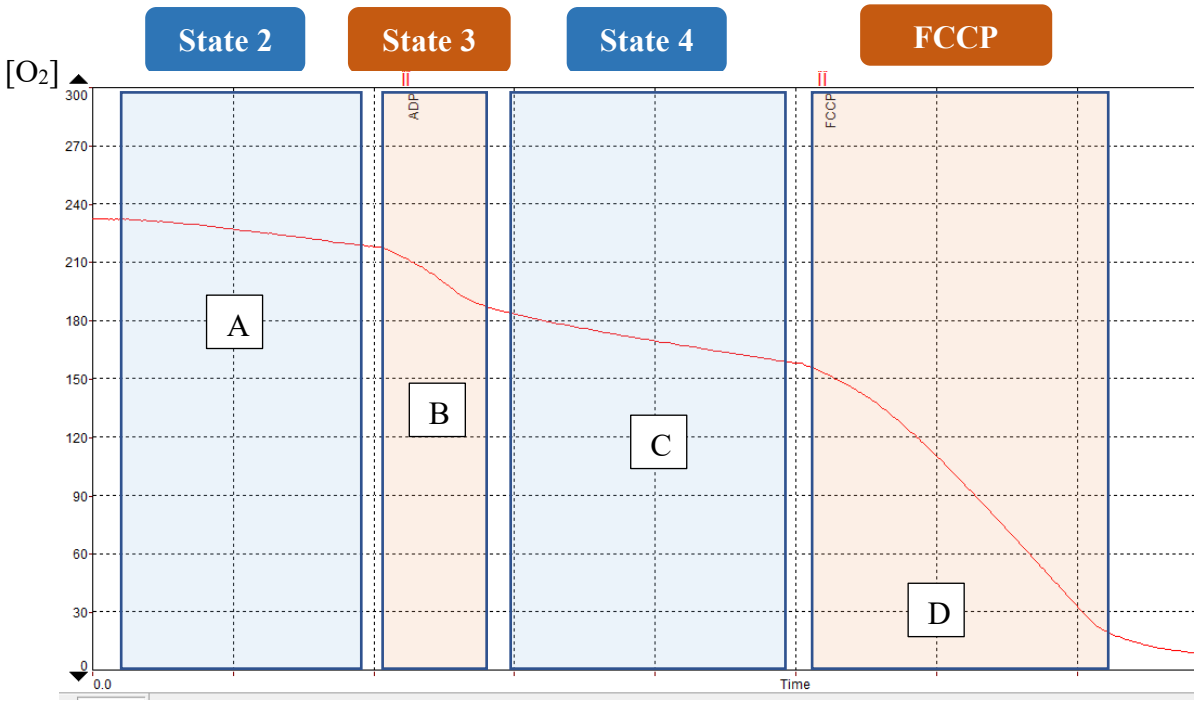

Figure 6. ***Oxygen consumption rate assay obtained with OxyGraph (Hansatech Instruments, Norfolk, England), comprising four mitochondrial metabolic states:*** *(A) State 2,a basal oxygen consumption rate; (B) State 3, an ADP-induced phosphorylative state, increasing the oxygen consumption rate; (C) State 4, the almost recovery to a basal oxygen consumption rate; (D) FCCP state, where due to the injection of an uncoupler the oxygen consumption rate is maximum in an attempt to reinstate the mitochondrial membrane potential.*

2.4.3.2. Mitochondrial Membrane Potential – Tetraphenylphosphonium$^+$ Electrode (TPP^+)

This assay has the objective of assess the mitochondrial membrane potential indirectly by measuring the amount of TPP^+ in medium using a TPP^+-sensitive electrode[87].

Mitochondrial inner membrane is extremely tight since it is a fundamental requirement to generate the electrochemical gradient used to force the protons to go through the ATP synthase, leading to the formation of ATP. Since there is a constant extrusion of protons from the mitochondrial matrix, it becomes negative which means that cationic compounds are attracted to the matrix[87]. TPP^+ is a cationic compound that is attracted to the mitochondrial matrix and it is able to cross the membranes due to its particular chemical structure with 4 aromatic rings that hide the phosphor positive center, allowing it to diffuse across the membranes freely. To measure mitochondrial membrane potential, a TPP^+-sensitive electrode containing tetraphenylboron as an ion exchanger and a saturated calomel electrode (SCE) was used as the reference. The electrodes were connected to a potentiometer and the measurements were registered in a paper chart recorder.

The mitochondrial membrane potential assays were performed in 1 mL of HRB in which mitochondria were suspended, at a mitochondrial protein concentration of 0.5 mg/ml. For complex I NADH dehydrogenase-ubiquinone oxidoreductase assays, 10 µL glutamate 0.5 mM/malate 1 mM were used. For complex II succinate dehydrogenase-ubiquinone oxidoreductase assays, 10 µL succinate 1 mM and 1 µL of rotenone 1.5 µM (inhibitor of Complex I) were used. To induce a mitochondrial phosphorylative state 8 µL of ADP 30 mM were added to the chamber.

The assay described above allows to indirectly assess the mitochondrial membrane potential by measuring the fluctuations TPP^+ in the medium (Figure 7). As above explained, the TPP^+, as a cation, can trespass membranes freely. When mitochondria are placed in the chamber, the TPP^+ immediately accumulates in the mitochondrial matrix, since it is charged negatively. A higher

mitochondrial membrane potential will lead to a greater accumulation of the cation, which allows to define the maximum membrane potential of mitochondria (ΔΨ). The addition of ADP will stimulate mitochondria to produce ATP and consequently the passage of protons through the ATP synthase causes a depolarization in the membrane potential of mitochondria, which we can observe by the increase of TPP^+ in the medium. The ETC increases its activity to reinstate the mitochondrial membrane potential, and when the added substrate is fully consumed, there is repolarization and the membrane potential returns to a basal level, which can be observed by the decrease of TPP^+ in the medium since it returns to the mitochondrial matrix. This stage can be defined as ΔΨ ADP. The amount of time that takes from the addition of ADP until its complete consumption comprises the lag phase, which can be an indicator of mitochondrial efficiency and coupling. For example, a rapid consumption of the ADP could indicate that there is a strong coupling between ATP synthase and the ETC.

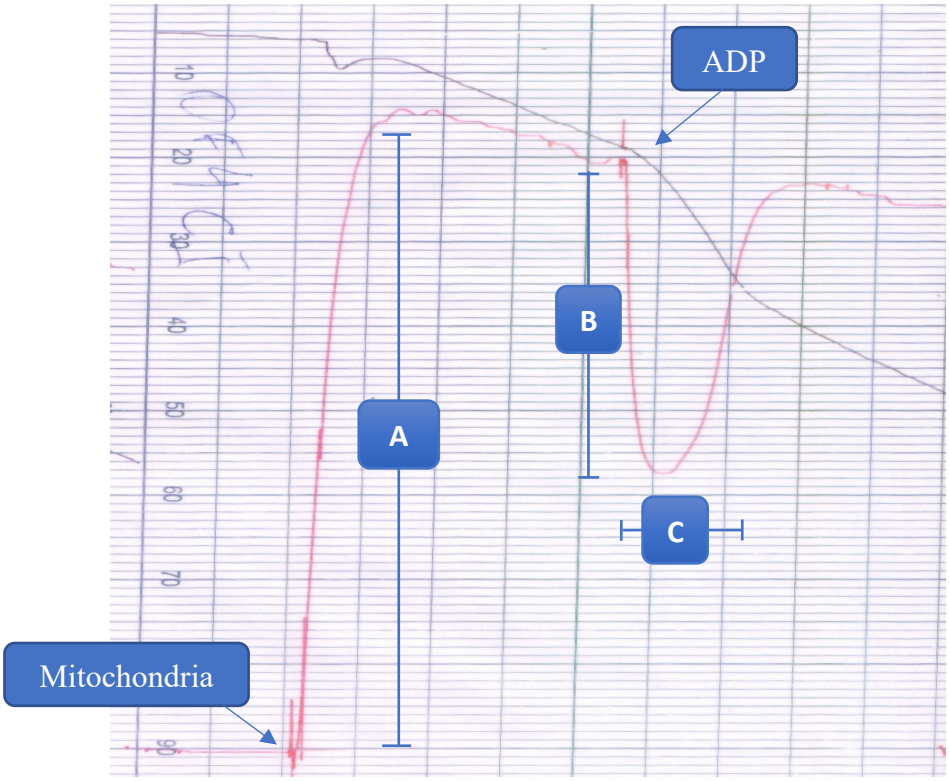

Figure 7. ***Paper chart exemplar of a mitochondrial membrane potential assay obtained with a TPP^+-selective electrode.*** *(A) Maximum potential, ΔΨ - it is defined by the capacity that mitochondria have to accumulate TPP^+. (B) Depolarization, ΔΨ ADP – it comprises the variation of mitochondrial membrane potential, caused by the addition of ADP. (C) Lag Phase - it comprises the amount of time that is necessary for the mitochondria to consume the whole amount of ADP added.*

2.5. Relative Gene Expression Profile Using qPCR

Real-Time Polymerase Chain Reaction (qPCR) is a widely used technique that allows to measure the RNA expression level, using specific primers, and to monitor that reaction due to the presence of a specific fluorescent probe. The assay can be divided in 3 different stages:

a) RNA extraction and purification;

b) RNA conversion to cDNA through reverse transcription PCR;

c) Assessment of the expression levels of specific target genes, through quantitative PCR.

2.5.1. RNA Extraction and Isolation

For sample preparation optimization, frozen cardiac tissue was weighted, and extraction was performed using three different protocols, based on the RNA quality and yield obtained the following protocol was chosen. It is important to weight the tissues in order to maintain a similar tissue mass for all samples ensuring an efficient yield and preventing saturation of extraction reagents.

Total RNA was extracted from 30 - 40 mg of cardiac tissue placing the tissue in a 2 mL eppendorf with 1 mL of TripleXtractor RNA extraction reagent (GRiSP Research Solutions, Porto, Portugal), a monophasic lysis solution of phenol and guanidine isothiocyanate, and mechanic homogenization with UltraTurrax T10 homogenizer from IKA (Staufen, Germany). When the tissue was completely lysed, 200 µL of chloroform were added followed by quick shake (15 sec) and an incubation at room temperature during 3 min. The samples were then centrifuged at 12 000 g for 15 min at 4ºC in a Heraeus Megafuge 40R Centrifuge (Thermo Fisher Scientific, Massachusetts, U.S.A.). Centrifugation with chloroform allowed to realize a sequential precipitation, separating the homogenate in 3 different phases (Figure 8). The lower phase consists in a reddish phenol-chloroform organic phase which contains proteins, the

interphase consists in a thin white phase which is the DNA, and the upper one is a colorless aqueous phase which contains RNA. The upper phase was retrieved (about 700 µL), carefully to avoid drawing any of the inter or the organic phases and placed in new 1.5 mL eppendorf to proceed for RNA purification protocol. The remaining phases were stored at -20ºC for posterior protein purification, which will be addressed later in the topic 2.6.1 Protein Extraction and Isolation.

The RNA purification was performed using RNeasy® Mini Kit (QIAGEN, Hilden, Germany)

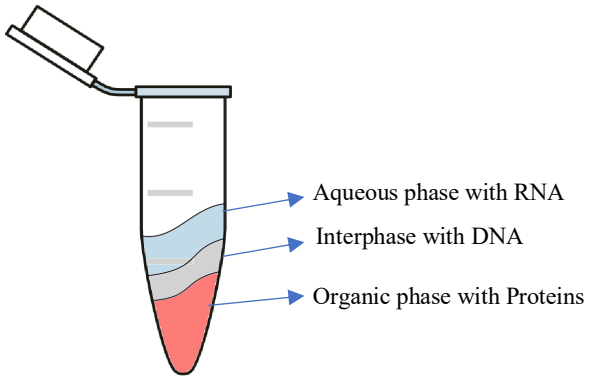

Figure 8. ***Schematic representation of the 3 different phases that are obtained when using TripleXtractor RNA extraction reagent (GRiSP Research Solutions, Porto, Portugal) for RNA extraction.***

and following the manufacturer´s instructions. Briefly, an equal volume of molecular grade ethanol 70% (700 µL) was added to each eppendorf containing the RNA aqueous phase, and the mixture was transferred to a spin column placed in 2 mL collection tube. The tubes were then centrifuged for at 8000 G for 15 sec at 4ºC. This step allowed to pass the mixture through the silica column, retaining the RNA due to its high affinity to positively charged phosphates in the silica composition. The flow-through is discarded and the column is placed in a new collection tube. As a washing step, 350 µL of buffer RW1 are added to the column, followed by another centrifugation at 8000 g for 15 sec at 4ºC. The following step consisted in the on-column DNA digestion, performed by the addition of 80 µL of DNase solution (10 µL DNase stock in 70 µL of RDD buffer) to the columns, followed by an incubation of 15 min at room-temperature. This step is crucial to obtain high degree of purity when extracting RNA, since it

will degrade any DNA that was bonded to the column. After the incubation, 350 µL of buffer RW1 are added to the column, followed by centrifugation at 8000 g for 15 sec at 4ºC, to wash the DNase and any debris resultant of DNA digestion. Then, 500 µL of RPE buffer was added to the columns, followed by centrifugation at 8000 g for 15 sec at 4ºC. This step was repeated; however, the centrifugation was 2 minutes long. The columns were then placed in new collection tubes and were centrifuged at full speed (24 000 g) for 1 minute to air-dry the columns membrane. Finally, the columns were placed in the final collection tubes of 1.5 mL and 40 µL of DNase/RNase-free water were added directly to the spin column membrane, and centrifugation followed at 8000 g for 1 min, to promote RNA elution. The column is then discarded and the flow-through collected consists of purified RNA. All the steps in this protocol were performed with sterile RNase-free materials, filtered tips, and RNase-free reagents to avoid contamination and RNA degradation. Further, the work area and the hands were cleaned using RNase*Zap*™ RNase decontamination solution (Invitrogen, California, U.S.A.).

2.5.2 RNA Quantification and Integrity

RNA quantification was performed in NanoDrop™ 2000 spectrophotometer (Thermo Fisher Scientific, Massachusetts, U.S.A.) using DNase/RNase-free water as blank reading, and then all RNA samples were quantified, and its purity assessed by the ratios of A260/A280 and A260/A230. Samples with a A260/A280 ratio between 1.9 and 2.1, and a A260/A230 ratio between 2 and 2.2, were considered with a good RNA purity.

To assess RNA integrity, Experion™ RNA StdSens (Bio-Rad, California, U.S.A.) was performed. Before starting the procedure, the Experion electrophoresis station electrode were clean, first with Bio-Rad electrode cleaning reagent for about 5 min, followed by another 5 min in RNase-free H_2O. The RNA samples and RNA ladder must be kept on ice; however, the remaining reagents of the kit need to equilibrate at room-temperature for 15 min before starting

the procedure. Next, the gel-staining solution was prepared by mixing 65 µL of filtered RNA gel and 1 µL of RNA staining solution, and 9 µL of this solution were pipetted into **GS** well will orange background (Figure 9, gel priming well), in order to prime the chip.

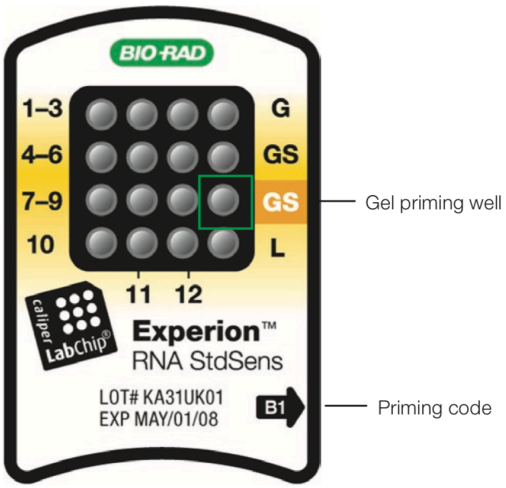

Figure 9. ***Experion™ RNA StdSens Chip representation.*** *Image taken from Experion™ RNA StdSens (Bio-Rad, California, U.S.A.) online protocol.*

This step was performed on the priming station, that uses pressure to inject the gel and fill the chip microtubes. To program the priming station the intensity of pressure "B" was selected, in accordance with the priming code printed on chip (Figure 7), and the priming was completed in one minute.

To prepare the samples, 2 µL of each sample were placed in new RNase-free microcentrifuge tubes. Also 1 µL of RNA ladder was placed in a new RNase-free microcentrifuge. The samples and the RNA ladder were then denatured for 2 min at 70º C.

The chip loading consists on pipetting 9 µL of gel-staining solution to the other **GS** well, followed by pipetting 9 µL of filtered gel in **G** well. The **L** well was filled with 1 µL of ladder plus 5 µL of loading buffer. Each remaining well (1-12) was loaded with 1 µL of sample plus 5 µL of loading buffer. After the chip loading was complete, it was vortexed to avoid bubbles, and placed in the Experion electrophoresis station. The quality of the samples was evaluated

considering the electrophoresis results by visualization of the ribosomal band integrity for both the 18S and 28S ribosomal RNA.

Only RNA samples that demonstrated consistent quality in purity and integrity were used.

2.5.2. RNA to cDNA: Reverse Transcriptase PCR

Synthesis of cDNA was performed using iScript™ cDNA Synthesis Kit (Bio-Rad, California, U.S.A.). After quantification 2 µg of RNA was aliquoted to a new RNase-free microcentrifuge tube and the final volume adjusted to 30 µL with RNase-free water for each sample. Then it was added 8 µL of supermix, and 2 µL of reverse-transcriptase (RT) to each sample in accordance with Table 3.

Table 3. iScript™ reaction components and volumes.

Volume RNA	Volume Supermix	Volume RT	Volume H2O	Total volume
Variable	8 µL	2 µL	Variable	40 µL

The complete reaction mix was then incubated in a thermal cycler, using the following protocol: 5 min at 25ºC, followed by 20 min at 46ºC, then 1 min at 95ºC, and finally hold at 4ºC. Also, a reaction mix containing all the components with the exception of RT was prepared and incubated alongside the remaining samples as a negative control (NRT).

2.5.3. Quantitative Polymerase Chain Reaction

With the cDNA obtained in from the reverse-transcription PCR, we assessed the expression levels of target genes through qPCR. Before the reaction itself, the samples were diluted in DNase/RNase-free water to a final cDNA concentration of 10 ng/µL. A pool of all samples was prepared by mixing 5 µL of each sample (Pool 1:1). From that pool, 20 µL were taken and 180

μL of DNase/RNase-free water was added to dilute the pool 10 times. (Pool 1:10). From this last pool, 20 μL were taken and 180 μL of DNase/RNase-free water was added to dilute the pool another 10 times (Pool 1:100). Finally, a negative control for qPCR, named Non-Template Control (NTC) was prepared, where the template, cDNA, was replaced by RNase-free water. The reaction was performed in hard-shell PCR 96-well plates. Each well was loaded with 7.5 μL of reaction mix and 2.5 μL of sample. The reaction mix consisted in 600 μL of SsoFast™ EvaGreen Supermix, 6 μL of primer forward and 6 μL of primer reverse, and finally 288 μL of DNase/RNase-free water.

The plates were incubated for qPCR in a CFX96 Touch™ Real-Time PCR Detection System (Bio-Rad, California, U.S.A.) and the reaction was set with the software CFX Manager™ 3.1 (Bio-Rad, California, U.S.A.) following the protocol provided at the SsoFast™ EvaGreen Supermix datasheet. The program used was 95ºC for 30 sec, to promote enzyme activation, followed by 40 cycles of amplification, with 5 sec at 95ºC for cDNA denaturation, followed by 5 sec at 55-65ºC to allow primer annealing/extension (see List of Primers – Table 4, since annealing temperature is variable according to the optimum annealing temperature of each primers pair). A melting curve program for quality control was immediately performed after the cycling program.

Fluorescence was detected from each well during the annealing step of each cycle, as well for housekeeping genes, internal controls, controls for efficiency of reverse transcription, PCR and the absence of contaminating genomic DNA. The values were exported to an Excel template file for analysis. Data were normalized for 18S, Beta-Actin and GAPDH housekeeping genes and analyzed with the ΔΔCt method, where Ct is the threshold cycle.

2.5.4. List of Primers

Table 4. List of primers used to assess expression of target genes.

Gene	Designation	Accession Nº	Primer F	Primer R	Optimal Extension ºC
RNA18S	18S Ribosomal RNA	NR_046237.1	ACTCAACACGGGAAACCTC	ACCAGACAAATCGCTCCAC	62.3
ACAA2	Acetyl-CoA Acyltransferase 2	NM_130433	CCTCAGTTCTTGGCTGTTCA	CCACCTCGACGCCTTAAC	63.7
ACOX1	Acyl-CoA Oxidase 1	NM_017340.2	GCAGACAGCCAGGTTCTTGATG	ACTCGGCAGGTCATTCAGGTAT	62
β-Actin	Beta-Actin	NM_031144.3	AGATCAAGATCATTGCTCCTCCT	ACGCAGCTCAGTAACAGTCC	63.2
GAPDH	Glyceraldehyde-3-Phosphate Dehydrogenase	NM_017008.4	GTCATCCCAGAGCTGAACGG	ACTTGGCAGGTTTCTCCAGG	62.2
HIF1α	Hypoxia Inducible Factor subunit alpha	NM_024359.1	CAAGCAGCAGGAATTGGAACG	CTCATCCATTGACTGCCCCA	60.9
LDHB	Lactate Dehydrogenase B	NM_012595.1	GGTGAAGGGAATGTACGGCAT	GAGCGACCTCATCGTCCTTC	62.2

LDHD	Lactate Dehydrogenase D	NM_010088893	TGCGTCCAGGAAGAGTCATT	CGATGCCATGTTCTCCGGTA	63.5
PGC1α	PPARG Coactivator 1 Alpha	NM_031347.1	GGGACGAATACCGCAGAGAG	CGGCGCTCTTCAATTGCTTT	61.7
POLmt	Mitochondrial RNA Polymerase	NM_001106766.1	GAGACAGGTACCTTCGATCTGG	GGTGGGTTTGTGTGTAGCCA	61.6
PPARα	Peroxisome Proliferator Activator Receptor Alpha	NM_013196	AGACTAGCAACAATCCGCCTTT	TGGCAGCAGTGGAAGAATCG	62.4
SOD2	Superoxide Dismutase 2	NM_017051.2	CGCGACCTACGTGAACAATC	CTCCAGCAACTCTCCTTTGG	62.9
TBP	TATA-box Binding Protein	NM_001004198.1	CCTATCACTCCTGCCACACC	CAGCAAACCGCTTGGGATTA	60.6
mTFA	Mitochondrial Transcription Factor A	NM_031326.1	AATGTGGGGCGTGCTAAGAA	TCGGAATACAGATAAGGCTGACAG	64.7
TnnT2	Cardiac Type Troponin T2	NM_012676.1	ATCCACAACCTAGAGGCCGA	CCCACGAGTTTTGGAGACTT	59.2

VDAC2	Voltage-Dependent Anion Channel 2	NM_031354.1	GACACCCGCAGATCACCTTT	ACATCCAGCTTTACCAACCCAAA	62.7

2.6. Protein Analysis by Western Blot

Western blot (WB) is a common technique in cellular and molecular biology, which allows the separation of a mixture of proteins by their molecular weight, regardless of the electrical charge, allowing the immunodetection enabling the identification and the relative abundance of proteins between samples[124]. The main phases of WB technique were: (1) separation of proteins based on their molecular weight; (2) transference from the gel to a solid support, such as a membrane; (3) tag selected protein using a specific primary antibody and then a proper secondary antibody to visualize the protein of interest[124].

2.6.1. Protein Extraction and Isolation

As aforementioned in 2.5.1, the samples were extracted using TripleXtractor RNA extraction reagent, that is able to separate the sample in three different phases, upon centrifugation with chloroform. For protein purification, the organic reddish phase containing proteins and DNA was used (Figure 8). Initially, 300 mL of ethanol 99.5% was added to each sample, and manual shaking was performed to promote homogenization, followed by 3 min of incubation at room-temperature. The samples were then centrifuged in a Heraeus Megafuge 40R Centrifuge at 2000 g for 5 min at a temperature of 4ºC. After centrifugation, the proteins were collected from the supernatant and placed in new tubes, the pellet that contains DNA was stored at -20ºC. It was added 1.5 mL of isopropanol to the protein supernatant and shook manually and allowed to incubate for 10 min at room temperature. The protein fraction was sedimented by centrifugation

at 12 000 g for 10 min at 4ºC, and the supernatant was discarded. The pellets were then washed with 2 mL of 0.3 M guanidine hydrochloride in 95% ethanol for 20 min. Samples were then centrifuged at 7500 g for 5 min at 4ºC, and the supernatant was discarded. This washing step was repeated another 2 times. Ensuing, 1 mL of ethanol 99.5% was added to each sample to detach the pellet and it was sonicated in a VCX 130 sonicator (Sonics & Materials Inc., Newtown, CT, U.S.A.) with a 2 mm probe using pulses of 5 sec at 60% amplitude (maximum of 130 watts) followed by one sec off. The sonication was performed until the pellet was dissolved promoting the resuspension. After, the samples were incubated for 20 min at room-temperature and centrifugated at 7500 g for 5 min at 4ºC. The supernatant was discarded, and the pelleted samples were allowed to air-dry on the benchtop.

The dried pellet was solubilized in 400 µL of 8 M Urea with 1% SDS supplemented with several inhibitors (0.5 mM phenylmethanesulfonylfluoride, 40 µL of protease inhibitor cocktail (104 mM AEBSF, 80 µM Aprotinin, 4 mM Bestatin, 1.4 mM E-64, 2 mM Leupeptin, and 1.5 mM Pepstatin A), 20 mM sodium fluoride, 10 mM of nicotinamide, 5 mM sodium butyrate, 0.5% DOC, and 1 mM sodium orthovanadate). The samples were centrifuged at 10 000 g for 10 min at 4ºC to remove the debris, and the pellet was discarded, and the proteins, soluble in the supernatant, stored at -80ºC for further analysis.

2.6.2. Protein Quantification and Sample Preparation

The protein was quantified using DC™ Protein Assay (Bio-Rad, California, U.S.A.) with the incorporation of reagent S, since the urea buffer contains detergent. The standard curve was performed using BSA diluted in the same buffer as the samples with the following BSA concentrations: 0.2 mg/mL, 0.5 mg/mL, 0.75 mg/mL, 1 mg/mL, 1.5 mg/mL. After assembling the reaction in a 96-well plate, there was an incubation of 15 min and then the absorbance was read at 750 nm. Standards and unknown samples were performed in triplicate. After protein

quantification, all the samples were diluted to the same final concentration of 1.8 mg/mL with *Laemmli* Blue (Bio-Rad, Hercules, California, USA) and stored at -80ºC until forward use.

2.6.3. Acrylamide Gel Preparation and Electrophoresis

The first steps consisted in preparation of the running station as well as assembly of the glass's apparatus were the gels are polymerized. The gel includes two different layers with different acrylamide percentage. The upper layer, called stacking gel, was prepared with 1.25 mL of 0.5 M Tris-HCL pH=6.8, 0.5 mL of 40% acrylamide/bis-acrylamide, 3.2 mL of MiliQ water, 100 µL of SDS 10%, 50 µL of APS 10%, and 5 µL TEMED. This gel is more acidic, and it has a smaller content of acrylamide (4%), meaning that it will generate a more porous grid, allowing the proteins to easily migrate and align at the top of the next layer. Also, it is in this gel that the 15-well 1.5 mm combs were insert, to generate the well were the protein was loaded.

The lower layer, named resolving gel, was prepared with 2.5 mL of 1.5 M Tris-HCL pH=8.8, 2.5 mL, 3 mL or 3.5 mL of 40% acrylamide/bis-acrylamide (according with the desired gels percentage), 4.9 mL, 4.4 mL, or 3.9 of MiliQ water (according with the desired gels percentage), 100 µL of SDS 10%, 50 µL of APS 10%, and 5 µL of TEMED. This gel is more basic and has a higher content in acrylamide since its purpose is to separate the proteins according to their molecular weight, meaning that the smaller the protein is the further it will pass across the gel. The percentage of acrylamide defines the percentage of the gel and must be adjusted according with the molecular weight of the protein of interest. For higher molecular weights, a lower percentage of acrylamide (8-10%) is desired, however if the protein of interest has a small molecular weight, a higher percentage of acrylamide (14-16%) is appropriate to allow a higher resolution. After gel polymerization, gels were assembled in the running station immersed in running buffer (250 mM Tris-base, 1.9 M glycine, and 1% SDS). The proteins are loaded in the wells formed on top of the stacking gel. A molecular weight marker was loaded

in the first well of each gel, the Precision Plus Protein™ Dual Color Standard (Bio-Rad, California, U.S.A.), with known molecular weights between 10 and 250 KDa. The samples were loaded dispensing 25 µg of protein in *Laemmli* Blue (15.6 µL) per well.

Electrophoresis was carried at 30 mA per gel until the sample buffer (blue) reach the bottom of the gel using a PowerPac™ HC High-Current Power Supply (Bio-Rad, California, U.S.A).

2.6.4. Electroblotting

After separation of proteins by SDS-PAGE, proteins were electrophoretically transferred from the gel to polyvinylidene fluoride (PVDF) membranes. The transfer was performed using two different methods: in the classic wet system, the transfer occurs totally submerged in transfer buffer (390 mM Glycine, 480 mM Tris base, 20 % Methanol, 10% SDS). The stacking gel was carefully removed, and the gel was placed on top of a filter paper, supported by a sponge, in the transfer cassette. On top of the gel it was placed methanol activated PVDF membrane, followed by filter paper and another sponge. The transfer cassette was closed and placed inside a Trans-Blot® Cell ((Bio-Rad, California, U.S.A.), paying attention to orient the cassette with the side of the gel towards the negative pole and the side with the PVDF membrane towards the positive pole. The transfer system was connected to a PowerPac™ HC High-Current Power Supply (Bio-Rad, California, U.S.A.) with cooling system and the transfer was performed at a constant voltage of 100 V during 90 min. After transfer conclusion the membrane was carefully removed, and the marker was labelled with a "-" for the blue bands (10, 15, 20, 37, 50, 100, 150, and 250 kDa) and a "+" for the pink bands (25 and 75 kDa).

The other transfer method involves a semi-dry method and was performed in a Transblot Turbo™ Transfer System (Bio-Rad, California, U.S.A.). The assembling of the transfer cassette started by soaking an ion reservoir stack in Transfer Buffer (75 mL MiliQ water, 25 mL of Transblot Turbo Transfer Buffer, and 25 mL Ethanol 99.5%) and placing it on the bottom of

the cassette correspondent to anode (+). Then on top of the reservoir stack the PVDF membrane rested, followed by gel on top of it. After this step, another ion reservoir stack was placed on top of the gel and the cassette was closed with the lid, that corresponded to the cathode (-). The cassette was then inserted into the transfer system and the transfer was performed at 2 A, for a period of 20 min.

After the transfer was concluded the membrane was carefully removed and the marker was labelled with a "-" for the blue bands and a "+" for the pink bands as described before.

2.6.5. Membrane Ponceau Labelling

The quality of the electrophoretic transfer was assessed by Ponceau staining with 0.1% Ponceau in 5% acetic acid. The membranes were left under stirring with 10-15 mL of Ponceau solution for 1-5 minutes. Then the membranes were washed with MiliQ water until the protein bands were clearly visible. The membrane was scanned for Ponceau signal quantification and then it was placed in MiliQ for full removal of Ponceau. Ponceau labelling were also used to confirm equal amount of protein loading, verification for artifacts in the membranes and to normalize the WB data[125].

2.6.6. Blocking and Immunodetection

The membranes were blocked during 2 h at RT with agitation with 5% Bovine Serum Albumin in TBS-T (20 mM Tris, 150 mM NaCl, 0.1% Tween 20) to reduce nonspecific binding. After the blocking step the membranes were washed three times in TBS-T and then stored in 50 mL tubes with ~45 mL of TBS-T.

For immunodetection, the primary antibodies (Table 5) were prepared in 50 mL conical tubes with 5 mL TBS-T with 1% BSA at concentrations that ranged from 1:500 to 1:1000. The membranes were incubated with the primary antibody for the protein of interest and were placed

in a roller overnight at 4ºC. After incubation with the primary antibody, the membranes were washed 3 times with TBS-T. The secondary horseradish peroxidase conjugated antibodies were prepared in 50 mL falcons with 5 mL TBS-T at a concentration of 1:5000 (Table 6) and were incubated for 2 h at room-temperature under agitation. After incubation with the HRP-secondary antibody, the membranes were washed again 3 times. The HRP-secondary antibodies will emit luminescence upon exposure to Clarity™ Western enhanced chemiluminescence (ECL) substrate (Bio-Rad, California, U.S.A.), allowing the detection of the primary antibody bonded to the protein of interest.

The immunodetection was performed using a VWR® Imager Chemi 5QE (VWR, Pennsylvania, U.S.A.), for image acquisition, the membranes where placed inside the acquisition chamber and centered within the capture field and 400 µL of ECL substrate were carefully spread on top of the membrane and the chamber was closed for image acquisition. The images were treated with ImageJ Fiji Software and bands density analysis was quantified using TotalLab™ TL120 Software (TotalLab, Newcastle, United Kingdom). Densities were normalized to Ponceau of the respective lane. The average value of the control group (NP_C_S) was assumed as one unit and the values of each sample were proportionally determined.

2.6.7. List of Antibodies

Table 5. Descriptive list of primary antibodies used.

Primary Antibody	Molecular Weight (kDa)	Dilution	Host Organism	Reference	Company
ß-Actin	43	1:5000	Mouse	MAB1501	Millipore

GLUT4	50-63	1:1000	Mouse	sc-53566	Santa Cruz Biotechnology
IL-6	21	1:1000	Mouse	sc-28343	Santa Cruz Biotechnology
IRS-1	170-185	1:1000	Mouse	sc-8038	Santa Cruz Biotechnology
LC3	16, 18	1:500	Rabbit	PD014	MBL International Corporation
mtTFA	25	1:500	Goat	sc-23588	Santa Cruz Biotechnology
MitoProfile® Total OXPHOS	18, 22, 29, 48, 54	1:500	Mouse	ab110411	Abcam
NDUFB8	18	1:500	Mouse	ab110258	Abcam
MTCO2	22	1:500	Mouse	ab110242	Abcam
SDHB	29	1:500	Mouse	ab14714	Abcam
UQCRC2	48	1:500	Mouse	ab14745	Abcam
ATP5A	54	1:500	Mouse	ab14748	Abcam

p62	47	1:1000	Rabbit	PM045	MBL International Corporation
SOD2	25	1:1000	Mouse	ab16956	Abcam
Tom20	20	1:1000	Rabbit	sc-11415	Santa Cruz Biotechnology
TNF-α	17, 26	1:1000	Mouse	sc-12744	Santa Cruz Biotechnology
Cardiac Troponin T	40	1:1000	Rabbit	5593	Cell Signaling

Table 6. Descriptive list of the secondary antibodies used.

Secondary Antibody	Dilution	Host Organism	Company	Reference
Anti-Goat	1:5000	Rabbit	Santa Cruz	2771
Anti-Mouse	1:5000	Horse	Cell Signaling	7076
Anti-Rabbit	1:5000	Goat	Cell Signaling	7074

2.7. Statistical Analysis

By definition, the experimental unit is the unit which could be independently assigned to any treatment. In this study, each pregnant or non-pregnant female were considered as an experimental unit. The outbred rats were randomly assigned to the groups. Whenever possible, we performed blind assessment on the determination of the parameters to be statistically analyzed.

Data are expressed as mean ± standard error. Normality was assessed by Kolmogorov-Smirnov normality test but was absent due to the reduced experimental number, so the non-parametric comparison between groups, as a whole, was performed using Kruskal-Wallis non-parametric ANOVA, as post-test, to assess which pairs were different, the multiple comparisons were performed using Mann-Whitney non-parametric t-test. Statistical tests were performed considering a significance level of $p=0.05$.

Statistical analyses were performed using GraphPad Prism version 6.01 (GraphPad Software, Irvine, CA. USA).

3. RESULTS

3.1 Establishment and characterization of a gestational diabetes mellitus rat model

3.1.1 Maternal characterization and glucose homeostasis

For the purpose of this work, our initial aim was to establish a physiological model of GDM, in which the state of glucose intolerance only appears during pregnancy. As maternal obesity is a main factor to develop GDM, in this study, we fed a high-fat-high-sugar diet to 6-weeks old female rats to potentiate obesity and mate them to induce pregnancy at 13 weeks old. Further we assessed the development of GDM during pregnancy through verification if the model mimics the clinical features of GDM during human pregnancy, characterized by glucose intolerance, mild hyperglycemia, hyperinsulinemia and, hyperlipidemia.

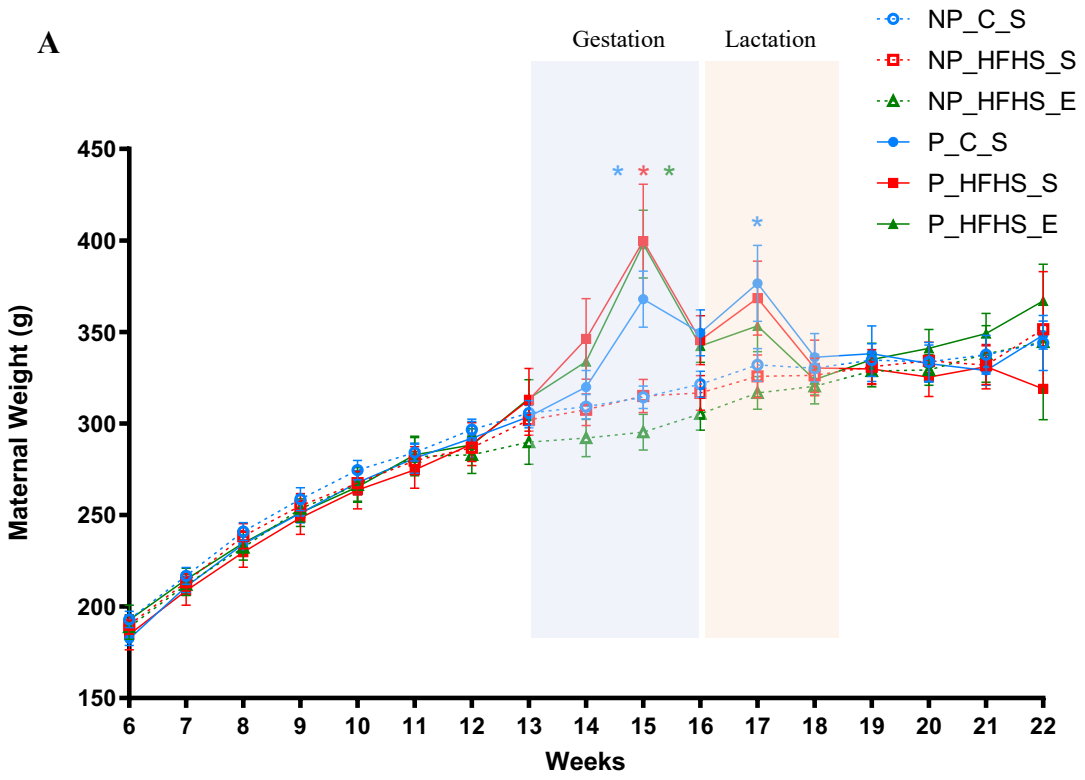

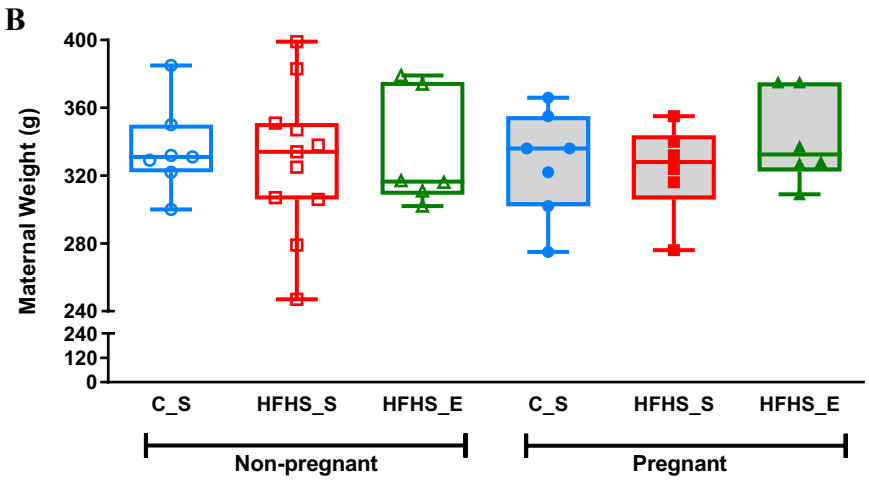

Figure 10. ***Maternal body mass determined weekly during the experimental procedure and before euthanasia.*** *(A) change in body weight over time. The data are expressed with means ± SEM. The comparison between groups was performed with t-test, corrected with Holm-Sidak method. *p≤0.05 for comparisons between P_C_S and NP_C_S; *p≤0.05 for comparisons between P_HFHS_S and NP_HFHS_S; and *p≤0.05 for comparisons between P_HFHS_E and NP_HFHS_E. (B) females body mass registered before the sacrifice (24 weeks old). The data are expressed in median ± quartiles with min to max. The comparison between groups were performed using Mann-Whitney non-parametric test (*p≤0.05).*

The HFHS-female rats consumed the HFHS diet 7 weeks before pregnancy and throughout pregnancy and lactation, and the effects of maternal diet and exercise on maternal body mass are shown in Figure 10 A.

The results revealed that neither diet nor exercise had a significant impact on the females' body mass at the sacrifice time point, 24 weeks old (Figure 10 B). However, during gestation (13 to 16 weeks old), there was an increase in the body mass of the pregnant dams. As expected, during pregnancy all pregnant groups presented higher body mass when compared to their non-pregnant homologues. Also, at 2 weeks post-partum the dams from P_C_S groups weighted on average 376 g ± 12.51 which represents a 12.5 % of increase comparing with the NP_C_S group, with an average weight of 334 g ± 10.30.

Thus, the consumption of the HFHS diet induced an increase in maternal gestational weight gain (Figure 11). This increase comprised the weight gained from the first day of pregnancy until the day of delivery. During this period the P_HFHS_S with a median of 156 g (min = 138; max = 200; p = 0.0023) experienced a 22.8 % increase in body weight comparing with the

control with a median of 127g (min = 70; max = 140; p = 0.0023). Regarding the exercised group, with a median of 120 (min = 113; max = 139), it showed no difference in gestational weight gain regarding the control group. However, it showed a 30 % decrease in the gestational weight gain when compared with the P_HFHS_S group (p = 0.0043). These results show that exercise during pregnancy could revert the excessive maternal gestational body weight gain even in the presence of a HFHS diet.

Heart mass was measured to understand if the experimental treatments or pregnancy could alter the cardiac weight due to lipid accumulation or muscle hypertrophy. However, no alterations were found regarding this parameter (data not shown). Also, no variation was observed in the heart mass/body mass ratio (data not shown).

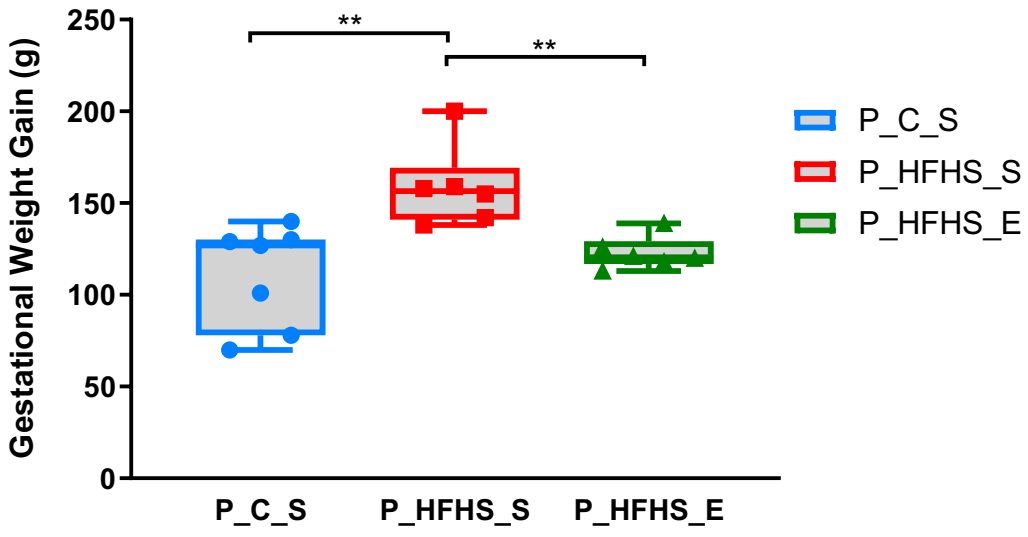

Figure 11. ***Maternal gestational body weight gain.*** *The data are expressed in median ± quartiles with min to max. The comparison between groups were performed using Mann-Whitney non-parametric test (*p≤0.05)*

The Oral Glucose Tolerance Test (OGTT) was applied to diagnose if a degree of glucose intolerance was developed, which could be related to insulin resistance and finally positively diagnose diabetic state. This was complemented with the tail prick testing. OGTTs were performed before pregnancy and at mid-pregnancy. Before mating, the ability to handling a load of 2mg/kg body weight of glucose was not different between the control and the HFHS group (Figure 12 A). However, during mid-pregnancy (Figure 12 B) the groups exhibited a distinct glycemic control, mirrored in distinct curves between the C and HFHS groups that culminate in differences in the area under the curve parameter (Figure 12 C). OGTT blood glucose levels were different at 15 minutes for C vs P_HFHS_S (106.0 ± 4.8 vs 143.0 ± 3.2; p<

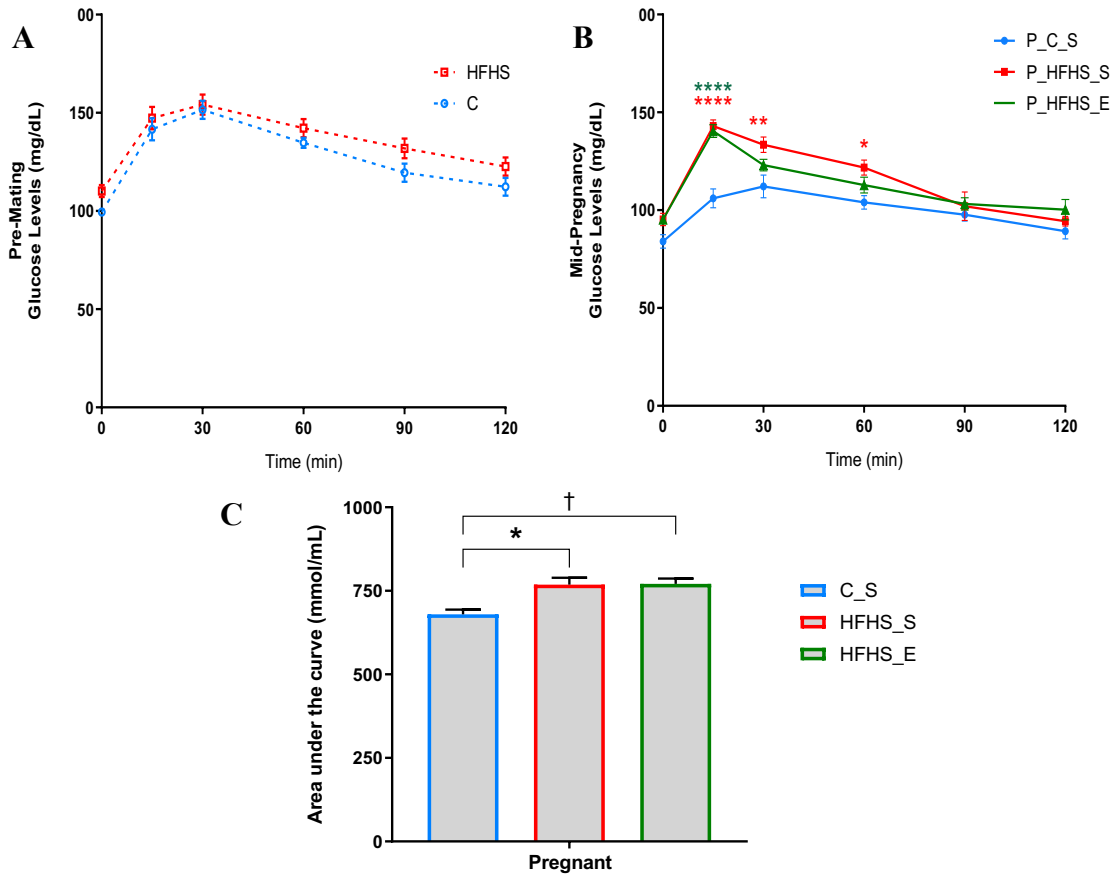

Figure 12. ***Oral Glucose Tolerance Test performed pre-mating and mid-gestation, presenting the blood glucose levels at 0, 15, 30, 60, 90, and 150 minutes after glucose ingestion, and respective post-mating AUC.*** *(A) Pre-mating levels are expressed as mean ± SEM, with comparison between Control (C, n=14) and High-Fat-High-Sugar (HFHS, n=22) groups performed with t-test corrected with Holm-Sidak method. (B) Mid-Pregnancy glucose levels are expressed as mean ± SEM, with comparison between pregnant: C_S (n=7); HFHS_S (n=6); HFHS_E (n=6) groups preformed with t-test corrected with Holm-Sidak method. ****p≤0.0001, **p≤0.01, *p≤0.05 for comparison of P_HFHS_S vs control, and ****p≤0.0001 for comparison of P_HFHS_E vs control. (C)Area under the curve values correspondent to the mid-pregnancy OGTT. The comparison between groups was performed using 2-way ANOVA, with the comparison between pregnant C_S (n=7) and HFHS_S (n=6) or HFHS_E (n=6) groups preformed with tukeys' test. † p≤0.1; and * p<0.05 for differences against control.*

0.000001) and for C vs P_HFHS_E (106.0 ± 4.8 vs 140.4 ± 3.3, p< 0.000001). These differences persist at 30 and 60 minutes between C and P_HFHS_S group (112.2 ± 5.9 vs 133.4 ± 3.9; p=0.0045 and 104.0 ± 3.5 vs 121.8 ± 3.9; p=0.019, respectively) (Figure 12 B). Furthermore, exercise seemed to reduce the impaired glucose tolerance induced by HFHS, since when comparing HFHS_S vs HFHS_E there is a tendency in HFHS_E to approximate with the C curve, without significant difference in glucose levels at 30 min of testing. Also, in the mathematical representation, the area under the curve correspondent to the mid-pregnancy OGTT test the same differences were observed. The HFHS_S (768.4 ± 31.42, p = 0.0452) developed a state of glucose intolerance comparing with the C_S (679.8 ± 28.87). Moreover, the HFHS_E (771 ± 30.39, p = 0.0527) showed only a tendency, which could suggest that exercise may revert the glucose intolerance state developed.

3.1.2 Characteristics of the offspring at birth.

The consumption of HFHS diet before and during gestation resulted in increased litter size. Control group had a median of 12 pups per litter (C=12, min. 11, max. 15). Moreover, P_HFHS_S had a median of 15.5 (min. 13, max. 18, p = 0.029 vs C) and P_HFHS_E had a median of 15 (min. 13, max. 16, p = 0.040 vs C) pups per litter (Figure 13 A). Other than the number, the litters also exhibited a different sex distribution, with significant difference between the number of males in the offspring of the P_C_S vs P_HFHS_S (5.57 ± 1.02 vs 8.68 ± 0.33, p = 0.032) (Figure 13 B).

Exercise during pregnancy was able to prevent the shift in the offspring sex distribution although it did not prevent the increase in litter size.

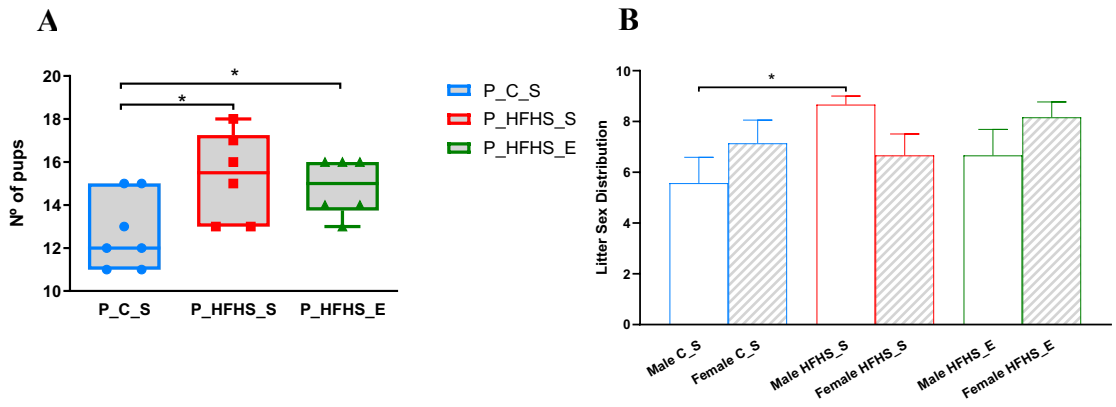

Figure 13. ***Maternal HFHS diet increased the litter size, recovered by exercise, and altered the litter sex distribution patterns.*** *(A)Litter size among the offspring of the experimental groups. The data are expressed as median ± quartiles with min to max. Comparisons were performed using Kruskal-Wallis non-parametric test followed by Mann-Whitney non-parametric t-test for multiple comparisons. (B) Sex distribution between male and female among the offspring of the experimental groups. The data are expressed as mean ± SEM. Comparisons were performed using Kruskal-Wallis non-parametric test followed by Mann-Whitney non-parametric t-test for multiple comparisons. (*p≤0.05).*

3.2 Mitochondrial Bioenergetics

3.2.1 A high-fat-high-sugar diet, isolated or when combined with exercise impairs complex I – dependent cardiac mitochondrial function oxygen consumption

Cardiac mitochondrial O_2 consumption was measured in isolated fractions using Clark-type electrode technique with the following steps/additions: basal, glutamate + malate (substrates of complex I, state 2), ADP (state 3), and FCCP (uncoupled state) to evaluate complex I – dependent cardiac mitochondrial function (Figure 14).

In state 2, a state in which the mitochondrial oxygen consumption is at a basal level, there was a 25 % increase in the OCR in the NP_HFHS_E with a median of -19.41 (min= -21.52, max= -16.26, p-value = 0.031) when compared with the NP_HFHS_S with a median of -15.48 (min= -21.12, max= -13.50). A similar result can be observed in the pregnant groups, with an increase of 23.7 % in the OCR of P_HFHS_E with a median of -18.78 (min= -24.29, max= -15.63, p-value = 0.026) when compared with P_HFHS_S with a median of -15.18 (min= -17.27, max= -13.42) (Figure 14 A). Regarding mitochondrial state 3, there were no differences in the OCR between the experimental groups (Figure 14 B). However, during state 4, which represents an oxygen consumption rate in which the mitochondrial respiration returns to a basal OCR, there was a 29.5 % increase in basal respiration of NP_HFHS_E with a median of -24.16 (min= -29.19, max= -18.85, p-value = 0.022) when compared with NP_C_S with a median of -18.66 (min= -21.15, max= -15.96), being also possible to observe a similar trend for NP_HFHS_S group (Figure 14 D). From the ratio between state 3 and state 4 it was possible to obtain the respiratory control ratio (RCR), is an indicator of the mitochondrial respiration coupling state. Regarding this parameter, the RCR of the NP_HFHS_E, with a median of 3.524 (min= 3.083, max= 5.884, p-value = 0.035), decreased 41.3 % when compared with the NP_C_S with a median of 6.006 (min= 4.758, max= 6.408). Also, there is a tendency that shows a slight decrease in the P_HFHS_E when comparing with the NP_C_S (Figure 14 C). Another indicator

often used in the literature to characterize mitochondrial state is the ADP/O ratio that allows to infer about the respiratory efficiency of mitochondria. The results showed a significant decrease in the ADP/O ratio of 24.3 % in the NP_HFHS_E with a median of 3.913 (min= 3.738, max= 4.427, p-value = 0.014) group when compared with the NP_C_S with a median of 4.940 (min=3.996, max= 9.570) group. Further, there is a tendency to a decrease in the NP_HFHS_S also when compared to the control (Figure 14 F).

FCCP was used to disrupt the membrane potential by allowing the movement of protons across the mitochondrial inner membrane, uncoupling the electron transport from the ATP synthase. This causes a maximum respiratory rate, since the ETC tries at all cost to restore the membrane potential. This was the measured parameter that registered more differences between the groups. A 5 % decrease in OCR of the NP_HFHS_S with a median of -139.7 (min= -161.7, max= -84.51, p-value = 0.027) compared to the NP_C_S with a median of -148.0 (min= -158.3, max= -114.4) was observed, decreasing even more, 34 %, when control is compared to NP_HFHS_ E with a median of -97.61 (min= -131.9, max= -93.38, p-value = 0.0047). A similar pattern is observed in the pregnancy groups, where there is an accentuated decrease of 20% in the OCR of the P_HFHS_E with a median of -111.5 (min= -123.0, max= -93.75, p-value = 0.0022) when compared with the P_C_S with a median of -140.2 (min= -175.8, max= -127.7). Also, when comparing the NP_C_S with the group with all the experimental variables, pregnancy, HFHS and exercise, there is a 24.7 % decrease in the maximum OCR with a p-value of 0.0082 (Figure 14 E). These results show that HFHS diet consumption decreased the electron transfer capacity, and the addition of exercise did not cause a recovery of the OCR consumption rate, instead it aggravated the effect of diet, becoming even lower the maximum OCR.

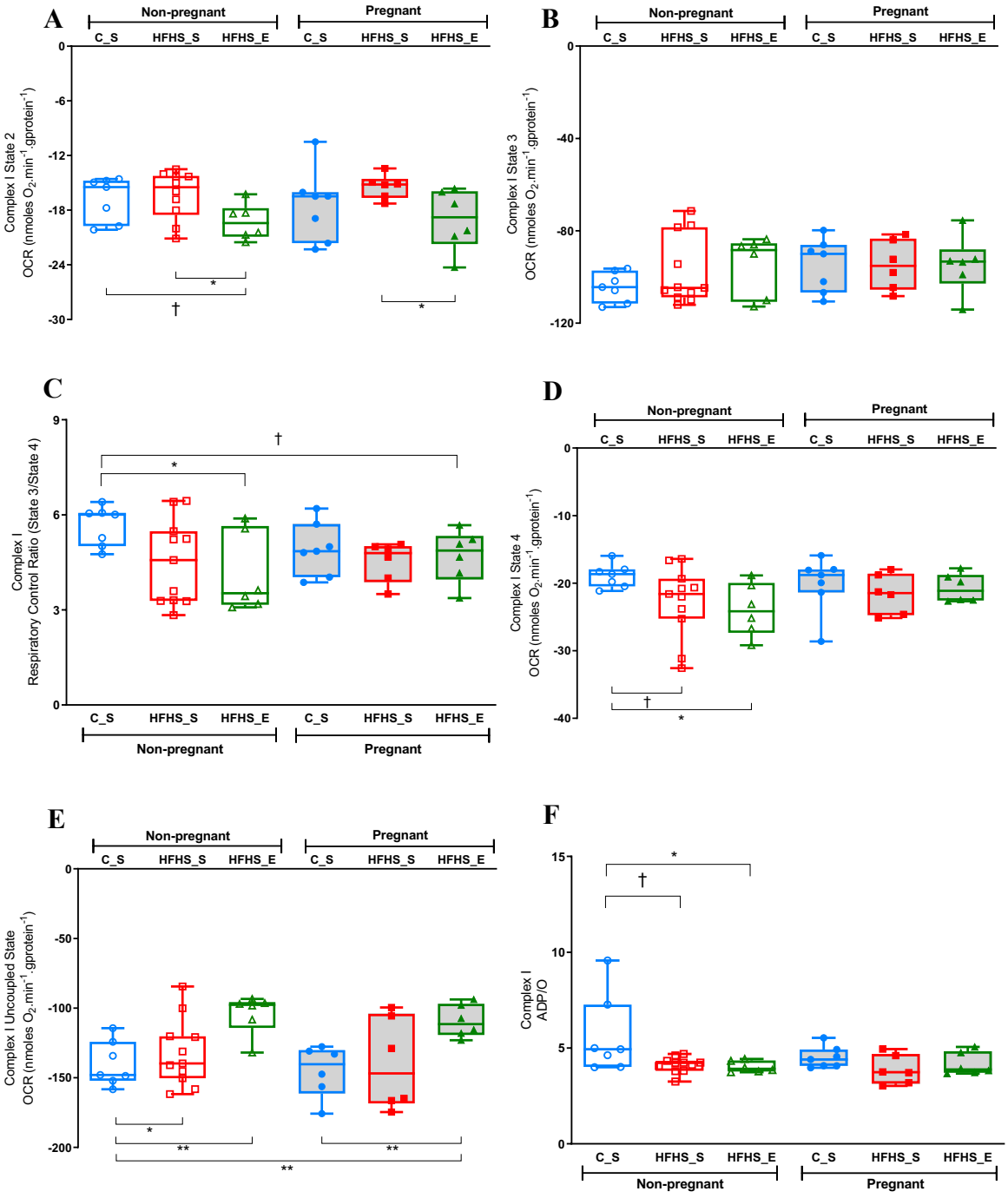

Figure 14. ***A high-fat-high-sugar diet, isolated or when combined with exercise alters complex I – dependent cardiac mitochondrial function oxygen consumption.*** *Mitochondrial respiratory parameters determined using complex I substrates, measured with Clark-type electrode. The data are expressed as medians ± quartiles with min to max. The comparison between groups as a whole was performed using Kruskal-Wallis non-parametric test, followed by Mann-Whitney test to determine which are the different groups. Statistical significance is represented as follows: † p≤0.1; *p≤0.05; **p≤0.01. (A) Mitochondrial state 2. (B) Mitochondrial state 3. (C) Mitochondrial Respiratory Control Ratio (RCR) determined by the ratio between state3 and state 4. (D) Mitochondrial state 4. (E) Mitochondrial uncoupled state induced with FCCP, causing maximum OCR. (F) ADP/O.*

3.2.2 Complex II – dependent cardiac mitochondrial function is minimally affected by a high-fat-high-sugar diet when combined with exercise

To evaluate complex II – dependent cardiac mitochondrial function, oxygen consumption rate was measured in isolated mitochondria with succinate as substrate, using Clark-type electrode technique allowing the determination of several respiratory parameters: state 2, state 3, state 4, uncoupled state, respiratory control ratio (RCR) and ADP/O, as described before (Figure 15). Complex II – dependent cardiac mitochondrial state 2, state 3, RCR, ADP/O and uncoupled state showed no significant differences between the groups. However, in state 4 it was observed a 17.5 % increase in oxygen consumption rate of the NP_HFHS_E with a median of -58.31 (min= -67.31, max= -51.55, p-value = 0.0023) group relative to the NP_C_S with a median of -49.61 (min= -55.16, max=-42.22) (Figure 15 D).

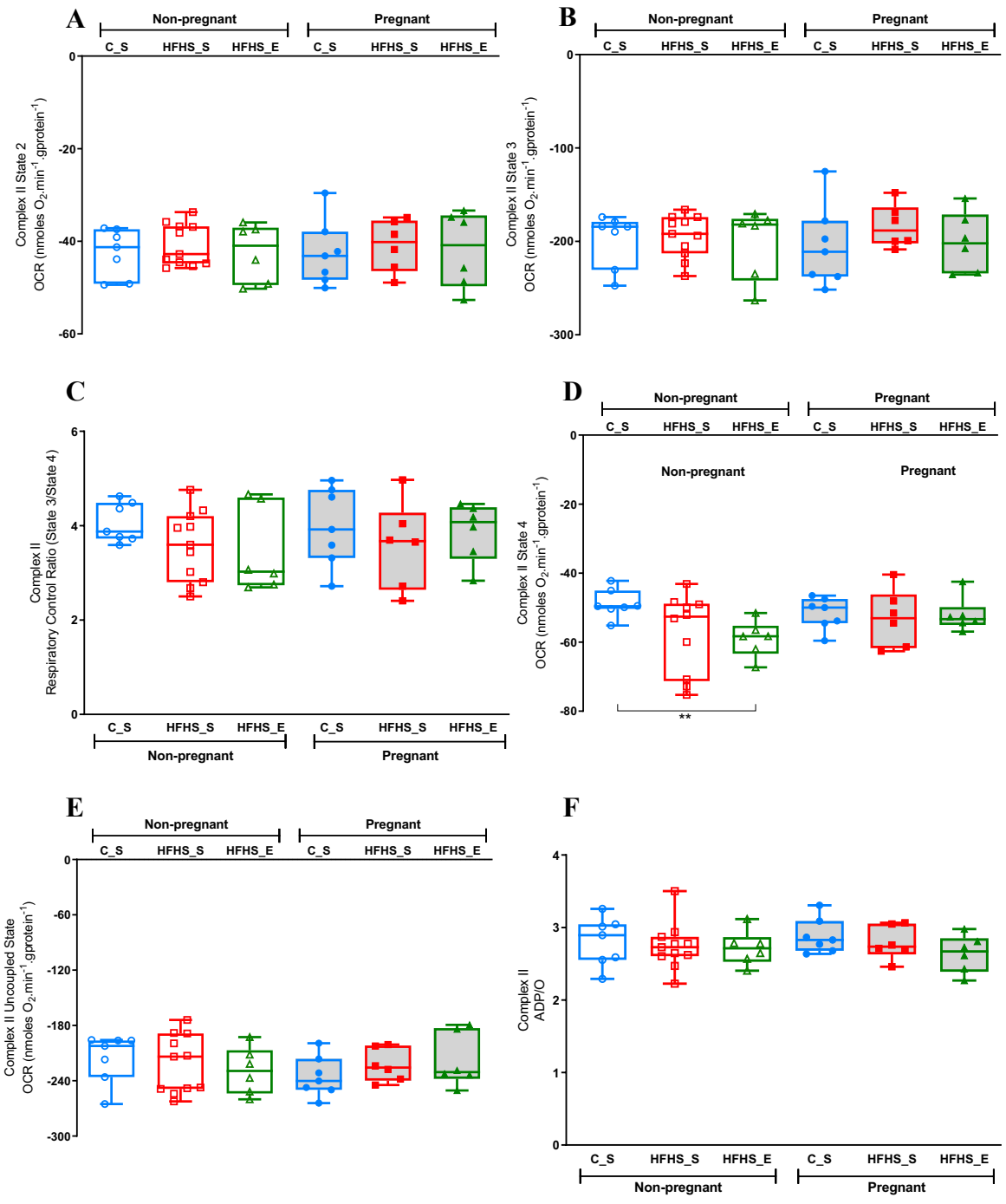

Figure 15. ***Complex II – dependent cardiac mitochondrial function is minimally affected by a high-fat-high-sugar diet when combined with exercise.*** *Mitochondrial respiratory parameters determined using complex II substrates, measured with Clark-type electrode technique. The data are expressed as medians ± quartiles with min to max. The comparison between groups as a whole was performed using Kruskal-Wallis non-parametric test, followed by Mann-Whitney test to determine which are the different groups. Statistical significance is represented as follows: † p≤0.1; *p≤0.05; **p≤0.01. (A) Mitochondrial state 2. (B) Mitochondrial state 3. (C) Mitochondrial Respiratory Control ratio. (D) Mitochondrial state 4. (E) Mitochondrial uncoupled state induced with FCCP, causing maximum OCR. (F) ADP/O.*

3.2.3 Pregnancy affects the cardiac mitochondrial membrane potential and high-fat-high-sugar and exercise modulate the mitochondrial repolarization time in pregnancy

Mitochondrial membrane potential was measured using a TPP^+ electrode that allows to indirectly determine parameters of the mitochondrial membrane potential, namely: the $\Delta\Psi_{max}$, $\Delta\Psi$ ADP, and lag phase (Figure 16). $\Delta\Psi_{max}$ represents the maximum variation in the mitochondrial membrane potential, and it is obtained in a basal mitochondrial respiratory state. Regarding complex I, there is a decrease in the maximum potential of the P_HFHS_E with a median of 176.8 (min= 171.9, max= 177.7, p-value = 0.026) when compared with the non-pregnant homologue NP_HFHS_E with a median of 178.2 (min= 176.7, max= 181.0) (Figure 16 A).

$\Delta\Psi$ ADP represents the variation on mitochondrial membrane potential upon depolarization induced by ADP injection. When complex I substrates were used, an increase of 12.3 % in the variation of mitochondrial membrane potential in the P_C_S with a median of -15.25 (min= -19.37, max= -14,64, p-value = 0.026), with a higher value of 21.6 %, in the P_HFHS_E with a median of -16.51 (min= -18.54, max= -15.18, p-value = 0.0012) both when compared with the NP_C_S with a median of -13.85 (min= -15.00, max= -11.98) (Figure 16 B). Regarding complex II, a significant increase of 19.7 % in NP_HFHS_S with a median of -12.02 (min= -14.29, max= -8.68, p-value = 0.020) was observed, comparing to NP_C_S with a median of -10.04 (min= -10.62, max= - 8.65), being this difference even greater, of 29.7 %, when NP_HFHS_E with a median of -13.02 (min= -23.18, max= -10.59, p-value = 0.0023) is compared to the control. (Figure 16 E). Furthermore, the results showed that P_C_S with a median of -12.87 (min= -17.93, max= -9.388, p-value = 0.038) has also a 28.2 % increased level of depolarization when comparing with NP_C_S, and again, there is a 23 % increase in

the mitochondrial membrane potential of P_HFHS_E with a median of -12.40 (min= -15.58, max= - 10.69, p-value = 0.0012) towards the same control (Figure 16 E).

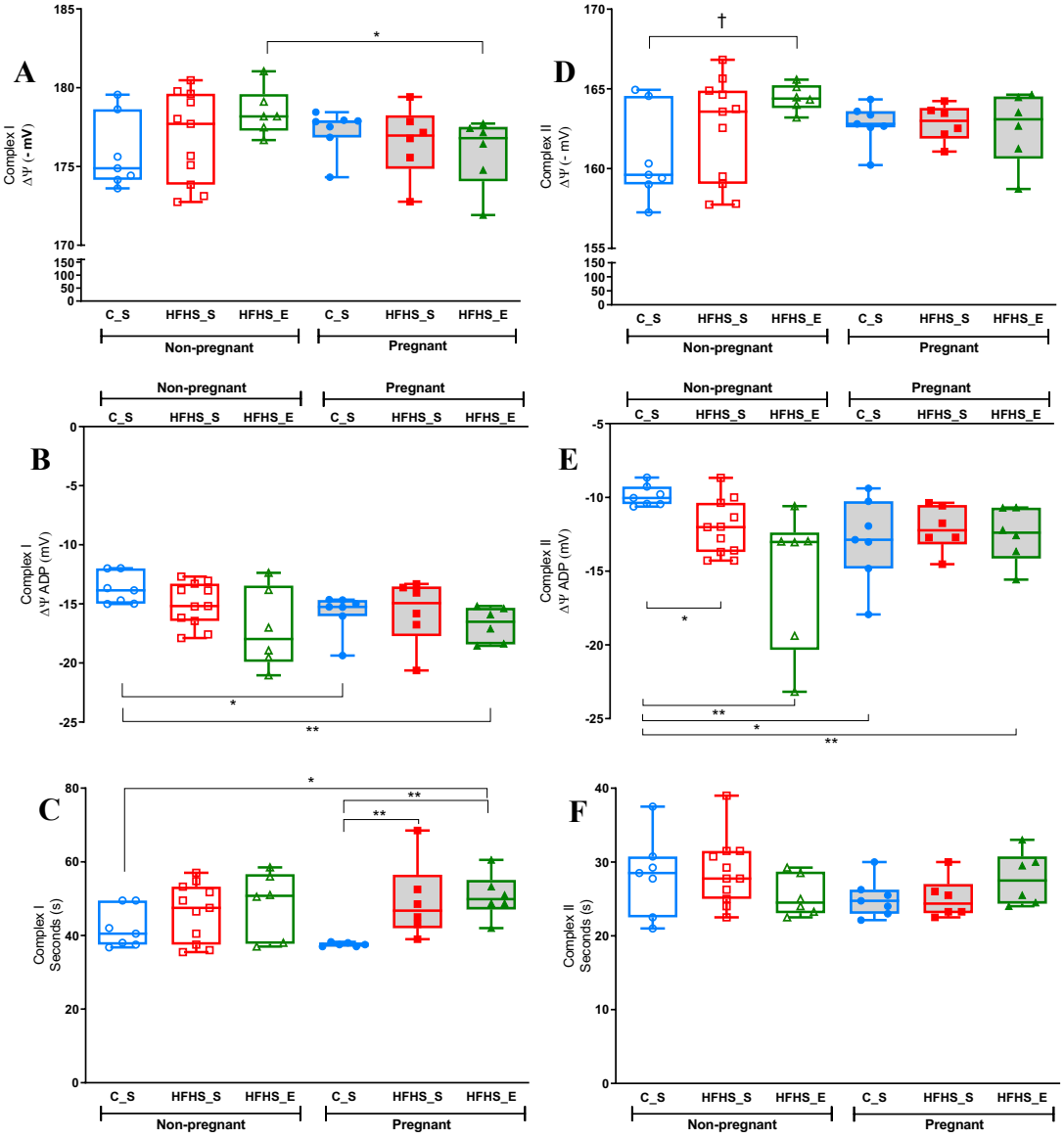

Figure 16. ***Pregnancy affects the cardiac mitochondrial membrane potential and high-fat-high-sugar and exercise modulate the mitochondrial repolarization time in pregnancy.*** *Mitochondrial Membrane Potential parameters measured with TPP+ electrode. The data are expressed as medians ± quartiles with min to max. The comparison between groups as a whole was performed using Kruskal-Wallis non-parametric test, followed by Mann-Whitney test to determine which are the different groups. Statistical significance is represented as follows: † p≤0.1; *p≤0.05; **p≤0.01. (A) $\Delta\Psi_{max}$ represents the maximum variation of the mitochondrial membrane potential obtained in a basal state when complex I substrates were used. (B) ΔΨ ADP represents the variation of the mitochondrial membrane potential when depolarization occurs, due to ADP injection. These results were obtained using complex I substrates. (C) Lag phase represents the period of time the goes from the beginning of depolarization, until complete reestablishment of mitochondrial membrane potential. These results were obtained using complex I substrates. (D) $\Delta\Psi_{max}$ represents the maximum variation of the mitochondrial membrane potential obtained in a basal state when complex II substrates were used. (E) ΔΨ ADP represents the variation of the mitochondrial membrane potential when depolarization occurs, due to ADP injection. These results were obtained using complex II substrates. (F) Lag phase represents the period of time the goes from the beginning of depolarization, until complete reestablishment of mitochondrial membrane potential. These results were obtained using complex II substrates.*

The lag phase represents the amount of time that goes from the beginning of depolarization, induced with ADP injection, until full usage of that substrate and reestablishment of the mitochondrial membrane potential. When complex I substrate were used, the lag phase was 33 % higher in the P_HFHS_E with a median of 49.88 (min= 42.00, max= 60.50, p-value = 0.012) and 24.7 % in the P_HFHS_S with a median of 46.75 (min= 39.00, max= 68.50, p-value = 0.015) groups versus the P_C_S with a median of 37.50 (min=37.00, max= 52.50). Also, the P_HFHS_E (p-value = 0.038) revealed to have a 23.2 % increased lag phase when compared to the NP_C_S with a median of 40.50 (min= 36.75, max= 49.50) groups (Figure 16 C).

Regarding complex II, no significant differences among the groups were detected **(**Figure 16 F).

3.3 Gene expression profiles

3.3.1 A high-fat-high-sugar diet, isolated or combined with exercise modulate the gene expression pattern

Next, the transcripts of several genes of interest were evaluated in order to better understand the results observed before and also to provide a broader characterization of the effects induced by the diet and exercise, with and without pregnancy in the cardiac tissue (Figure 17). For these results, the data were presented as expression profiles considering different comparations, attempting to give an overall picture of the expression of the chosen genes. The results show that there is a significant decrease in the transcription level of mitochondrial transcription factor A (mTFA) in the expression profile comparing the NP_HFHS_E (0.164 ± 0.083, p-value = 0.048) with the NP_HFHS_S group (Figure 17 B). Regarding the mitochondrial-related genes, no other significant alteration was found. Regarding genes related with fatty acid metabolism, significant decrease was observed in Peroxisome Proliferator Activator Receptor Alpha (PPARα) in the expression profile that compares NP_HFHS_E (0.257 ± 0.104) with NP_C_S (Figure 17 C). Also, a tendency was observed for a decrease in the expression levels of PPARα when NP_HFHS_E is compared with NP_HFHS_S. Furthermore, regarding the expression pattern of ACOX1 there are a similar increasing tendency both when comparing the NP_HFHS_E group with the NP_C_S and with the NP_HFHS_S group. Moreover, there is a significant increase in the expression levels of the ACAA2 gene when comparing the P_HFHS_S (2.032 ± 0.25) with the P_C_S. Also, a tendency is observed when the P_HFHS_E is confronted with the P_C_S group. Overall the results are focused mainly in the genes involved in the fatty acid metabolism.

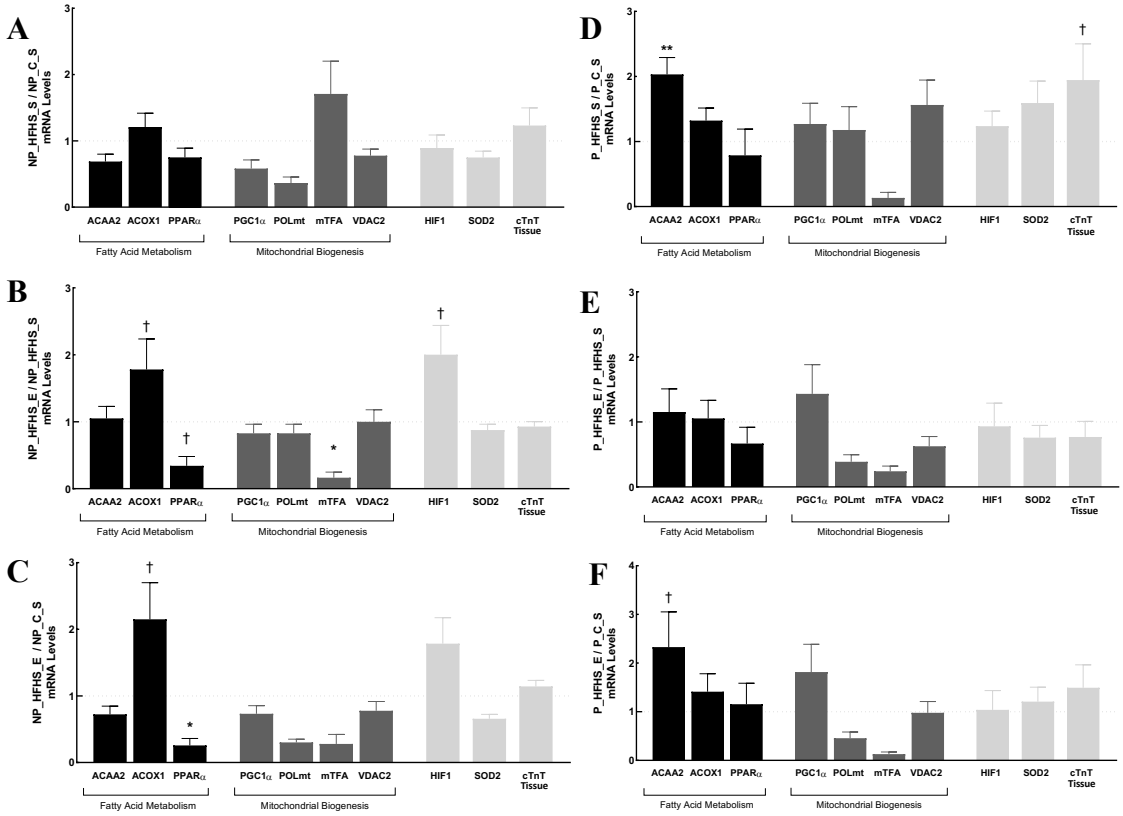

Figure 17. ***A high-fat-high-sugar diet, isolated or combined with exercise modulate the gene expression pattern.*** *The transcripts expression levels were determined by qPCR technique and were normalized by the expression levels of 3 housekeeping genes as references: 18s, β-Actin and GAPDH. In each graph, the expression profile resultant of the comparison of one group towards the other is shown. The data are expressed as means ± SEM. The comparison between groups was performed with Mann-Whitney non-parametric t -test. Statistical significance is represented as follows: † p≤0.1; *p≤0.05; **p≤0.01. (A) mRNA expression profile of NP_HFHS_S compared with the NP_C_S group where its expression level for each gene was matched to 1 and the levels of NP_HFHS_S are presented as fold variation. (B) mRNA expression profile of NP_HFHS_E compared with the NP_HFHS_S group where its expression level for each gene was matched to 1 and the levels of NP_HFHS_E are presented as fold variation. (C) mRNA expression profile of NP_HFHS_E compared with the NP_C_S group where its expression level for each gene was matched to 1 and the levels of NP_HFHS_E are presented as fold variation. (D) mRNA expression profile of P_HFHS_S compared with the P_C_S group where its expression level for each gene was matched to 1 and the levels of P_HFHS_S are presented as fold variation. (E) mRNA expression profile of P_HFHS_E compared with the P_HFHS_S group where its expression level for each gene was match to 1 and the levels of P_HFHS_E are presented as fold variation. (F) mRNA expression profile of P_HFHS_E compared with the P_C_S group where its expression level for each gene was match to 1 and the levels of P_C_E are presented as fold variation.*

3.3.2 Pregnancy by itself mildly modifies certain gene transcription patterns, however it influences the effects of HFHS diet and exercise

This topic shows the mRNA transcripts modulations in the cardiac tissue that were promoted by pregnancy as the main factor. When pregnancy control was compared to the non-pregnant control, no significant alterations were detected; however, it was possible to distinguish two

different tendencies, a decrease in PPARα levels (0.468 ± 0.157) and a tendency for an increase in the expression levels of Hypoxia Inducible Factor 1 (HIF1) (1.982 ± 0.313) (Figure 18 A). Moreover, when the pregnancy was associated with a high-fat-high-sugar diet and compared to the NP_HFHS_S groups, a greater effect of pregnancy was detected confirming the increase in HIF1 (2.474 ± 0.466, p-value = 0.023). Also, in the same comparison a significant decrease in the levels of mTFA transcript (0.124 ± 0.078, p-value = 0.028), and a highly significant increase in the mRNA expression levels of ACAA2 (2.137 ± 0.271, p-value = 0.0048) were measured (Figure 18 B).

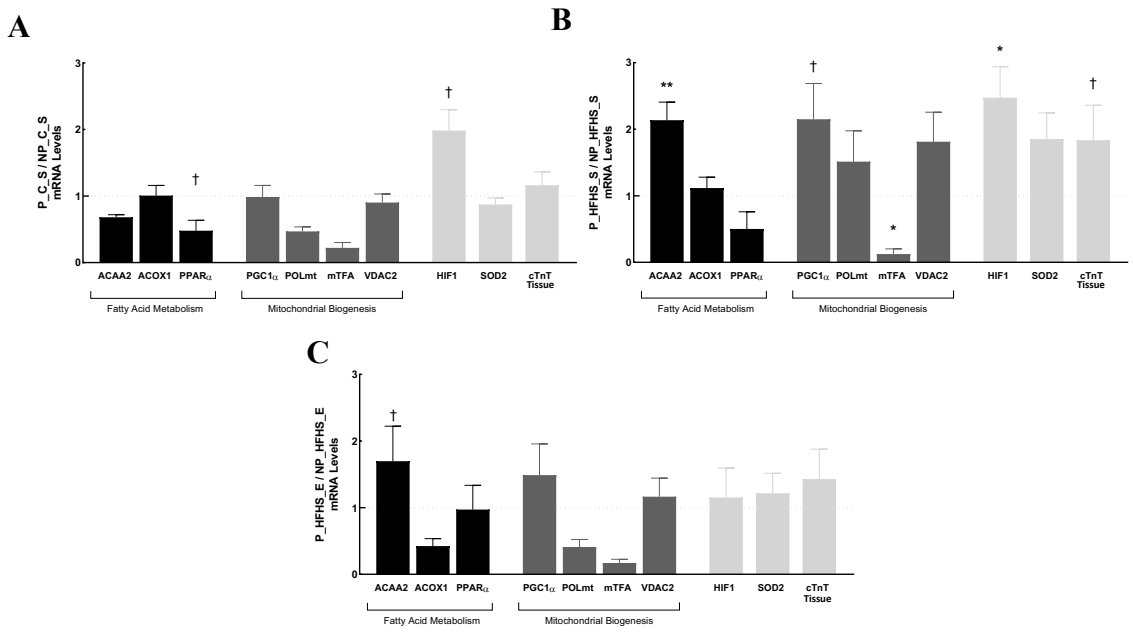

Figure 18. ***Pregnancy by itself mildly modifies certain gene transcription patterns, however it influences the effects of HFHS diet and exercise.*** *The mRNA expression levels of the genes were determined by qPCR technique and normalized by the expression levels of 3 housekeeping genes as references: 18s, β-Actin and GAPDH. In each graph it is presented an expression profile resultant of the comparison of one group towards the other. The data are expressed as means ± SEM. The comparison between groups was performed with Mann-Whitney non-parametric t -test. Statistical significance is represented as follows: † p≤0.1; *p≤0.05; **p≤0.01. (A) mRNA expression profile of P_C_S compared with the NP_C_S group where its expression level for each gene was matched to 1 and the levels of P_C_S are presented as fold variation. (B) mRNA expression profile of P_HFHS_S compared with the NP_HFHS_S group where its expression level for each gene was matched to 1 and the levels of P_HFHS_S are presented as fold variation. (C) mRNA expression profile of P_HFHS_E compared with the NP_HFHS_E group where its expression level for each gene was matched to 1 and the levels of P_HFHS_E are presented as fold variation.*

In the last graph, a less conspicuous effect of pregnancy when the P_HFHS_E group is compared to the NP_HFHS_E group is observed. Nevertheless, a tendency was observed in increase in the ACAA2 expression levels (1.697 ± 0.527) (Figure 18 C).

Overall, the pregnancy when combined with the HFHS diet produced a greater impact on the mRNA expression profile.

3.4 Protein level profiles

3.4.1 A high-fat-high-sugar diet, isolated or combined with exercise altered the protein level of mitochondrial related proteins

Several interest proteins were selected to allow a broad perspective of possible alterations that could be induced by the experimental conditions. The results revealed that the protein levels of mitochondrial ETC proteins were decreased. Namely, a decrease in the protein level of complex IV when NP_HFHS_S (0.308 ± 0.143, p-value= 0.0381) group was compared with NP_C_S (Figure 18 A). Moreover, the exercise, when in combination with the diet greatly caused a decrease in the protein level of Complex III subunit (NP_HFHS_E; 0.247 ± 0.069, p-value = 0.017), comparing to levels of the NP_HFHS_S group (Figure 18 B). That decrease is accentuated even more when the NP_HFHS_E (0.337 ± 0.094, p-value= 0.0079) group is compared with the NP_C_S (Figure 18 C). Other mitochondrial protein that showed significant differences was TOM20, being increased when diet is combined with exercise (NP_HFHS_E; 1.486 ± 0.047, p-value= 0.042) comparing with NP_HFHS_S group (Figure 18 B). Overall, no other significant alteration was detected in the remaining protein levels.

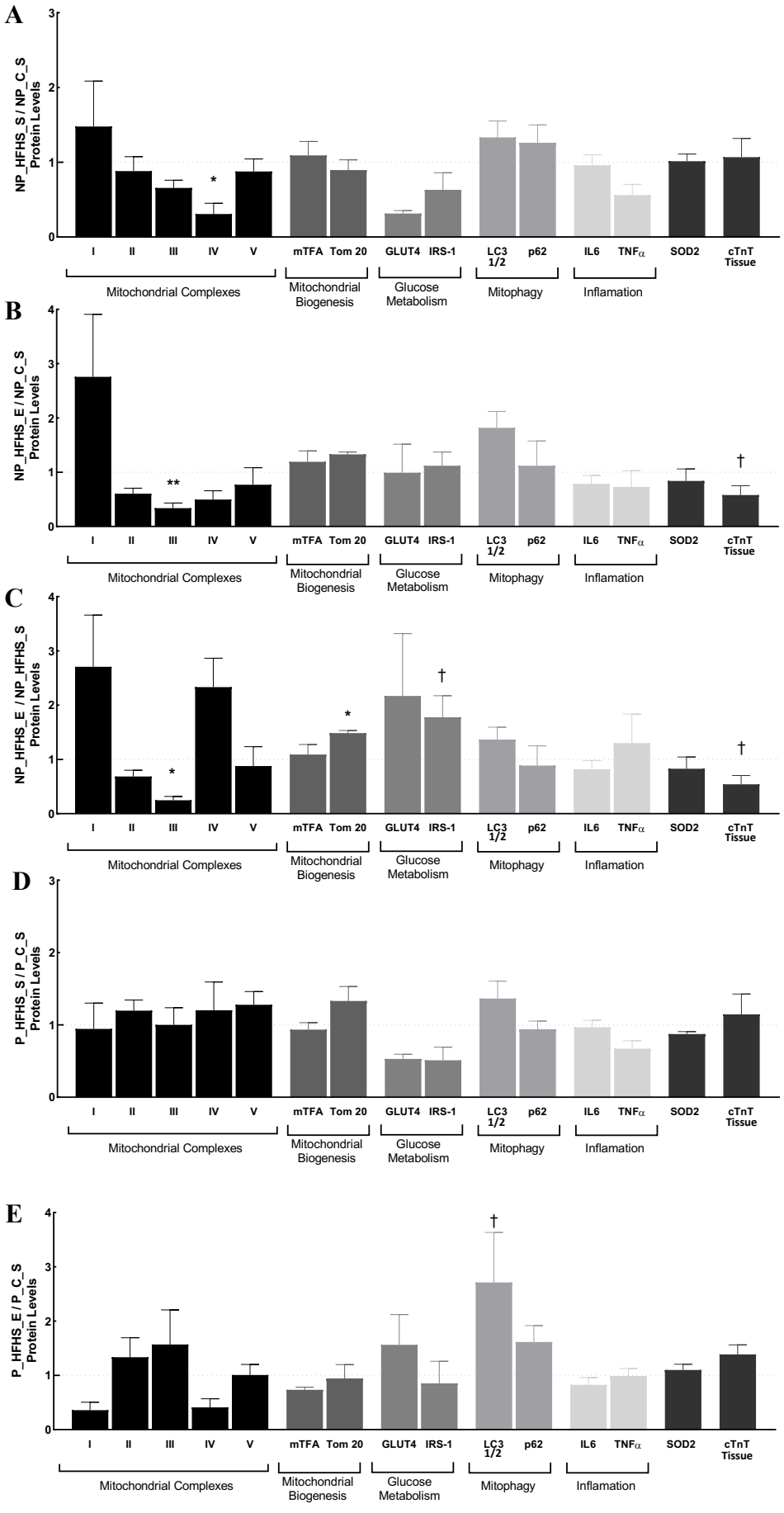
A
NP_HFHS_S / NP_C_S Protein Levels
B
NP_HFHS_E / NP_C_S Protein Levels
C
NP_HFHS_E / NP_HFHS_S Protein Levels
D
P_HFHS_S / P_C_S Protein Levels
E
P_HFHS_E / P_C_S Protein Levels
I II III IV V
mTFA Tom 20
GLUT4 IRS-1
LC3 1/2 p62
IL6 TNFα
SOD2
cTnT Tissue
Mitochondrial Complexes
Mitochondrial Biogenesis
Glucose Metabolism
Mitophagy
Inflamation

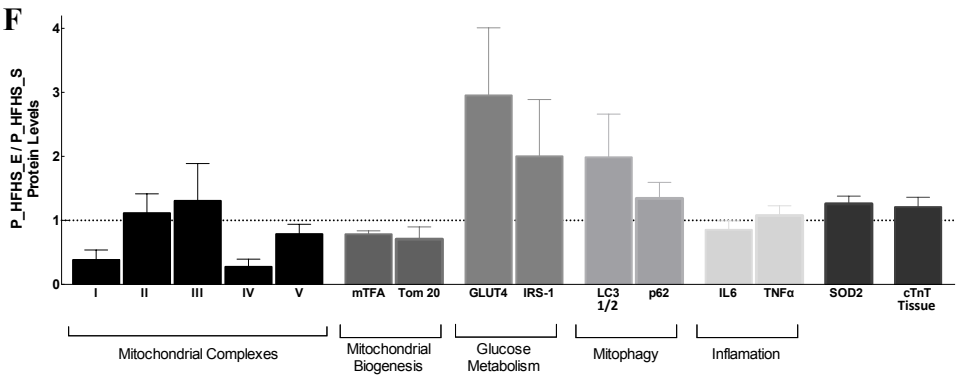

Figure 19. ***High-fat-high-sugar diet, isolated or combined with exercise altered the protein level of mitochondrial related proteins****. Different profiles of protein levels according to the band density of each group. The band density was normalized by Ponceau and the values are presented as fold variation between the compared groups. (A) Protein level profile of NP_HFHS_S compared to the NP_C_S; (B) Protein level profile of NP_HFHS_E compared to the NP_HFHS_S; (C) Protein level profile of NP_HFHS_E compared to the NP_C_S; (D) Protein level profile of P_HFHS_S compared to the P_C_S; (E) Protein level profile of P_HFHS_E compared to the P_HFHS_S; (F) Protein level profile of P_HFHS_E compared to the P_C_S; The data are expressed as means ± SEM. The comparison between groups was performed with Mann-Whitney non-parametric t -test. Statistical significance is represented as follows: † p≤0.1; *p≤0.05; **p≤0.01.*

3.4.2 Pregnancy mediates alterations in protein levels promoted by the HFHS diet and the exercise when combined

When performing the characterization of the pregnancy-modulated mitochondrial proteins between the sedentary animals with control diet (P_C_S vs NP_C_S) almost no significant alteration in the pattern of protein level was detected, or even when the same comparison was made between the animals with the HFHS diet (P_HFHS_S vs NP_HFHS_S). Nevertheless, there is a tendency for an increase in the protein level of Complex IV subunit MTCO1 when the P_HFHS_S group is compared to the NP_HFHS_S group (Figure 19A and 19B).

However, when HFHS diet and exercise are combined during pregnancy (P_HFHS_E) a series of alterations appear compared to the respective non-pregnant group (NP_HFHS_E). A highly significant increase is observed in the protein level of cTnT (2.701 ± 0.346, p-value = 0.0087), which is not observed in any other comparison. A decrease is observed in the protein level of complex III UQRC2 subunit (0.791 ± 0.320, p-value = 0.0317). Also, a tendential decrease is observed in the protein levels of Tom20. In general, mitochondrial related proteins seem to be

more altered in the results presented, with a great increase in the levels of cardiac troponin T, a cardiac regulatory protein that control the calcium mediated interactions between actin and myosin and is used as a marker for cardiac damage when detected in the serum.

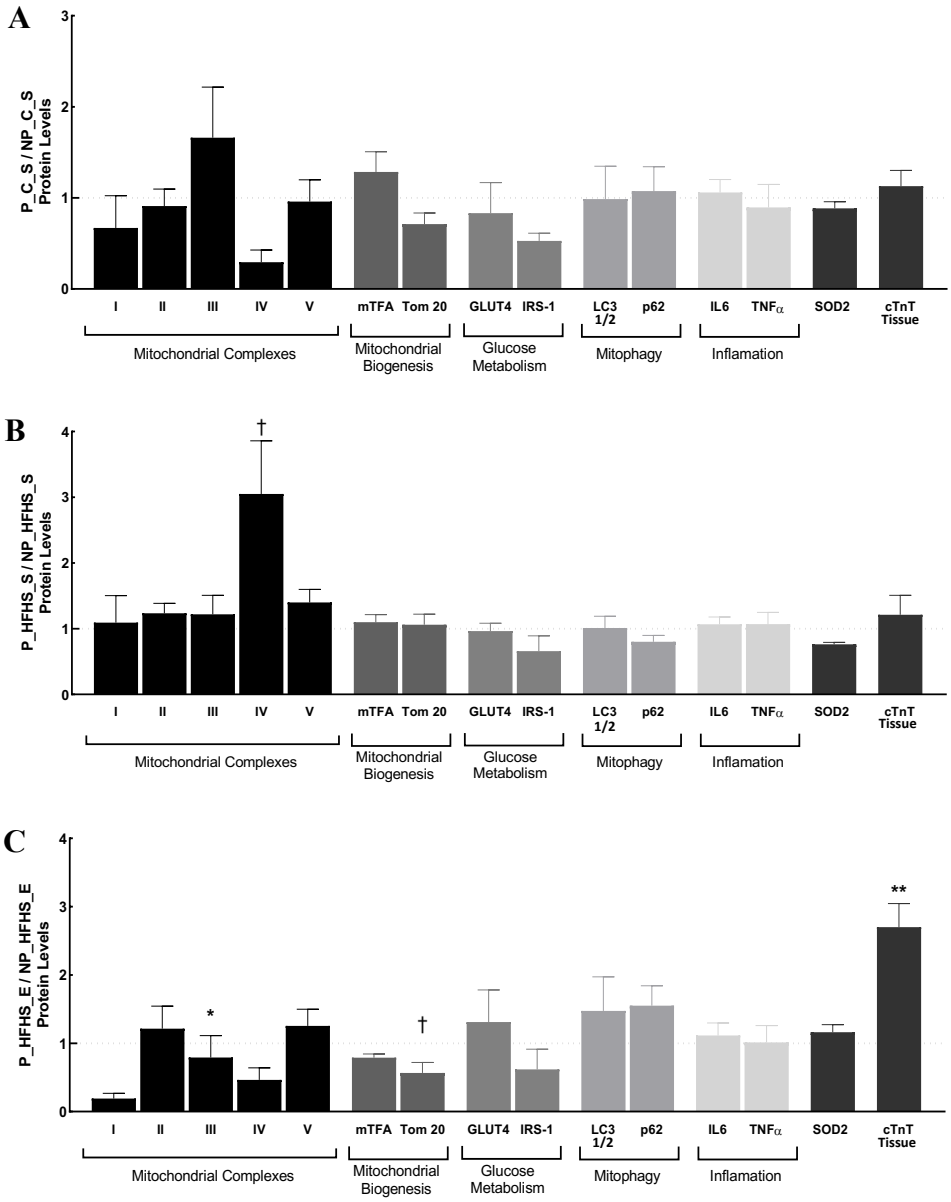

Figure 20. ***Pregnancy-mediated alterations in the protein levels of key proteins.*** *The present graphs represent different profiles of protein levels according to the band density of each group. The band density was normalized by Ponceau and the values are presented as fold variation between the compared groups: (A) Protein level profile of P_C_S compared to the NP_C_S; (B) Protein level profile of P_HFHS_S compared to the NP_HFHS_S; (C) Protein level profile of P_HFHS_E compared to the NP_HFHS_E; The data are expressed as means ± SEM. The comparison between groups was performed with Mann-Whitney non-parametric t -test. Statistical significance is represented as follows: † p≤0.1; *p≤0.05; **p≤0.01.*

4. DISCUSSION

4.1 A Gestational diabetes mellitus model or a high-fat-high sugar model?

GDM has increased its incidence in the last years being the most common disease that can occur during pregnancy[126]. The main risk factor that has been contributing to this trend is the worldwide increasing levels of obesity, highly related to a rise in sedentary lifestyle and unhealthy food consumption, especially in developed countries[13,39,126]. Further, it has already been described that consumption of a HFHS diet in rodent model could successfully mimic hallmarks of gestational diabetes mellitus, namely a state of glucose intolerance, development of insulin resistance, and hyperglycemia.[11]. An excessive gestational weight gain has also been considered as another feature of GDM, nevertheless gestational weight gain is a physiological event that occurs naturally during pregnancy due to tissue growth, fluid retention and fetal development.[1,11].

For the purpose of this work, it was important to develop a model that mimicked hallmarks of GDM which would allow the accurate study of the pathological events that follow a GDM pregnancy. Given that, we fed a rodent model with a diet rich in dextrin (11,1%), sucrose (20,4%) and crude fat (23%), an HFHS diet to induce GDM hallmarks.

As aforementioned, an excessive gestational weight gain can be considered a hallmark of GDM. In our results, we observed that the group fed with an HFHS diet had a significant increase of 54% in the gestational weight gain compared with the control which had a normal weight gain associated with pregnancy. Further we saw that the exercised group showed no difference comparing to the control group (P_HFHS_E vs P_C_S) and that had a gestational weight gain 30% lower than the HFHS sedentary group, meaning that exercise was able to revert the excessive gestational weight gain that was caused by the ingestion of an HFHS diet and a

sedentary style (P_HFHS_S vs P_HFHS_E). Moreover, during the lactation period that follows birth, P_C_S continued to show a higher weight, when compared with the NP_C_S, however it is possible to observe also that the P_HFHS_E group has a weight behavior that is closer to the non-pregnant control, which suggests that exercise contributed towards a faster recovery of the pregestational weight. Although no statistical significance was observed, the HFHS_S group had an apparent slower recovery, being closer to the weight level of the P_C_S group. It has already been shown that exercise could lead to a quicker recovery after a pregnancy[127–129]. Studying maternal obesity in a rodent model, Vega et al. found that exercise could recover several metabolic parameters that were deregulated in obese mothers, such as increased blood levels of insulin, cholesterol, glucose, triglycerides, and leptin[128]. With exercise, those levels returned to levels similar to the controls; however, in terms of maternal weight they saw that exercise did not alter this parameter[128]. Nonetheless, it is important to remember that part of the gestational weight gain results of fat accumulation, so that the mother can support the child during the lactation period. Contrarily, breastfeeding requires a high level of energy that causes a negative pressure on energy equilibrium leading to maternal weight loss and ideally recovery of the pregestational weight[130]. Therefore, since exercise also causes an increase in the energy requirements, we believe that the P_HFHS_E group has an apparent quicker recovery due to the effect of exercise. With these data presented before we can assume that our results suggest that exercise could be a powerful approach to manage not only the percentage of weight gain during gestation but also to improve the postpartum recovery of the maternal pregestational weight.

To evaluate the glucose homeostasis, OGTT was performed since it is the gold standard diagnosis to detect any sort of intolerance to glucose. The test was performed in two different time points, before a pregnancy state and in the second week of gestation. Since GDM is often defined as a state of glucose intolerance with first onset during pregnancy, it was crucial that

the ingestion of a HFHS diet did not cause an imbalance in the glucose homeostase before pregnancy. Our results showed that there were no differences in glucose levels measured in the OGTTs performed to the non-pregnant animals that were fed a control diet and to the ones fed with a HFHS diet. Interestingly, when the same procedure was performed during pregnancy, we found significant differences in the glucose levels, specifically 15, 30 and 60 minutes after the ingestion of glucose, reporting an impaired glucose metabolism. Those results suggest that the animals that were fed with an HFHS diet developed a degree of glucose intolerance. So, the impaired glucose metabolism and increased gestational weight gain, hallmarks of GDM were successfully reproduced. Similar results were observed in studies performed by Pereira et al [9]. Surprisingly the P_HFHS_S group also exhibited increased litter size, with a median of 15.5 pups per litter. It has being described, in a mild gestational hyperglycemic rat model that when the litter size exceeds 15 newborns the macrosomia is less than 5%[131]. Perhaps increasing the litter size can be an alternative way to spend the excess of nutrients in polytomous species, representing an alternative route of the macrosomia in the monotocous human. Moreover, the explanation for this event could lie in a basic phenomenon of species survival. One of the most powerful driving forces of natural selection is the abundance/availability of food, and many species can alter their reproductive strategies accordingly[132]. In cases of food restriction, some species can delay the fertile period, or decrease the size of the litter in order to improve fitness and do not spare endogenous energy resources. This are common trade-offs observed in the nature that can also be observed when there is plenty of food supplies. The fertile period of the females is more frequent or even constant, and the number of pups in each gestation is also increased. This could be the explanation for a higher number of pups in the litter from the animals that were fed an HFHS diet, simply because they had access to a more caloric diet that allowed to allocate a greater amount energy to produce a greater litter size. However, it is

important to highlight that the mechanisms that drive these processes are not clearly understood nor were evaluated in the present work.

The arguments presented above allow to affirm that through ingestion of a HFHS diet it was possible to mimic some of the features of GDM, and that this is an accurate model to study the disease.

Regarding the group that was fed with an HFHS diet but practiced exercise during pregnancy the results showed that the degree of glucose intolerance developed by this group was lower, since P_HFHS_E only showed a significant increase in the glucose level in the first time point after the ingestion of glucose (15 min), being able to obtain similar glucose levels to P_C_S in the remaining tested time points, which suggest that physical activity could have minimized the impact of diet and improved glucose metabolism. Moreover, there are already evidences showing that physical activity could be a powerful mechanism to regulate glucose homeostase and improve insulin sensitivity in non-pregnant subjects[133]. Nevertheless, P_HFHS_E also developed a degree of glucose intolerance when compared with P_C_S, meaning that the protocol of exercise applied was unable to completely reverse the effects of the excessive diet. As a future perspective, an interesting parameter that could be measured is the pre- and mid-pregnancy insulin plasma levels, since they could have revealed if the HFHS diet had induced alterations in the insulin levels, showing another GDM hallmark, that is already described as being altered with first onset during pregnancy[9].

4.2 Cardiac mitochondrial function modulation by pregnancy, high-fat-high-sugar induced GDM and exercise

As aforementioned, mitochondria play a crucial role in cardiac cells being absolutely essential for the energy demands that a beating heart requires. In a pregnancy with GDM, the challenge that the heart is subjected to increases substantially, and that could be the underlying reason for

the incidence of cardiovascular diseases in the years that follow a diabetic pregnancy[21]. Further, this could mean that during a GDM pregnancy, the stress to which cardiomyocytes are subjected could lead to a degree of mitochondrial dysfunction that later in life can progress and emerge a cardiovascular disease. This study aims to understand if physical exercise could play preventive role, avoiding a future cardiovascular disease through improvement of mitochondrial function during pregnancy.

Mitochondrial function was measured in isolated mitochondria through Clark-type electrode technique to assess the oxygen consumption rate and the variations in the mitochondrial membrane potential, that allows to extrapolate about the electron transfer capacity of the ETC, how coupled is the transport of electrons to the production of ATP, and about the state of permeability of the inner mitochondrial membrane.

Concerning mitochondrial bioenergetics data, we observed two main features. The first one was that complex I appeared to play a determinant role in the effects caused by the experimental variables since it presented more alterations in the parameters measured, comparing with the results showed in complex II-dependent OCR. The second was that the majority of alterations were observed in the non-pregnant groups, often without alterations in the pregnant groups. Meaning that pregnancy by itself, as a variable, is acting as a "double-agent", since it can outcrop alterations in mitochondrial bioenergetics, as well as protect against others.

Regarding complex I involvement, when oxygen consumption was based on complex I substrates (G/M), the mitochondria from the groups exposed to an HFHS diet and exercise had an increased basal respiration, namely in state 2. In this state, only endogenous substrates are consumed so the oxygen consumption is at the minimum rate. However, this rate can become higher due to proton leakage in cases where the mitochondrial inner membrane is not well sealed, allowing the passage of protons and causing a variation in the mitochondrial membrane potential[134]. Also, the passage of protons through the ATP synthase without ATP production or

through the cycle of cations could be responsible for increased basal oxygen consumption. These events will trigger the ETC to restore the membrane potential, leading to higher oxygen consumption rate. For that reason, state 2 is sometimes named in the literature as proton leak. Although this increase in basal respiration was not observed in the sedentary groups, we cannot directly assume that exercise was the cause of the rise in the basal respiration. Further, we hypothesized that the diet may already be a challenge for mitochondria, since previous work related that diet could alter hepatic mitochondrial membrane lipid composition and disrupts bioenergetics[135]. However, in our model HFHS diet is still a manageable challenge to which mitochondria are able to cope. However, when a variable such as exercise is added to the equation the two challenges may be too overwhelming and hidden alterations start to appear. This pattern is observed again in state 4, which comprises the return to basal oxygen consumption rate after complete phosphorylation of ADP. Again, there is increased basal OCR which could be derived from proton leak. A possible explanation for these results could reside in the overexpression of mitochondrial uncoupling proteins (UCPs)[136]. These proteins are able to facilitate the transport of protons from the mitochondrial matrix to the intermembranar space, disrupting the mitochondrial membrane potential and uncoupling the ETC from the ATP synthase, causing an increase in the OCR[137].

A recent study on diabetic cardiomyopathy induced with a high-fat diet in a rodent model showed that mitochondria from diabetic mice had upregulated protein levels of uncoupling protein 2 (UCP2), which are known to increase their expression with enhanced fatty acid metabolism[136]. Wang and colleagues described that mitochondria with high levels in UCP2 had an increased OCR in state 4. Contrarily, the exercised mice exhibited a lower state 4, and decreased protein levels of UCP2, which suggests that mitochondria from exercised mice had better coupling[136]. In other study, it was reported that in Akita mice with type I diabetes, myocytes had a higher abundance of fatty acid-oxidation proteins, which was correlated with

the development of diabetic cardiomyopathy[138]. Interestingly, in our qPCR results we observed that the diet caused a tendential overexpression of ACOX1 in the non-pregnant groups. Also, in the pregnant groups diet isolated or in combination with exercise also led to overexpression of ACAA2. Both these genes encode proteins that are involved in the catabolic process of fatty acids[139,140]. These results may suggest that the fatty acid metabolism is enhanced which could lead to proton leakage, through UCP overexpression. However, in our data, the exercise combined with an HFHS diet exerted the opposite effect to the one observed in the UCPs study, since exercise was not able to revert the increased OCR in state 4. Nevertheless, as a future perspective, it would be interesting to measure the protein levels of UCPs in the cardiac tissue of the experimental groups to better understand these results. Further, we calculated the RCR through the ratio of state 3, a state of ADP stimulated respiration which increase oxygen consumption rate, by state 4 which follows state 3 and represents the return to a basal oxygen consumption rate. This parameter allows to infer about the coupling capacity of the mitochondria, and again the results pointed that the combination of diet and exercise decreased the RCR in the non-pregnant groups, which is in accordance with the hypothesis presented before. Also, the same result was obtained when we measured the number of ATP molecules formed per oxygen consumed (ADP/O), which can be used to infer the efficiency of respiration. Since the amount of ADP added is the same, if mitochondria require more oxygen to fully phosphorylate the ADP added to the system, then this means that there is oxygen being consumed without being used to produce ATP. Following, it suggests that mitochondrial coupling is impaired. Interestingly, by measuring the amount of time to fully consume ADP, no differences were observed in the non-pregnant groups. However, in the pregnant groups, we observed that diet induced a slower ADP phosphorylation rate, requiring longer time to phosphorylate the same quantity of ADP, and this effect was exacerbated by exercise. Despite the alterations in lag phase duration, no alterations in the RCR or in the ADP/O was registered.

This was an interesting outcome, since if mitochondria are slower to phosphorylate a same amount of ADP, then it may be possible to observe some fluctuations in the coupling and efficiency indicators, or some fluctuations between groups in the OCR measured in state 3. Likewise, in the literature, studies, not only in cardiac mitochondria, revealed that increased lag phase also have decreased state 3, and consequently alterations in the ADP/O ratio or the RCR[141–143]. Nevertheless, it is important to salient that the ADP/O is often the last parameter to be disturbed. Also, in a study of type I diabetes, cardiac mitochondria from diabetic mice showed decreased state 3 when measured with complex I substrates glutamate/malate[138]. Moreover, Ascensão and colleagues found that doxorubicin treatment in a rodent model caused decreased state 3 and prolongated lag phase in cardiac mitochondria, and that exercise could revert this deleterious effect of doxorubicin and restore state 3 with shorter lag phase[144]. Although our results point to an opposite direction it is important to highlight that our results were obtained in a different novel model, with meager characterization in the literature, that may not be directly comparable to the results obtained in the studies aforementioned.

Finally, regarding complex I, the parameter that revealed a greater amount of alterations was the uncoupled respiration. To obtain this state, FCCP was used to dissipate the mitochondrial membrane potential causing maximum electron transport rate and consequentially maximum OCR. In pregnant and non-pregnant groups, the same pattern was observed. The consumption of an HFHS cause a decrease in the OCR in the uncoupled state which was highly accentuated when exercise and the HFHS diet were combined. In this state, the ETC is stimulated, due to mitochondrial membrane potential dissipation, to transport electrons at the maximum capacity, thus it is natural that when a system is driven to the limit the alterations or anomalies are revealed. Again, our results point out that we have a degree of mitochondrial uncoupling due to the combination of exercise with the HFHS diet, since mitochondria from those groups cannot achieve the same maximum oxygen consumption rate as controls. Somehow the

interaction between the two treatments hindered the ETC maximum capacity, which is in accordance with our data with increases in the OCR of state 2, state 4 and in lag phase, as well as decreased ADP/O ratio and RCR. In male type I diabetic mice, it was found that the maximum electron transport capacity was decreased in cardiac mitochondria and that this event was correlated with reduced ATP production, alterations in mitochondrial cristae, and coordinated repression of OXPHOS which points out the central role of mitochondria dysfunction in the pathophysiology of diabetic cardiomyopathy[138].

Regarding complex II, an increase in the state 4 was detected, similar to the observed in complex I, where the interaction between HFHS diet and exercise caused an increase in the basal respiration after state 3, which could be related with proton leakage, however in no other parameter alterations were detected, leading us to believe that complex II had a secondary role in the effects promoted by the experimental variables.

It is known that complex I-linked respiration has been associated with decreased state 3 oxygen consumption rates in rodents with cardiac failure and accordingly, similar studies pointed out that early defects in complex I-linked respiration and in fatty acid oxidation could lead to cardiac failure, being this one of the major causes of death in diabetic patients[37,38,145]

After all, why is complex I more affected than complex II? We wondered if somehow the expression levels of complex I or II were altered or even if any other complexes could be downregulated. By western blot technique we measured the protein levels of one subunit of each complex of the ETC and one subunit of ATP synthase. One interesting result was the decreased expression of complex III subunit UQCRC2 namely in the NP_HFHS_E, meaning that the combination of diet and exercise caused a downregulation in the expression levels of this subunit, which may alter the ETC capacity. In fact two of the most common supercomplexes in mitochondria are composed by complex I, III and IV, namely supercomplex I/III and supercomplex I/III/IV, which is the main supercomplex also named respirasome[146].

Thus, if there is a depletion in the UQCRC2 subunit of the complex III, it may cause a malfunction in the electron transfer capacity of the supercomplex, thus the complex I-dependent mitochondrial alterations, may not be directly due to a malfunction in complex I, but due to complex III. In a study with streptozotocin-diabetic mice using BN-PAGE, the authors identified that complex III was not able to assemble properly which was also correlated with decreased activity[147]. Further, two other subunits of complex III were overexpressed, however this occurred as a compensatory mechanism trying to restore the complex III activity during diabetes[147]. Thus, as future perspective it would be interesting to explore the protein levels of other subunits of complex I and III to see if there is a similar behavior and better enlighten our knowledge about our work. Moreover, Shägger and colleagues have shown that alterations in the complexes that form the respirasome can lead instability in complex I, and impair the respirasome assembly[148]. More specifically, alterations that led to loss of complex III proper assembly impaired the formation of the respirasome which is essential for the stability of complex I, the major point of entrance of respiratory chain substrates[148]. A study on skeletal muscle of T2D patients submitted to an exercise protocol showed that the exercised patients exhibited increased protein levels of UQCRC2 which was positively correlated with physical exercise, which is a result that goes against our findings in our work[149]. Overall, we can say that our results suggest that there is a degree of mitochondrial dysfunction promoted by the ingestion of an HFHS diet being exacerbated in combination with exercise. This mitochondrial dysfunction may be related with proton leak caused by an excessive fatty acid oxidation, leading to mitochondrial uncoupling and ROS production, already known to be involved in the pathophysiology of diabetic cardiomyopathy[42]. Also, the alterations in the protein level of complex III subunit UQCRC2, support the hypothesis that complex I has a determinant role in the degree of mitochondrial dysfunction generated. The absence of complex III may impair the respirasome formation which is essential for proper assembly and stability of complex I. Thus

since complex I is compromised due to complex III absence and impaired respirasome formation, the the electron transport capacity of the ETC is decreased, which could lead to mitochondrial dysfunction. It will be highly relevant to perform the visualization of supercomplexes activity by in-gel stains for the different ETC complexes to clarify these results.

Returning to the two main features observed in this work, the second one concerns pregnancy as variable by itself. Pregnancy, as mentioned before, is an extremely demanding process to which the mother undergoes major physiological alterations in order to cope with the demands of gestation. Further, it is likely that at cellular and molecular level, such alterations may occur to. However, the actual literature regarding alterations in the cardiac mitochondria during pregnancy are somewhat scarce. We believe that our work provides novel information regarding the maternal cardiac mitochondrial respiratory states modulation after different types of pregnancies, which could lead to a better knowledge on how to approach each individual during and after the pregnancy to improve fetal and maternal pregnancy outcomes.

In our results, the pregnancy variable acted as a "double agent". Either it was responsible for alterations in the mitochondrial membrane potential and OCR, or, reverted variations that were observed in the non-pregnant controls exposed to an HFHS diet in combination with exercise.

Regarding complex II, no alterations were registered regarding the OCR. Only in complex I a tendency was registered when comparing the RCR of the NP_C_S group with the P_HFHS_E. The combination of pregnancy with the HFHS diet and exercise led to a decrease in the RCR, although with poor statistical significance. Nevertheless, this does not mean that pregnancy was a variable with no influence on the cardiac mitochondrial OCR. Interestingly, we observed that pregnancy appeared to be able to recover some of the alterations that were observed in the non-pregnant group. Being pregnant recovered the decrease in the RCR that were observed in the NP_HFHS_E group when in comparison with the non-pregnant control group. And it decreased

the OCR of state 4 that had been observed in the NP_HFHS_E, which suggested that pregnancy may be able to lower basal OCR, suggesting that it promoted a better mitochondrial coupling. The same effect was observed for complex II. Regarding mitochondrial membrane potential, pregnancy also induced an increased mitochondrial depolarization observed in the pregnant control groups when using complex I and II substrates. This could corroborate the hypothesis that pregnancy may improve mitochondrial coupling since a higher mitochondrial depolarization induced by ADP phosphorylative state 3 is associated with a better coupling ETC and ATP synthase leading to a higher capacity to produce ATP[141]. Given that we hypothesized that if pregnancy induces maternal alterations in order for the organism to cope with the demands of pregnancy, then it may also induce a series of mitochondrial adaptations that will contribute to a better mitochondrial performance during pregnancy. Thus, as a future perspective it would be interesting to explore which mechanisms are in motion during pregnancy that improve mitochondrial bioenergetics and how in fact that improvement is occurring. For example, an evaluation of mitochondrial dynamics like fusion and fission through measurement of proteins such as Drp1, Opa1, Mitofusins 1 and 2, and Fis1, or even electron microscopy would be interesting to understand the mitochondrial network state and the mitochondrial cristae structure. Although we hypothesized a putative protective effect of pregnancy towards the challenges exerted by the ingestion of an HFHS diet alone or combined with exercise, in some parameters that protective effect was not observed, for example, in the uncoupled state or state 2 using G/M substrate to feed complex I. In the pregnant groups, the diet in combination with exercise increased the OCR in a basal state, and it decreased the maximum OCR with the addition of an uncoupler.

These series of conflicting results regarding pregnancy highlight the impact that new studies could have to better understand and characterize the pregnancy-mediated cardiac mitochondrial alterations and their interactions with diet and exercise.

CONCLUSIONS AND FUTURE PERSPECTIVES

It has become evident, in recent decades, that the prevalence of metabolic-rooted pathologies is increasing, with incidence levels of obesity, diabetes, non-alcoholic fatty liver disease, metabolic syndrome and CVD rising every year. One metabolic disease that as followed this trend, is GDM, that emerges as the most common disease that occurs during pregnancy. Moreover, GDM being such a prominent disease, is fundamental to better understand its mechanisms in order to improve prevention, diagnosis, treatment, and management of long-term effects.

With this work, we provide a maternal cardiac mitochondrial bioenergetics characterization without precedent, with focus on the phosphorylative capacity of cardiac mitochondria of a rodent model of GDM. We also test the impact that a protocol of physical exercise could have as a putative non-pharmacological approach to counteract the maternal negative long-term implications that follow a diabetic pregnancy. Finally, we provide for the first time, to our knowledge, new data on the pregnancy-derived cardiac mitochondrial bioenergetics adaptations.

We were able to successfully induce multiple hallmarks of GDM through the ingestion of an HFHS diet, that promoted glucose intolerance, excessive gestational weight gain, and hyperglycemia. Moreover, it increased the number of pups per litter and altered the sex distribution pattern, increasing the number of males. We found that the consumption of an HFHS diet isolated or in combination with exercise led to a degree of mitochondrial dysfunction which possible roots in the excessive FA oxidation that may have caused mitochondrial uncoupling and consequent decreased efficiency. Also, we found decreased protein levels of complex III subunit UQCRC2 which led us to believe that the apparent major role of complex I is in fact resultant of deficient respirasome (CI/III/IV) assembly. Regarding pregnancy, we

found that it may have a mild protective effect on cardiac mitochondria since it promoted an apparent recovery of the mitochondrial coupling.

Finally, and to answer the major question in the title of this work, our data suggest that physical exercise did not exert a protective effect on maternal cardiac mitochondria, and in fact aggravated the negative outcomes promoted by the ingestion of an HFHS diet. Nevertheless, it is important to have in account the enormous number of evidences about the beneficial and cardioprotective effects of exercise. Given that, we propose a theory that is a possible explanation for our results. We believe that the initial challenge promoted by the HFHS diet was manageable and promoted slight alterations in the mitochondrial state. However, the combination with exercise, which acts as a "second-hit stress" may hindered the ability of mitochondria to remodel, leading to a state of mitochondrial dysfunction. Nevertheless, we were able to observe some of the beneficial effects of exercise such as recovery of a physiological gestational weight gain, prevention of the shift in the offspring sex distribution and improved management of blood glucose homeostasis.

In the future, this work should follow two different paths:

a) we suggest that a possible way to better understand the protective effect of exercise could be to reduce the intensity of the exercise, or the time frame where it is applied, since the exercise protocol may have been too demanding or applied too late to counteract the challenge of diet.

b) we suggest focusing on mitochondrial adaptations that may emerge during pregnancy, which will allow to better understand the extent of adaptations that occur, so that the mother is able to cope with pregnancy demands. A greater enlightening on these phenomena would not only improve the medical approach in cases of disease, but also in cases where there is a healthy pregnancy allowing better medical-advisement, follow-up, and improve maternal pregnancy outcome.

In conclusion, this work adds new important knowledge about the most emerging disease in pregnancies nowadays, and we hope that it may contribute to a better comprehension of the disease mechanisms, improve the medical approach to cases of GDM, and one day contribute to decrease the burden of aging-related cardiovascular disease.

APPENDIX

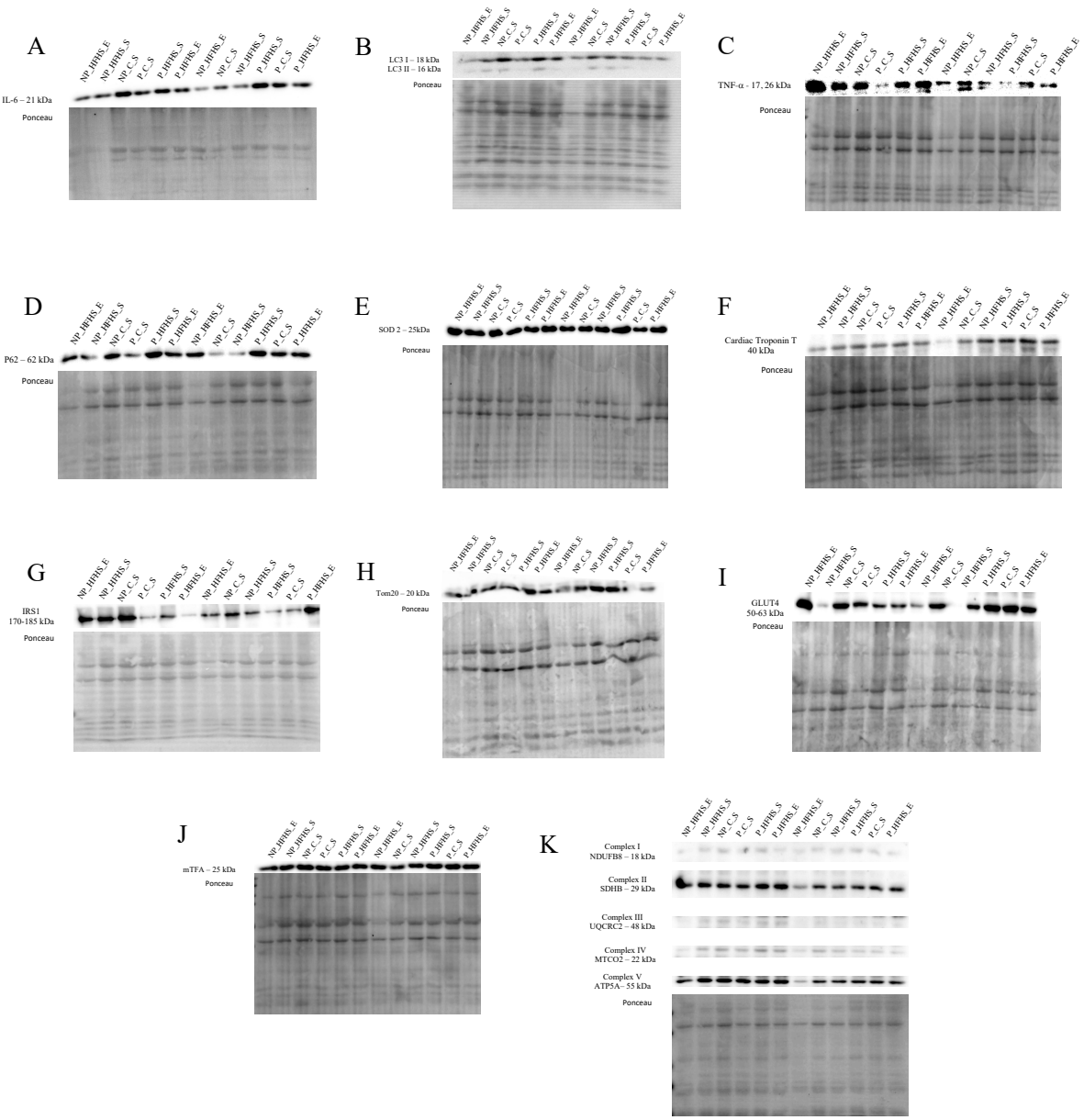

Figure 21. ***Protein levels of cardiac tissue samples from all 6 experimental groups (NP_C_S n= 6; NP_HFHS_S n= 7; NP_HFHS_E n = 5; P_C_S n= 6; P_HFHS_S n= 6 and P_HFHS_E n=6), normalized with ponceau****. The presented images were obtain by Western blot and represent alterations in the protein levels of: (A) IL-6; (B) LC3 I and LC3 II; (C) TNF α ; (D) p62; (E) SOD2; (F) Cardiac Troponin T; (G) IRS-1; (H) Tom20; (I) GLUT4; (J) mTFA; (K) OXPHOS complexes I (NDFUB8), II (SDHB), III (UQCRC2), IV (MTCO1), Complex V (ATP5A). The presented images are representative of 3 independent experiments. Ponceau staining was used to normalize the protein levels.*

REFERENCES

1. Tan, E. K. & Tan, E. L. Alterations in physiology and anatomy during pregnancy. *Best Pract. Res. Clin. Obstet. Gynaecol.* **27**, 791–802 (2013).
2. Larciprete, G. *et al.* Body composition during normal pregnancy: Reference ranges. *Acta Diabetol.* **40**, 225–232 (2003).
3. Pugsley, M. K. & Tabrizchi, R. The vascular system. An overview of structure and function. *J. Pharmacol. Toxicol. Methods* **44**, 333–40 (2014).
4. Crossley, D. A., Burggren, W. W., Reiber, C. L., Altimiras, J. & Rodnick, K. J. Mass transport: Circulatory system with emphasis on nonendothermic species. *Compr. Physiol.* **7**, 17–66 (2017).
5. San-Frutos, L. *et al.* Hemodynamic changes during pregnancy and postpartum: a prospective study using thoracic electrical bioimpedance. *J. Matern. Neonatal Med.* **24**, 1333–1340 (2011).
6. Melchiorre, K., Sharma, R. & Thilaganathan, B. Cardiac structure and function in normal pregnancy. *Curr. Opin. Obstet. Gynecol.* **24**, 413–421 (2012).
7. Carbillon, L., Uzan, M. & Uzan, S. Pregnancy, vascular tone, and maternal hemodynamics: a crucial adaptation. *Obstet. Gynecol. Surv.* **55**, 574–81 (2000).
8. Thornburg, K. L., Jacobson, S. L., Giraud, G. D. & Morton, M. J. Hemodynamic changes in pregnancy. *Semin. Perinatol.* **24**, 11–4 (2000).
9. Kametas, N. A., McAuliffe, F., Hancock, J., Chambers, J. & Nicolaides, K. H. Maternal left ventricular mass and diastolic function during pregnancy. *Ultrasound Obstet. Gynecol.* **18**, 460–466 (2001).
10. Grady, K. M. (Kathryn M. ., Howell, C., Cox, C. (Charles) & Royal College of Obstetricians and Gynaecologists (Great Britain). *Managing obstetric emergencies and trauma : the MOET course manual.* (RCOG Press, 2007).

11. Pereira, T. J. *et al.* Maternal obesity characterized by gestational diabetes increases the susceptibility of rat offspring to hepatic steatosis via a disrupted liver metabolome. *J. Physiol.* **593**, 3181–3197 (2015).

12. Diabetes gestacional | Atlas da Saúde. Available at: http://www.atlasdasaude.pt/publico/content/diabetes-gestacional. (Accessed: 20th July 2018)

13. Catalano, P. M., Kirwan, J. P., Haugel-de Mouzon, S. & King, J. Gestational Diabetes and Insulin Resistance: Role in Short- and Long-Term Implications for Mother and Fetus. *J. Nutr.* **133**, 1674S-1683S (2003).

14. DeSisto, C. L., Kim, S. Y. & Sharma, A. J. Prevalence estimates of gestational diabetes mellitus in the United States, Pregnancy Risk Assessment Monitoring System (PRAMS), 2007-2010. *Prev. Chronic Dis.* **11**, E104 (2014).

15. Obesity and overweight. Available at: http://www.who.int/news-room/fact-sheets/detail/obesity-and-overweight. (Accessed: 20th July 2018)

16. Sonagra, A. D., Biradar, S. M., K, D. & Murthy D S, J. Normal pregnancy- a state of insulin resistance. *J. Clin. Diagn. Res.* **8**, CC01-3 (2014).

17. Kaaja, R. & Rönnemaa, T. Gestational diabetes: pathogenesis and consequences to mother and offspring. *Rev. Diabet. Stud.* **5**, 194–202 (2008).

18. Desoye, G. & Hauguel-de Mouzon, S. The human placenta in gestational diabetes mellitus. The insulin and cytokine network. *Diabetes Care* **30 Suppl 2**, S120-6 (2007).

19. Menon, R. K. *et al.* Transplacental Passage of Insulin in Pregnant Women with Insulin-Dependent Diabetes Mellitus. *N. Engl. J. Med.* **323**, 309–315 (1990).

20. Billionnet, C. *et al.* Gestational diabetes and adverse perinatal outcomes from 716,152 births in France in 2012. *Diabetologia* **60**, 636–644 (2017).

21. Pereira, T. J., Moyce, B. L., Kereliuk, S. M. & Dolinsky, V. W. Influence of maternal

overnutrition and gestational diabetes on the programming of metabolic health outcomes in the offspring: experimental evidence. *Biochem. Cell Biol.* **93**, 438–451 (2015).

22. Gilmore, L. A., Klempel-Donchenko, M. & Redman, L. M. Pregnancy as a window to future health: Excessive gestational weight gain and obesity. *Semin. Perinatol.* **39**, 296–303 (2015).
23. Gestational diabetes - NHS.UK. Available at: https://www.nhs.uk/conditions/gestational-diabetes/. (Accessed: 25th June 2018)
24. Marcinkevage, J. A. & Narayan, K. M. V. Gestational diabetes mellitus: Taking it to heart. *Prim. Care Diabetes* **5**, 81–88 (2011).
25. Bellamy, L., Casas, J.-P., Hingorani, A. D. & Williams, D. Type 2 diabetes mellitus after gestational diabetes: a systematic review and meta-analysis. *Lancet* **373**, 1773–1779 (2009).
26. Noctor, E. *et al.* ATLANTIC-DIP: prevalence of metabolic syndrome and insulin resistance in women with previous gestational diabetes mellitus by International Association of Diabetes in Pregnancy Study Groups criteria. *Acta Diabetol.* **52**, 153–160 (2015).
27. Roth, G. A. *et al.* Global, Regional, and National Burden of Cardiovascular Diseases for 10 Causes, 1990 to 2015. *J. Am. Coll. Cardiol.* **70**, 1–25 (2017).
28. Townsend, N. *et al.* Cardiovascular disease in Europe: epidemiological update 2016. *Eur. Heart J.* **37**, 3232–3245 (2016).
29. WHO. World Heart Federation. World Stroke Organization. Global Atlas on Cardiovascular disease prevention and control. *Publ. by World Heal. Organ. Collab. with World Hear. Fed. World Hear. Fed. World Stroke Organ.* 155 (2011). doi:NLM classification: WG 120
30. Abajobir, A. A. *et al.* Global, regional, and national age-sex specific mortality for 264

causes of death, 1980-2016: a systematic analysis for the Global Burden of Disease Study 2016. *Lancet* **390**, 1151–1210 (2017).

31. Teufel, E. J. Risk Factors for Cardiovascular Disease. in *Encyclopedia of Cardiovascular Research and Medicine* 307–314 (Elsevier, 2018). doi:10.1016/B978-0-12-809657-4.99837-5
32. Risk factors - World Heart Federation - World Heart Federation. Available at: https://www.world-heart-federation.org/resources/risk-factors/. (Accessed: 20th July 2018)
33. Lippi, G. & Guidi, G. Risk factors for cardiovascular disease (CVD). *Hear. UK* **166**, 710 (2002).
34. Chomistek, A. K. *et al.* Healthy Lifestyle in the Primordial Prevention of Cardiovascular Disease Among Young Women. *J. Am. Coll. Cardiol.* **65**, 43–51 (2015).
35. Yu, E. *et al.* Diet, lifestyle, biomarkers, genetic factors, and risk of cardiovascular disease in the nurses' health studies. *Am. J. Public Health* **106**, 1616–1623 (2016).
36. Finks, S. W. *et al.* Key Articles of Dietary Interventions that Influence Cardiovascular Mortality. *Pharmacother. J. Hum. Pharmacol. Drug Ther.* **32**, e54–e87 (2012).
37. World Health Organization. *Noncommunicable diseases country profiles 2014*.
38. Chatterjee, S., Khunti, K. & Davies, M. J. Type 2 diabetes. *Lancet* **389**, 2239–2251 (2017).
39. Abel, E. D. Free fatty acid oxidation in insulin resistance and obesity. *Heart and metabolism : management of the coronary patient* **48**, 5–10 (2010).
40. Abdul-Ghani, M. *et al.* Cardiovascular Disease and Type 2 Diabetes: Has the Dawn of a New Era Arrived? *Diabetes Care* **40**, 813–820 (2017).
41. Cardiomyopathy | National Heart, Lung, and Blood Institute (NHLBI). Available at: https://www.nhlbi.nih.gov/health-topics/cardiomyopathy#Types. (Accessed: 20th June

2018)

42. Boudina, S. & Abel, E. D. Diabetic cardiomyopathy revisited. *Circulation* **115**, 3213–3223 (2007).

43. Kolwicz, S. C., Purohit, S., Tian, R. & Tian, R. Cardiac metabolism and its interactions with contraction, growth, and survival of cardiomyocytes. *Circ. Res.* **113**, 603–16 (2013).

44. Murphy, E. *et al. Mitochondrial Function, Biology, and Role in Disease: A Scientific Statement from the American Heart Association*. *Circulation Research* **118**, (2016).

45. Hopmans, T.-E. J. P. *et al.* [Increased risk of type II diabetes mellitus and cardiovascular disease after gestational diabetes mellitus: a systematic review]. *Ned. Tijdschr. Geneeskd.* **159**, A8043 (2015).

46. Hiersch, L. & Yogev, Y. Management of diabetes and pregnancy - When to start and what pharmacological agent to choose? *Best Pract. Res. Clin. Obstet. Gynaecol.* **29**, 225–236 (2015).

47. Langer, O. Pharmacological treatment of gestational diabetes mellitus: point/counterpoint. *Am. J. Obstet. Gynecol.* **218**, 490–499 (2018).

48. Hyer, S., Balani, J. & Shehata, H. Metformin in Pregnancy: Mechanisms and Clinical Applications. *Int. J. Mol. Sci.* **19**, (2018).

49. Polasek, T. M., Doogue, M. P. & Thynne, T. R. J. Metformin treatment of type 2 diabetes mellitus in pregnancy: update on safety and efficacy. *Ther. Adv. drug Saf.* **9**, 287–295 (2018).

50. Priya, G. & Kalra, S. Metformin in the management of diabetes during pregnancy and lactation. *Drugs Context* **7**, 212523 (2018).

51. Donovan, P. J. & McIntyre, H. D. Drugs for gestational diabetes. *Aust. Prescr.* **33**, 141–144 (2010).

52. Ripsin, C. M., Kang, H. & Urban, R. J. Management of blood glucose in type 2 diabetes mellitus. *Am. Fam. Physician* **79**, 29–36 (2009).

53. Powers, M. A. *et al.* FROM THE ACADEMY Diabetes Self-Management Education and Support in Type 2 Diabetes: A Joint Position Statement of the American Diabetes Association, the American Association of Diabetes Educators, and the Academy of Nutrition and Dietetics. *J. Acad. Nutr. Diet.* **115**, 1323–1334 (2015).

54. Wu, C.-Y. *et al.* The association of physical activity with all-cause, cardiovascular, and cancer mortalities among older adults. *Prev. Med. (Baltim).* **72**, 23–29 (2015).

55. Akki, A., Smith, K. & Seymour, A. M. L. Compensated cardiac hypertrophy is characterised by a decline in palmitate oxidation. *Mol. Cell. Biochem.* **311**, 215–224 (2008).

56. Kumar, V., Santhosh Kumar, T. R. & Kartha, C. C. Mitochondrial membrane transporters and metabolic switch in heart failure. *Heart Fail. Rev.* 1–13 (2018). doi:10.1007/s10741-018-9756-2

57. Davidoff, A. J., Davidson, M. B., Carmody, M. W., Davis, M.-E. & Ren, J. Diabetic cardiomyocyte dysfunction and myocyte insulin resistance: role of glucose-induced PKC activity. *Mol. Cell. Biochem.* **262**, 155–63 (2004).

58. Monti, D. A., Sufian, M. & Peterson, C. Potential role of mind-body therapies in cancer survivorship. *Cancer* **112**, 2607–2616 (2008).

59. Lopaschuk, G. D., Ussher, J. R., Folmes, C. D. L., Jaswal, J. S. & Stanley, W. C. Myocardial Fatty Acid Metabolism in Health and Disease. *Physiol. Rev.* **90**, 207–258 (2010).

60. Fillmore, N., Mori, J. & Lopaschuk, G. D. Mitochondrial fatty acid oxidation alterations in heart failure, ischaemic heart disease and diabetic cardiomyopathy. *Br. J. Pharmacol.* **171**, 2080–90 (2014).

61. Ussher, J. R. *et al.* Stimulation of glucose oxidation protects against acute myocardial infarction and reperfusion injury. *Cardiovasc. Res.* **94**, 359–369 (2012).

62. Dyck, J. R. B. *et al.* Malonyl Coenzyme A Decarboxylase Inhibition Protects the Ischemic Heart by Inhibiting Fatty Acid Oxidation and Stimulating Glucose Oxidation. *Circ. Res.* **94**, (2004).

63. BHAGAVAN, N. V. Lipids I: Fatty Acids and Eicosanoids. *Med. Biochem.* 365–399 (2002). doi:10.1016/b978-012095440-7/50020-2

64. Stanley, W. C. & Chandler, M. P. Energy Metabolism in the Normal and Failing Heart : Potential for Therapeutic Interventions. 115–130 (2002).

65. Lopatin, Y. M. *et al.* Rationale and benefits of trimetazidine by acting on cardiac metabolism in heart failure. *Int. J. Cardiol.* **203**, 909–915 (2016).

66. Gladden, L. B. Lactate metabolism: a new paradigm for the third millennium. *J Physiol* **558**, 5–30 (2004).

67. Kolwicz, S. C., Tian, R. & Tian, R. Glucose metabolism and cardiac hypertrophy. *Cardiovasc. Res.* **90**, 194–201 (2011).

68. Shipley, M. T. & Ennis, M. Functional organization of. *J. Neurobiol.* **30**, 123–176 (1996).

69. Jeffery, C. J., Bahnson, B. J., Chien, W., Ringe, D. & Petsko, G. A. Crystal structure of rabbit phosphoglucose isomerase, a glycolytic enzyme that moonlights as neuroleukin, autocrine motility factor, and differentiation mediator. *Biochemistry* **39**, 955–964 (2000).

70. Usenik, A. & Legiša, M. Evolution of allosteric citrate binding sites on 6-phosphofructo-1-kinase. *PLoS One* **5**, e15447 (2010).

71. Berry, A. & Marshall, K. E. Identification of zinc-binding ligands in the Class II fructose-1,6-bisphosphate aldolase of Escherichia coli. *FEBS Lett.* **318**, 11–16 (1993).

72. Mande, S. C. *et al.* Crystal structure of recombinant human triosephosphate isomerase at

2.8 A resolution. Triosephosphate isomerase-related human genetic disorders and comparison with the trypanosomal enzyme - 1994 - World Health.pdf. 810–821 (1994).

73. Brassard, J., Gottschalk, M. & Quessy, S. Cloning and purification of the Streptococcus suis serotype 2 glyceraldehyde-3-phosphate dehydrogenase and its involvement as an adhesin. *Vet. Microbiol.* **102**, 87–94 (2004).

74. Chiarelli, L. R. *et al.* Molecular insights on pathogenic effects of mutations causing phosphoglycerate kinase deficiency. *PLoS One* **7**, e32065 (2012).

75. Johnsen, U. & Schönheit, P. Characterization of cofactor-dependent and cofactor-independent phosphoglycerate mutases from Archaea. *Extremophiles* **11**, 647–657 (2007).

76. Erli Zhang, §,∥, John M. Brewer, ⊥, Wladek Minor, ∇, Lionel A. Carreira, # and & Lukasz Lebioda*, §. Mechanism of Enolase: The Crystal Structure of Asymmetric Dimer Enolase−2-Phospho-d-glycerate/Enolase−Phosphoenolpyruvate at 2.0 Å Resolution†,‡. (1997). doi:10.1021/BI9712450

77. Gupta, V. & Bamezai, R. N. K. Human pyruvate kinase M2: a multifunctional protein. *Protein Sci.* **19**, 2031–44 (2010).

78. Gudiksen, A. *et al.* Lack of Skeletal Muscle IL-6 Affects Pyruvate Dehydrogenase Activity at Rest and during Prolonged Exercise. *PLoS One* **11**, e0156460 (2016).

79. Lacombe, M. L., Tokarska-Schlattner, M., Boissan, M. & Schlattner, U. The mitochondrial nucleoside diphosphate kinase (NDPK-D/NME4), a moonlighting protein for cell homeostasis. *Lab. Investig.* **98**, 582–588 (2018).

80. Akram, M. Citric Acid Cycle and Role of its Intermediates in Metabolism. *Cell Biochem. Biophys.* **68**, 475–478 (2014).

81. Lushchak, O. V., Piroddi, M., Galli, F. & Lushchak, V. I. Aconitase post-translational modification as a key in linkage between Krebs cycle, iron homeostasis, redox signaling,

and metabolism of reactive oxygen species. *Redox Rep.* **19**, 8–15 (2014).

82. Milana A. B. Applegate, Kenneth M. Humphries, and & Szweda*, L. I. Reversible Inhibition of α-Ketoglutarate Dehydrogenase by Hydrogen Peroxide: Glutathionylation and Protection of Lipoic Acid†. (2007). doi:10.1021/BI7017464

83. Chinopoulos, C. & Seyfried, T. N. Mitochondrial Substrate-Level Phosphorylation as Energy Source for Glioblastoma: Review and Hypothesis. doi:10.1177/1759091418818261

84. Rutter, J., Winge, D. R. & Schiffman, J. D. Succinate dehydrogenase - Assembly, regulation and role in human disease. *Mitochondrion* **10**, 393–401 (2010).

85. Dimauro, S. & Schon, E. A. Mitochondrial Respiratory-Chain Diseases. 2656–2668 (2003).

86. Nicholls, D. G. & Ferguson, S. J. Bioenergetics 3rd Edition. *Full Text via CrossRef| View Rec. Scopus| Cited By Scopus* 1–333 (2002).

87. Palmeira, C. M. *Mitochondrial Bioenergetics*. **810**, (2012).

88. Rich, P. R. & Maréchal, A. The mitochondrial respiratory chain. *Essays Biochem.* **47**, 1–23 (2010).

89. Yoshida, M., Muneyuki, E. & Hisabori, T. ATP synthase - A marvellous rotary engine of the cell. *Nat. Rev. Mol. Cell Biol.* **2**, 669–677 (2001).

90. Boyer, P. D. Catalytic site occupancy during ATP synthase catalysis. *FEBS Lett.* **512**, 29–32 (2002).

91. Kayama, Y. *et al.* Diabetic cardiovascular disease induced by oxidative stress. *Int. J. Mol. Sci.* **16**, 25234–25263 (2015).

92. Trewin, A., Berry, B. & Wojtovich, A. Exercise and Mitochondrial Dynamics: Keeping in Shape with ROS and AMPK. *Antioxidants* **7**, 7 (2018).

93. Morales-Alamo, D. *et al.* Skeletal Muscle Pyruvate Dehydrogenase Phosphorylation and

Lactate Accumulation During Sprint Exercise in Normoxia and Severe Acute Hypoxia: Effects of Antioxidants. *Front. Physiol.* **9**, 188 (2018).

94. Pingitore, A. *et al.* Exercise and oxidative stress: Potential effects of antioxidant dietary strategies in sports. *Nutrition* **31**, 916–922 (2015).

95. Jin, H. *et al.* Mitochondria-targeted antioxidants for treatment of Parkinson's disease: Preclinical and clinical outcomes. *Biochim. Biophys. Acta - Mol. Basis Dis.* **1842**, 1282–1294 (2014).

96. Sawyer, D. B. *et al.* Role of oxidative stress in myocardial hypertrophy and failure. *J. Mol. Cell. Cardiol.* **34**, 379–88 (2002).

97. Sabri, A., Hughie, H. H. & Lucchesi, P. A. Regulation of Hypertrophic and Apoptotic Signaling Pathways by Reactive Oxygen Species in Cardiac Myocytes. *Antioxid. Redox Signal.* **5**, 731–740 (2003).

98. Ide, T. *et al.* Mitochondrial Electron Transport Complex I Is a Potential Source of Oxygen Free Radicals in the Failing Myocardium. *Circ. Res.* **85**, 357–363 (1999).

99. Zhang, C. *et al.* Aberrant expression of oxidative stress related proteins affects the pregnancy outcome of gestational diabetes mellitus patients. *Am. J. Transl. Res.* **11**, 269–279 (2019).

100. Lappas, M. *et al.* The Role of Oxidative Stress in the Pathophysiology of Gestational Diabetes Mellitus. *Antioxid. Redox Signal.* **15**, 3061–3100 (2011).

101. Karacay, Ö. *et al.* A quantitative evaluation of total antioxidant status and oxidative stress markers in preeclampsia and gestational diabetic patients in 24–36 weeks of gestation. *Diabetes Res. Clin. Pract.* **89**, 231–238 (2010).

102. Gaweł, S., Wardas, M., Niedworok, E. & Wardas, P. [Malondialdehyde (MDA) as a lipid peroxidation marker]. *Wiad. Lek.* **57**, 453–5 (2004).

103. Russell, A. P., Foletta, V. C., Snow, R. J. & Wadley, G. D. Skeletal muscle mitochondria:

A major player in exercise, health and disease. *Biochim. Biophys. Acta - Gen. Subj.* **1840**, 1276–1284 (2014).

104. Sarvas, J. L., Otis, J. S., Khaper, N. & Lees, S. J. Voluntary physical activity prevents insulin resistance in a tissue specific manner. *Physiol. Rep.* **3**, 1–11 (2015).

105. Antunes, J. M. M., Ferreira, R. M. P. & Moreira-Gonçalves, D. Exercise Training as Therapy for Cancer-Induced Cardiac Cachexia. *Trends Mol. Med.* (2018). doi:10.1016/j.molmed.2018.06.002

106. Marques-Aleixo, I. *et al.* The beneficial role of exercise in mitigating doxorubicin-induced Mitochondrionopathy. *Biochim. Biophys. Acta - Rev. Cancer* **1869**, 189–199 (2018).

107. Sklempe Kokic, I., Ivanisevic, M., Kokic, T., Simunic, B. & Pisot, R. Acute responses to structured aerobic and resistance exercise in women with gestational diabetes mellitus. *Scand. J. Med. Sci. Sports* **28**, 1793–1800 (2018).

108. DHS: Exercise During Pregnancy. Available at: http://www.dhs.state.il.us/page.aspx?item=48889. (Accessed: 21st July 2018)

109. Pregnancy and Exercise. Available at: https://www.webmd.com/baby/guide/exercise-during-pregnancy#1. (Accessed: 21st July 2018)

110. Hinman, S. K., Smith, K. B., Quillen, D. M. & Smith, M. S. Exercise in Pregnancy: A Clinical Review. *Sports Health* **7**, 527–31 (2015).

111. Viña, J. *et al.* Mitochondrial biogenesis in exercise and in ageing. *Adv. Drug Deliv. Rev.* **61**, 1369–1374 (2009).

112. Koh, J.-H. *et al.* PPARβ Is Essential for Maintaining Normal Levels of PGC-1α and Mitochondria and for the Increase in Muscle Mitochondria Induced by Exercise. *Cell Metab.* **25**, 1176-1185.e5 (2017).

113. Chow, S. L. Diabetes and exercise. *Am. J. Nurs.* **88**, 178–180 (1988).

114. Perry, C. G. R. *et al.* Repeated transient mRNA bursts precede increases in transcriptional and mitochondrial proteins during training in human skeletal muscle. *J. Physiol.* **588**, 4795–4810 (2010).

115. Xi, Q.-L. *et al.* Mitofusin-2 prevents skeletal muscle wasting in cancer cachexia. *Oncol. Lett.* **12**, 4013–4020 (2016).

116. Article, A., Journal, T. & Article, A. The role of alterations in mitochondrial dynamics andPGC-1α over-expression in fast muscle atrophy followinghindlimb unloading. 1–33 doi:10.1113/jphysiol.2014.286740.This

117. Leduc-Gaudet, J.-P. *et al.* Mitochondrial morphology is altered in atrophied skeletal muscle of aged mice. *Oncotarget* **6**, 17923–37 (2015).

118. Ong, S.-B. *et al.* Inhibiting mitochondrial fission protects the heart against ischemia/reperfusion injury. *Circulation* **121**, 2012–22 (2010).

119. Zhang, L. & Zhang, L. Voluntary oral administration of drugs in mice. *Protoc. Exch.* 1–10 (2011). doi:10.1038/protex.2011.236

120. Cora, M. C., Kooistra, L. & Travlos, G. Vaginal Cytology of the Laboratory Rat and Mouse. *Toxicol. Pathol.* **43**, 776–793 (2015).

121. Pereira, S. P. *et al.* Dioxin-induced acute cardiac mitochondrial oxidative damage and increased activity of ATP-sensitive potassium channels in Wistar rats. *Environ. Pollut.* **180**, 281–90 (2013).

122. Silva, A. M. & Oliveira, P. J. Evaluation of Respiration with Clark Type Electrode in Isolated Mitochondria and Permeabilized Animal Cells. in 7–24 (Humana Press, 2012). doi:10.1007/978-1-61779-382-0_2

123. GORNALL, A. G., BARDAWILL, C. J. & DAVID, M. M. Determination of serum proteins by means of the biuret reaction. *J. Biol. Chem.* **177**, 751–66 (1949).

124. Mahmood, T. & Yang, P.-C. Western blot: technique, theory, and trouble shooting. *N.*

Am. J. Med. Sci. **4**, 429–34 (2012).

125. Romero-Calvo, I. *et al.* Reversible Ponceau staining as a loading control alternative to actin in Western blots. *Anal. Biochem.* **401**, 318–320 (2010).
126. Chiefari, E., Arcidiacono, B., Foti, D. & Brunetti, A. Gestational diabetes mellitus: an updated overview. *J. Endocrinol. Invest.* **40**, 899–909 (2017).
127. Hall, D. C. & Kaufmann, D. A. Effects of aerobic and strength conditioning on pregnancy outcomes. *Am. J. Obstet. Gynecol.* **157**, 1199–1203 (1987).
128. Vega, C. C. *et al.* Exercise in obese female rats has beneficial effects on maternal and male and female offspring metabolism. *Int. J. Obes.* **39**, 712–719 (2015).
129. Connelly Freyder, S. Exercising while pregnant. *J. Orthop. Sports Phys. Ther.* **10**, 358–365 (1989).
130. Lambrinou, C. P., Karaglani, E. & Manios, Y. Breastfeeding and postpartum weight loss. *Curr. Opin. Clin. Nutr. Metab. Care* **22**, 413–417 (2019).
131. Cisse, O. *et al.* Mild Gestational Hyperglycemia in Rat Induces Fetal Overgrowth and Modulates Placental Growth Factors and Nutrient Transporters Expression. *PLoS One* **8**, (2013).
132. Beavers, K. M. *et al.* Effect of Exercise Type During Intentional Weight Loss on Body Composition in Older Adults with Obesity. *Obesity* **25**, 1823–1829 (2017).
133. JELLEYMAN, C. *et al.* Associations of Physical Activity Intensities with Markers of Insulin Sensitivity. *Med. Sci. Sport. Exerc.* **49**, 2451–2458 (2017).
134. Gnaiger, E. *Mitochondrial Pathways and Respiratory Control An Introduction to OXPHOS Analysis*. *Mitochondrial Physiology Network* (2014).
135. Vial, G. *et al.* Effects of a high-fat diet on energy metabolism and ROS production in rat liver. *J. Hepatol.* **54**, 348–356 (2011).
136. Wang, S. Y. *et al.* Exercise enhances cardiac function by improving mitochondrial

dysfunction and maintaining energy homoeostasis in the development of diabetic cardiomyopathy. *J. Mol. Med.* (2020). doi:10.1007/s00109-019-01861-2

137. Arsenijevic, D. *et al.* Disruption of the uncoupling protein-2 gene in mice reveals a role in immunity and reactive oxygen species production. *Nat. Genet.* **26**, 435–439 (2000).
138. Bugger, H. *et al.* Tissue-specific remodeling of the mitochondrial proteome in type 1 diabetic akita mice. *Diabetes* **58**, 1986–1997 (2009).
139. Yang, Y. *et al.* MIR-152 Regulates Apoptosis and Triglyceride Production in MECs via Targeting ACAA2 and HSD17B12 Genes. *Sci. Rep.* **8**, 1–10 (2018).
140. Vluggens, A. *et al.* Functional significance of the two ACOX1 isoforms and their crosstalks with PPARα and RXRα. *Lab. Investig.* **90**, 696–708 (2010).
141. Alves, M. G., Oliveira, P. J. & Carvalho, R. A. Mitochondrial preservation in celsior versus histidine buffer solution during cardiac Ischemia and reperfusion. *Cardiovasc. Toxicol.* **9**, 185–193 (2009).
142. Alves, M. G., Soares, A. F., Carvalho, R. A. & Oliveira, P. J. Sodium hydrosulfide improves the protective potential of the cardioplegic histidine buffer solution. *Eur. J. Pharmacol.* **654**, 60–67 (2011).
143. Pereira, G. C. *et al.* Mitochondrionopathy phenotype in doxorubicin-treated wistar rats depends on treatment protocol and is cardiac-specific. *PLoS One* **7**, (2012).
144. Ascensão, A. *et al.* Acute exercise protects against calcium-induced cardiac mitochondrial permeability transition pore opening in doxorubicin-treated rats. *Clin. Sci.* **120**, 37–49 (2011).
145. Rosca, M. G. & Hoppel, C. L. Mitochondrial dysfunction in heart failure. *Heart Fail. Rev.* **18**, 607–622 (2013).
146. Davies, K. M., Blum, T. B. & Kühlbrandt, W. Conserved in situ arrangement of complex i and III2 in mitochondrial respiratory chain supercomplexes of mammals, yeast, and

plants. *Proc. Natl. Acad. Sci. U. S. A.* **115**, 3024–3029 (2018).

147. Munusamy, S. *et al.* Alteration of renal respiratory Complex-III during experimental type-1 diabetes. *BMC Endocr. Disord.* **9**, 1–9 (2009).

148. Schägger, H. *et al.* Significance of respirasomes for the assembly/stability of human respiratory chain complex I. *J. Biol. Chem.* **279**, 36349–36353 (2004).

149. Hussey, S. E. *et al.* Effect of exercise on the skeletal muscle proteome in patients with type 2 diabetes. *Med. Sci. Sports Exerc.* **45**, 1069–1076 (2013).